Climate and Land Use/Cover Change Impacts on the Ecologically Relevant Flow Metrics in the Cahaba River Watershed

by

Furkan Dosdogru

A thesis submitted to the Graduate Faculty of
Auburn University
in partial fulfillment of the
requirements for the Degree of
Master of Science

Auburn, Alabama
August 6, 2016

Keywords: Climate change, Land use/cover change, SWAT, CMIP5,
Ecologically relevant flow metrics, Flow regime alteration

Approved by

Latif Kalin, Chair, Professor, School of Forestry and Wildlife Sciences
Luke J. Marzen, Professor, Department of Geosciences, College of Sciences and Mathematics
Li Dong, Assistant Professor, School of Forestry and Wildlife Sciences & Department of Geosciences, College of Sciences and Mathematics

Abstract

This study explored the impacts of land use/cover (LULC) and climate change on hydrological responses, particularly low-flow regimes, in the rapidly urbanizing upper Cahaba River basin in north-central Alabama. The Cahaba River is identified as the longest free-flowing river in the state of Alabama, and The Nature Conservancy noted it as one of the only eight "Hotspot of Biodiversity" in the contiguous United States. Past, present, and future potential streamflow responses to LULC and climate changes were analyzed based on ecologically relevant flow metrics. We used 38 key flow metrics that capture high, low, and median flow, as well as flashiness, which are known to have significant impacts on flora and fauna. These flow metrics, thus the ecology, will certainly be affected by LULC and climate change. Daily streamflow was produced from 1988 to 2013 using historical climate and LULC data with the Soil and Water Assessment Tool (SWAT). Streamflow data from the periods of 1988-1993 and 2008-2013 were used for model calibration and validation, respectively. The SWAT-CUP calibration and uncertainty program was used for this purpose. For the base periods, the effects of different land cover maps were also analyzed by using "National Land Cover Data (NLCD)" and "Digitized Landsat 5 TM Data". Future daily streamflows were generated with SWAT using bias corrected and downscaled CMIP5 climate data for the years 2035 to 2060 with eleven climate models under two different representative concentration pathways (RCP 2.6 and RCP 8.5). For the future LULC data, USGS EROS future projected dataset (250-meter resolution) was used. The daily streamflow from each period were fed into the Indicators of Hydrological Alterations (IHA) software to

calculate the 38 flow metrics in each period. Differences in the metrics were assessed, which may hint for increase/decrease in native species' density that may have occurred in the past or might occur in the future.

Keywords: Climate change, Land use/cover change, SWAT, CMIP5, Ecologically relevant flow metrics, Flow regime alteration

Acknowledgments

I am extremely grateful to my major advisor, Dr. Latif Kalin, for his instruction, guidance, and patience throughout my Master's program at Auburn University. I am thankful to my committee members, Dr. Luke J. Marzen and Dr. Li Dong, for always helping me with their expertise and valuable time. I am indebted to the Republic of Turkey Ministry of Forestry and Water Affairs. Without their financial support this study would not have been possible. I would also like to recognize and thank my colleagues Yuanzhi Yao, Mehdi Rezaeianzadeh and Megan Bartholomew for their help during multiple stages of this research.

I would also like to acknowledge the World Climate Research Programme's Working Group on Coupled Modelling, which is responsible for CMIP, and I thank the climate modeling groups (listed in Table III-2.) for producing and making available their model output. For CMIP the U.S. Department of Energy's Program for Climate Model Diagnosis and Intercomparison provides coordinating support and led development of software infrastructure in partnership with the Global Organization for Earth System Science Portals.

Finally, I dedicate this work to my family, Aysel Dosdogru, Turan Dosdogru, Gokhan Dosdogru, Bugra Dosdogru, and Dr. Tugce Arman for their love and support. You have always been with me during my enjoyable and difficult times and I hope this never ends. I love you all.

Table of Contents

Abstract ii

Acknowledgments iv

List of Tables vii

List of Figures viii

Chapter I - Introduction 1

Chapter II - Modeling Impacts of Land Use/Cover Change in the Upper Cahaba River Watershed 7

Abstract 7

Introduction 8

Methodology 12

Results and discussion 25

Summary and conclusion 29

References 31

Chapter III - Individual, Combined and Synergistic Impacts of Land Use/Cover and Climate Change on the Ecologically Relevant Flow Metrics 52

Abstract 52

Inroduction 54

Methodology 59

Results and discussion 69

Summary and conclusion 78

References 81

Chapter IV – Summary and Conclusions..... 112

Appendices..... 116

List of Tables

Table II-1. Land use/cover classes and changes in the Upper Cahaba River watershed. 38

Table II-2. Characteristics of the Upper Cahaba River watershed. 39

Table II-3. Input data used in the SWAT model and data sources. 40

Table II-4. Calibrated model parameters and fitted values for each LULC datasets. 41

Table II-5. Sensitivity ranks and *p*-values of two different LULC datasets. 42

Table II-6. Calibration and validation results. 43

Table II-7. Differences in mean and seasonal streamflows for the datasets. 44

Table III-1. Input data used in the SWAT model and data sources. 90

Table III-2. List of the CMIP5 climate models used in this study under RCP 2.6 and 8.5 scenarios. 91

Table III-3. Summary of hydrological parameters used in the IHA to characterize flow regime and their ecosystem influences. 92

Table III-4. Model experiment setup. 93

List of Figures

Figure II-1. Study area. 45

Figure II-2. 1950-2014 Upper Cahaba River watershed climate averages (NOAA). 46

Figure II-3. LULC datasets used in this study. 47

Figure II-4. Observed and simulated mean monthly streamflows based on the NLCD land use map for the calibration (a) and validation (b) periods. 48

Figure II-5. Observed and simulated mean monthly streamflows based on the digitized Landsat 5 TM imageries land use map for the calibration (a) and validation (b) periods. 49

Figure II-6. Mean monthly streamflow changes due to LULC changes (1988-2013). 50

Figure II-7. Changes in average seasonal streamflows. 50

Figure II-8. Exceedence probability of calibration (a) and validation (b) periods for both LULC datasets. 51

Figure III-1. LULC datasets used in this study. 94

Figure III-2. Cumulative distribution functions (CDFs) for historical (observed) maximum temperature data, historical conditions of a GCM and the bias-corrected historical GCM. 95

Figure III-3. Cumulative distribution functions (CDFs) for historical (observed) precipitation data, historical conditions of a GCM and the bias-corrected historical GCM. 96

Figure III-4. Seasonal mean temperature and precipitation variation from the baseline period according to 11 climate models under RCP 2.6 and 8.5 emission scenarios. 97

Figure III-5. Magnitude of monthly water conditions (Only climate change, group 1). 98

Figure III-6. Magnitude and duration of annual extreme water conditions (Only climate change, group 2). 99

Figure III-7. Timing of annual extreme water conditions of all scenarios. Only land use/cover change (2045 LULC + historical climate), only climate change (2011 LULC + future climate), combined impacts (2045 LULC + future climate) (Group 3). 100

Figure III-8. Rate and frequency of water condition changes (Only climate change, group 4). 101

Figure III-9. Monthly low flows (Only climate change, group 5 - EFCs). 102

Figure III-10. Magnitude and duration of annual extreme water conditions (Only LULC, group 2.) 103

Figure III-11. Monthly low flows (Only LULC, group 5 - EFCs) 103

Figure III-12. Magnitude of monthly water conditions (Combined impacts – IHA group 1). 104

Figure III-13. Magnitude and duration of annual extreme water conditions (Combined impacts, IHA group 2). 105

Figure III-14. Rate and frequency of water condition changes (Combined impacts – IHA group 4). 106

Figure III-15. Monthly low flows (Group 5 (EFC) - Combined impacts – IHA group 5). 107

Figure III-16. LULC, climate, combined and synergic impacts on mean monthly percentage change of streamflow. 108

Figure III-17. Changes in magnitude and duration of annual extreme water conditions (Synergistic impact). 109

Figure III-18. LULC, climate, combined and synergistic impact on monthly low flows (Synergistic impact). 110

Figure III-19. 25-year flow duration curves (FDCs) under projected future climate and 2011 LULC data. 111

Figure III-20. 25-year flow duration curves (FDCs) under projected future climate and 2045 LULC data. 111

Chapter I - INTRODUCTION

Climate and land use/cover (LULC) change are both key drivers of significant changes in watershed hydrology. Understanding impacts of alterations in climate and land use on eco-hydrological processes in a watershed is crucial to sustaining water resources for multiple uses. The impacts of urbanization on watershed hydrology has been known since the late sixties (Leopold, 1968). Human activities play important roles in hydrology and water resources. Water resources are under stress due to increasing urbanizing landscapes and population. The effects of such changes on ecosystems and sustainable development have gained considerable concern (Vorosmarty et al. 2000; Yang et al. 2008; Li et al. 2009; Ma et al. 2009). Impacts on hydrological processes, such as, recharge to groundwater, runoff, and infiltration, are reflected in the balance of supply/demand of water sources, which in turn significantly influence the economy, environment, and ecosystems. LULC change alters the surface roughness and the pathway that impacts the timing of discharge which leads to shifts in the river flow (Chen et al., 2004). Thus, LULC change can result in alteration of flood frequency (Brath et al. 2006), baseflow (Wang et al., 2006) and average annual discharge (Costa et al., 2003).

Climate change has numerous direct and indirect impacts on the hydrological processes and water resources of basins (Schulze, 2000; Li et al., 2007a). Increasing concentrations of atmospheric greenhouse gasses, and consistent global warming are almost certainly responsible for important changes in global climatic patterns (IPCC, 2007; Xu et al., 2011). Alterations in the availability of water resources are expected to be among the most significant results of projected

climate changes (IPCC, 2007; Kingston and Taylor, 2010). Concerns about the hydrological system will have implications for discharge quantity and timing, as well as on ecosystem dynamics. Therefore, quantifying current and future freshwater availability is a critical aspect of adapting to changing and variable climate because the availability of water is linked to ecosystem health, LULC change and regional conflicts (Schuol et al., 2008).

The significance of flow regimes for river ecosystem has been well documented (Richter et al., 2003). According to Dudgeon et al. (2006), river biodiversity is associated with low flow events that restrict overall habitat availability and quality and with high flow events that affect the river channel shape and allow access to differently disconnected floodplain habitats. Many characteristics of the flow regime, especially seasonality, interannual variability and timing of specific flow events, influence life history patterns like recruiting and spawning (Dudgeon et al., 2006). However, there is an enormous gap in the literature that studies generally explored combined and/or individual impacts of LULC and climate change on hydrological regime of rivers. Further, the effects of these changes on ecologically relevant hydrologic characteristics should be assessed for understanding and efficient planning, management and sustainable development of watersheds.

In this study, the Soil and Water Assessment Tool (SWAT) was utilized to explore changes in flow regimes under the past, present, and future LULC and climate conditions in the upper Cahaba River Watershed, which eventually drains into the Mobile River. Indicators of Hydrologic Alterations software (IHA) with 38 key flow metrics was used to evaluate the alterations in ecologically relevant flow metrics.

Objectives

The overarching goal of this study is to analyze the impacts of LULC and climate change on hydrological responses, particularly on ecologically sensitive flows, in the Upper Cahaba River watershed. This is accomplished through two specific analyzes that are presented in two individual chapters (Chapter II and III). The main objectives are:

1. To explore how the hydrologic regime of the Upper Cahaba River watershed responds to land use/cover (LULC) and climate change, and to analyze the influences of different LULC datasets on watershed model outputs.
2. To examine how changes in flow in the Upper Cahaba River watershed will affect the ecologically relevant flow metrics.

General outline

This thesis focuses on the above mentioned two objectives. The thesis is divided into two main chapters: Chapter II and III. Each chapter is presented as a research paper with an abstract, introduction, literature review, methodology, results, conclusions and references. Chapter I serves as a general introduction covering the topics in Chapter II and III, and outlines the basis of the two studies.

Chapter II presents research on how changes in LULC affect watershed streamflow in the Upper Cahaba River watershed. It also presents sensitivity of watershed model to different LULC datasets. Chapter III presents impacts of LULC and climate change on ecologically relevant flow metrics under 46 experiments. Chapter IV is a general conclusion of the results that synthesizes the results presented in Chapter II and III.

REFERENCES

Brath, A., Montanari. A., Moretti, G. (2006). Assessing the effect on flood frequency of land use change via hydrological simulation (with uncertainty). J. Hydrol., 324(1–4):141–153.

Chen, J., Li, X. (2004). Simulation of hydrological response to land-cover changes. Chinese J. Appl. Ecol., 15(5), 833–836.

Costa, M.H., Botta, A., Cardille, J.A. (2003). Effects of large-scale changes in land cover on the discharge of the Tocantins River, Southeastern Amazonia. J. Hydrol., 283:206–217.

Dudgeon, D., Arthington, A. H., Gessner, M. O., Kawabata Z.-I., Knowler, D. J., Leveque, C., Naiman, R. J., Prieur-Richard, A.- H., Soto, D., Stiassny, M. L. J., and Sullivan, C. A. (2006). Freshwater biodiversity: importance, threats, status and conservation chal- lenges, Biological Reviews, 81:163–182.

IPCC, (2007). Climate Change 2007: Synthesis Report. Contribution of Working Groups I, II and III to the Fourth Assessment Report of the Intergovernmental Panel on Climate Change [Core Writing Team, Pachauri, R.K and Reisinger, A. (eds.)]. IPCC, Geneva, Switzerland, 104 pp.

Kingston, D.G., Taylor, R.G. (2010). Sources of uncertainty in climate change impacts on river discharge and groundwaterin a headwater catchment of the Upper Nile Basin, Uganda. Hydrol. Earth Syst. Sci. 14:1297–1308, http://dx.doi.org/10.5194/hess-14-1297-2010

Leopold, L. (1968). Hydrology for urban land planning—A guidebook on the hydrologic effects of urban land use, U.S. Geol. Surv. Circ., 554, 18 pp.

Li, L.J., Jiang, D.J., Li, J.Y. (2007a). A summary and perspective of forest vegetation impacts on water yield. J. Nat. Resour., 22(2): 211–224.

Li, Z., Liu, W., Zhang, X., Zheng, F. (2009). Impacts of land use change and climate variability on hydrology in an agricultural catchment on the Loess Plateau of China. J. Hydrol., 377:35–42.

Ma, X., Xu, J.C., Luo, Y., Aggarwal, S.P., Li, J.T. (2009). Response of hydrological processes to land-cover and climate changes in Kejie watershed, south-west China. Hydrol. Process,. 23:1179–1191.

Richter, B. D., Matthew, R., Harrison, D. L., and Wigington, R. (2003). Ecologically sustainable water management: managing river flows for ecological integrity. Ecol. Appl., 13:206–224.

Schulze R E. (2000). Hydrological responses to land use and climate change: a southern African perspective. AMBIO. 29(1):12–22.

Schuol, J., Abbaspour, K.C., Srinivasan, R., Yang, H. (2008). Estimation of freshwater availability in the West African sub-continent using the SWAT hydrologic model. J. Hydrol., 352(1–2): 30–49.

Vorosmarty C.J., Green, P., Salisbury, J., Lammers, R.B. (2000). Global water resources: vulnerability from climate change and population growth. Science, 289:284–288.

Wang, G.X., Zhang, Y., Liu, G.M., Chen, L. (2006). Impact of land-use change on hydrological processes in the Maying River basin, China. Science in China Series D: Earth Sciences, 49(10):1098–1110.

Xu, H., Taylor, R.G., Xu, Y., (2011). Quantifying uncertainty in the impacts of climate change on river discharge in sub- catchments of the Yangtze and Yellow River Basins, China. Hydrol. Earth Syst. Sci. 15, 333–344, http://dx.doi.org/ 10.5194/hess-15-333-2011.

Yang, T., Zhang, Q., Chen, D.Y., Tao, X., Xu, C.Y., Chen, X. (2008). A spatial assessment of hydrologic alteration caused by dam construction in the middle and lower Yellow River, China. Hydrol. Process. 22:3829–3843.

Chapter II - Modeling Impacts of Land Use/Cover Change in the upper Cahaba River Watershed

Abstract

This chapter explored the impacts of land use/cover (LULC) change on hydrological responses in the rapidly urbanizing upper Cahaba River basin in north-central Alabama. Daily streamflow was produced from 1988 to 2013 using historical climate and LULC data with the Soil and Water Assessment Tool (SWAT). Streamflow data from the periods of 1988-1993 and 2008-2013 were used for model calibration and validation, respectively. The SWAT-CUP calibration and uncertainty program was used for this purpose. The effects of different LULC maps were also analyzed by using "National Land Cover Data (NLCD)" and "Digitized Landsat 5 TM" LULC maps. According to the NLCD and digitized LULC data results, the major land cover type for the watershed was forest for the years 1992 and 2011. Both NLCD and digitized Landsat 5 TM data provided very similar land cover information for the Upper Cahaba River watershed. The study results exhibited that discrepancy between the NLCD and digitized Landsat 5 TM did not have a significant impact on the model outputs of annual streamflows. In addition to this, these datasets did not have strong impacts on monthly streamflows for the watershed. However, significant impacts of these datasets were observed in seasons.

Keywords: Land use/cover change, SWAT, SWAT-CUP, NLCD, ERDAS, Flow regime alterations

1. INTRODUCTION

Land use/cover (LULC) change is a key driver of significant changes in water resources and flow regimes around the world. It is a significant component affecting various processes regards to hydrology in river basins. LULC change alters the surface roughness and the pathway that impacts the timing of discharge which leads to shifts in the river flow (Chen et al., 2004). Thus, LULC change can result in alteration of flood frequency (Brath et al. 2006), base-flow (Wang et al., 2006) and average annual discharge (Costa et al., 2003). Understanding impacts of alterations in LULC on hydrological processes in a watershed is crucial to sustaining water resources for multiple uses. Therefore, comprehensive assessment at the watershed system scale is critical for understanding impacts of LULC changes on hydrological cycles for effective planning, management and sustainable development of watersheds. This study performs a local scale assessment using simulation and statistical modeling to investigate impacts of LULC changes and LULC datasets on streamflow within the Upper Cahaba River watershed for the period of 1988-2013.

The impacts of urbanization on watershed hydrology has been known since the late sixties (Leopold, 1968). Human activities play important roles in hydrology and water resources. Water resources are under stress due to increasing urbanizing landscapes and population. The effects of such changes on ecosystems and sustainable development have gained considerable concern (Vorosmarty et al. 2000; Yang et al. 2008; Li et al. 2009; Ma et al. 2009). Impacts on hydrological processes, such as, recharge of groundwater, runoff, and infiltration, are reflected in the balance of supply/demand of water sources, which in turn significantly influence the economy, environment, and ecosystems.

A number of studies have investigated the linkages between LULC and hydrological processes (Fohrer et al. 2001, Guo et. al. 2008, Jin et al. 2009, Mao et al. 2009, Mango et al. 2011, Li et al. 2010, Archer et al. 2010, Liu et al. 2014). Studies have shown that changes in vegetation cover (i.e. deforestation or afforestation) can affect water circulation and spatio-temporal variations in the distribution of water resources that changes in LULC cause to reduction or increase in water yield. They observed that forested/vegetated catchments have greater infiltration rates, thus lower runoff. For example, Mango et al. (2011) and Guo et. al. (2008) used the SWAT model to explore combined impacts of LULC and climate change on hydrological processes in the upper Mara River, Kenya and Poyan Lake basin, China, respectively. Their simulation results indicated that deforestation and urbanization effect seasonal variation in streamflow, reduce dry season flows and intensify peak flows. However, their study claimed that land use/cover changes have a smaller impact than climate change on streamflow. On contrary to this, Li et al. (2010) assessed that LULC can have a greater impact on the Taoer River (China) streamflow. The results of this study indicated climate change and LULC were responsible for approximately 45% and 55% increases in mean annual discharge, respectively. These kinds of changes have been observed in catchments ranging from less than 1 km^2 to over 1000 km^2 (Shi et al., 2000), and these studies differ in their study area, hydrological models, and climate and LULC data.

Chen and Arnold (2005) used the SWAT model with no calibration to assess the influence of two different LULC datasets (the National Land Cover Dataset (NLCD) and Global Land Cover Characterization (GLCC)) on streamflow. They found that the source of LULC information slightly affected streamflow simulations. The differences between two simulated annual streamflows were assessed approximately 7%. The NLCD produced higher streamflow predictions compared to GLCC and the NLCD produced annual simulations closer to annual measurements.

In a similar paper, El-Sadek and Irvem (2014) used three different types of LULC datasets (the Coordinated Information on the Environment (CORINE), Global Land Cover Characterization (GLCC), and Global Land Cover (GlobCover)) by using calibrated SWAT model to assess differences in simulating streamflow and sediment yield from the Seyhan River watershed, Turkey. They found that the sensitivity of the SWAT model to the LULC maps with different spatial resolutions was extremely low in the monthly discharge and sediment simulations.

As mentioned above, there are several studies in the literature focusing on the effects of LULC change and different LULC datasets on hydrology. However, questions still exist in hydrological responses to different LULC datasets. Hydrological modelers around the world generally use available datasets based on accessibility of datasets in their study areas, such as the NLCD or GLCC to run hydrologic models. These datasets have different spatial, spectral and temporal resolutions. For instance, in the United States, the National Land Cover Dataset (NLCD) is often used for national as well as regional scale studies. The NLCD 2011 is a 16-class land cover classification scheme similar to the Anderson land use/cover classification system (Anderson et al., 1976). On the contrary, GLCC uses 24 classes based on the United States Geological Survey (USGS) LULC scheme. Both of these regional-scale datasets are based on the unsupervised classification where the outcomes are based on the software analysis of a satellite image without the user providing sample classes.

Watershed modeling needs accurate LULC datasets to accurately parameterize the physical system. Therefore, LULC datasets are crucial inputs for assigning parameters related to the hydrology. SWAT model requires inputs of LULC data for delineating hydrologic response units (HRUs) and assessing sediment, agricultural chemicals yields, and water over watershed (Neitsch et al., 2011). SWAT uses the SCS (Soil Conservation Service) curve number method to estimate

surface runoff from each HRU. A curve number is assigned to each HRU on the basis of their hydrologic soil group and LULC. The LULC data should indicate the surface features properly. For instance, urbanization in a watershed increases the impervious surface area, which increases surface runoff and reduces infiltration. This decreased infiltration results in reduced groundwater recharge and eventually decreased baseflow contribution to streamflow. As a result of this, low flows are intrinsically related to infiltration process. Thus, it is very critical to understand the uncertainties in streamflow prediction associated with LULC data source.

In this chapter, the Soil and Water Assessment Tool (SWAT), a semi-physically based distributed hydrologic model, was utilized with two different LULC datasets (regional-scale NLCD and basin-scale digitized satellite imageries) to explore changes in flow regimes under the historical climate and LULC conditions in the Upper Cahaba River Watershed. To understand impacts of the LULC datasets, the satellite imageries of 1992 and 2011 years were digitized by using supervised classification methods. Representatives of specific classes were selected with knowledge on the study area. The main objectives of this chapter are:

1. To explore how the hydrologic regime of the upper Cahaba River responds to land use/cover (LULC) change, mainly urbanization.
2. To examine the influence of LULC datasets (i.e., NLCD and digitized Landsat 5 TM imageries) on watershed model outputs.

2. METHODOLOGY

2.1. Study Area

The Cahaba River is the third largest and the longest tributary of the Alabama River (HUC 031502), which drains into the Mobile Bay. It is also Alabama's longest free-flowing river with a watershed area of 4,727 km^2 including a portion of St. Clair, Jefferson, Shelby, Bibb, Tuscaloosa, Chilton, Perry, and Dallas Counties. The Cahaba River extends for 307 kilometers from its source, near Trussville in St. Clair County, south to the Alabama River. The drainage area lies completely within the state of Alabama. Its headwaters are placed within the Alabama Ridge and Valley physiographic zone and eventually flow southwest within the East Gulf Coastal Plain. This is the only point within the 48 contiguous states where the geological landscape changes suddenly from mountainous regions directly to a coastal plain. This accounts for the unique landscape and aesthetic beauty in the watershed, as well as its well-known biodiversity (ADEM Upper Cahaba River Watershed TMDL, 2013).

Elevations within the basin range from nearly 440 meter above sea level in Shelby County to 30 meter at the confluence with the Alabama River. According to the Nature Conservancy, the Cahaba River and its major tributaries support 69 rare and imperiled species, making it one of the most various aquatic ecosystems in the United States. Amongst them, the most well known is the Cahaba lily (*Hymenocallis coronaria*). Once abundant in the Southeast, Cahaba lilies have been wiped out from many areas due to flow fluctuations. Today, because they require swift and shallow water (Davenport, 1996), they are only abundant in certain regions.

This study particularly focuses on the upper portion of the Cahaba River basin (Figure II-1. - Hydrologic Unit Code: AL03150202), which, since the 1990's, is a rapidly developed urban area

(ADEM Upper Cahaba River Watershed TMDL, 2013). The upper side of Cahaba River watershed drains a large part of the city of Birmingham, AL. According to the United States Census Bureau (http://www.census.gov/), the city's population has decreased from 260,602 (1992) to 211,985 (2011). However, due to expansion of the Birmingham metropolitan area, percentage of urban area within the watershed have increased from 9.34% (1992 NLCD) to 35.68% (2011 NLCD) (Table II-1.). Based on the USGS EROS projected future land cover data (http://landcover-modeling.cr.usgs.gov/projects.php, accessed on 8/20/2015), it is also expected that the urban areas will increase by approximately 12.26% over the next 35 years. (Table II-1.). The portion of the drainage area in our study area extends upstream from St. Clair County and encompasses in Jefferson, Shelby, and Bibb counties. The catchment area for this study is 1416 km^2. The climate of the area (Table II-2 and Figure II-2 and.) is mainly humid with a mean annual rainfall of 142.9 cm. Mean rainfall is typically higher during the spring and winter and slightly lower during summer and fall. Mean monthly minimum and maximum temperatures for the upper Cahaba River basin range from approximately 10.34 °C to 23.44 °C, respectively (NOAA, 1/1/1950-12/31/2014). Lastly, there are 16 United States Geological Survey (USGS) streamflow gauges and 6 weather stations within the watershed boundaries. (Figure II-1.). Due to the availability of continuous flow data and distance from the model's outlet, the USGS Cahaba River near Acton AL (Station Number: 02423500) station was chosen as a discharge station for calibration and validation periods. This station has 76 years (since 10/01/1938) of continuous flow data.

2.2. Watershed Model

The latest version of the Soil and Water Assessment Tool (ArcSWAT 2012.10.18) that runs on ArcGIS was used for preparing the input data and processing the output files (http://swat.tamu.edu/software/arcswat/). The SWAT model is a semi-physically based,

continuous-time, hydrological, and agricultural management practice simulation model that assesses impacts of land management practices on water quantity and quality in complex watersheds (Arnold et al., 1998). The main components of ArcSWAT (ArcGIS-ArcView extension and graphical user input interface for SWAT) are weather, hydrology, sedimentation, soil properties, loads and flows of nutrients, crop growth, pesticides, land management, stream routing, and agricultural management. The ArcSWAT model utilizes geographic information system (GIS) and digital elevation model (DEM) to delineate watersheds and extract the stream network.

SWAT runs on daily step and is capable of continuous simulation over a long time period (Gassman et al., 2007). It is suitable to evaluate the long-term influence of land management practices on water, sediment and agricultural chemical yields in heterogeneous watersheds with varying land use, soils and management conditions (Arnold et al., 1998; Neitsch et al., 2011). SWAT is one of the most commonly applied watershed models worldwide and has been applied in a variety of studies around the world. Some example applications are: plant growth in the Yellow River , China (Luo et al., 2008); erosion in the Keleta watershed, Ethiopia (Tibebe et al. 2011); nutrient transport and transformation in Iowa watersheds (ranging size from 2,000 to 18,000 km^2), IA, USA (Jha et al., 2004a); pesticide transport in Orestimba Creek, CA, USA (Luo and Zhang, 2009); sediment transport in the Rock River, WI, USA (Kirsch et al., 2002); water management in the Cedar Creek Reservoir, TX, USA (Debele et al., 2008); snowmelt in the Upper Rhone River watershed, Switzerland (Rahman et al., 2013); land use change in the Zanjanrood basin, Northwest Iran (Ghaffari et al., 2010); climate change impact assessment in the upper Mississippi River Basin, MS, USA (Jha et al., 2006); and combined impacts of LULC and climate change in the Brahmaputra basin, South Asia (Pervez and Henebry 2015). It is also worth that there were 155

scientific articles about impacts of LULC change on hydrology and/or water quality in the SWAT Literature Database as of 5/12/2016. (https://www.card.iastate.edu/swat_articles/INDEX.ASPX).

In order to characterize spatial heterogeneity, ArcSWAT divides a basin into multiple sub-basin based on drainage areas of tributaries. Depending on the homogeneity and combination of land use, soils and slope characteristics, each sub-basins are split into multiple hydrological response units (HRUs). Each HRU is expected to be spatially uniform in climate, LULC, soil, and topography. The ArcSWAT model simulates surface runoff, infiltration, percolation, evapotranspiration (ET), and deep and shallow aquifer flow (Arnold et al. 1998). SWAT simulates the hydrological cycle based on the following water balance equation in the soil profile:

$$SW_t = SW_0 + \sum_{i=1}^{t}(R_{day} - Q_{surf} - E_a - w_{seep} - Q_{gw}) \quad (1)$$

where SW_t is the final soil water content (mm H_20), SW_0 is the initial soil water content (mm H_20), t is the time (days), R_{day} is the amount of precipitation on day i (mm H_20), Q_{surf} is the amount of surface runoff on day i (mm H_20), E_a is the amount of evapotranspiration on day i (mm H_20), w_{seep} is the amount of percolation and bypass flow exiting the soil profile bottom on day i (mm H_20), Q_{gw} is the amount of return flow on day i (mm H_20).

2.2.1. Model Setup and Input Data

The geographic information system interface ArcSWAT (ArcSWAT 2012.10.18) was used to parametrize the model for the upper Cahaba River watershed. The watershed was delineated from a 10-meter DEM (available at https://gdg.sc.egov.usda.gov – downloaded on 9/27/2015). The basin was subdivided into 45 sub-basins with a threshold area of 600 ha. The outlet near to USGS discharge station was selected to be the final outlet of the upper Cahaba River watershed (Figure

II-1.). To further characterize the sub-basins for dominant soil types and land use, the multiple Hydrological Response Unit (HRU) option was performed. The detailed model setup process and input data (Table II-3.) are described in the following sections.

2.2.1.1. Weather Data

SWAT requires daily precipitation (*pcp*), maximum and minimum air temperature (T_{min} and T_{max}), solar radiation (*slr*), wind speed (*wnd*), and relative humidity (*hmd*) as meteorological inputs. The daily precipitation and maximum/minimum air temperature data were obtained from the highest-quality spatial climate gridded dataset (4 km cell size) of PRISM (PRISM Climate Group, Oregon State University, http://prism.oregonstate.edu, accessed on 8/20/2015). The other data; solar radiation, wind speed, and relative humidity data were obtained from the National Centers for Environmental Prediction (NCEP) Climate Forecast System Reanalysis (CFSR) database (http://rda.ucar.edu/ accessed on 8/21/2015).

2.2.1.2. Observed streamflow

The daily measured discharge data for the period 1983-2013 was obtained from the United States Geological Survey National Water Information System website (USGS Station Name: Cahaba River near Acton AL, Station Number: 02423500, http://waterdata.usgs.gov/nwis accessed on 8/21/2015). This station is located in Jefferson County, AL (Figure II-1. - Drainage area: 595.65 km^2; Latitude 33°21'48" Longitude 86°48'47" NAD27). Daily discharge data in that station have been collected for over 78 years (since 1938) and are operated in cooperation with the Alabama Department of Environmental Management (ADEM). Daily observed streamflow averages 10.23 m^3/sec, although it can vary from 0.07 m^3/sec to 385.11 m^3/sec, during late summer flow conditions and at peak flow conditions during late fall and winter, respectively. The daily

discharges were used for model calibration (1988-1993) and validation (2008-2013) in the SWAT Calibration and Uncertainty Program (SWAT-CUP).

2.2.1.3. Digital Elevation Model (DEM)

The model utilized a 10-meter digital elevation model (DEM), which was downloaded from the USDA Geospatial Data Gateway (available at https://gdg.sc.egov.usda.gov – downloaded on 6/17/2015). The DEM (Figure II-1.) was used to delineate the surface drainage of the watershed, along with 45 subwatersheds.

2.2.1.4. LULC Data

LULC changes impact various components of the hydrologic cycle, such as surface runoff, erosion, recharge, and evapotranspiration either directly or indirectly. To better understand the impacts of change in land use/cover on hydrology in the upper Cahaba River watershed (1416 km^2), two different LULC data (NLCD and processed Landsat 5 TM scenes) were used. The National Land Cover Database (NLCD) is a publicly available dataset at 30-meter resolution (available at http://www.mrlc.gov/ - accessed on 6/12/2015). The second dataset was digitized from Landsat 5 TM scenes (details are provided below *LULC Data Generation from Satellite Images* section) for the years of 1992 and 2011. The two LULC dataset were compared to observe the differences in LULC, especially in urbanized areas. Then, each of these LULC maps were used separately as a land use data in baseline period (1988-2013). Since these historical maps had different LULC classifications, reclassification process were applied to all LULC maps so that the original categories were classified into five classes to make them consistent with SWAT's own database. The classes are water (1), urban (2), forest (3), agriculture (4), and wetland (5).

2.2.1.5. Soil Data

The model incorporated soil types obtained from SSURGO database, certified database by United States Department of Agriculture – Natural Resources Conservation Service Soils (USDA-NRCS, available at https://gdg.sc.egov.usda.gov - accessed on 7/17/2015), was used as the soil data source (Table II-3.). The dominant soil texture in the upper Cahaba River watershed are sand (67.2%), clay (17.5%) and silt (15.3%) (Table II-2.).

2.2.1.6. Sub-basins and Hydrological Response Units (HRUs)

The model with 45 sub-basins was obtained at the end of the process. The sub-basins were then divided into hydrologic response units (HRUs), which are unique combinations of soil and land cover types. As a result, the watershed was discretized into 557 and 540 HRUs for the 1992 and 2011 NLCD LULC datasets, respectively. On the contrary, 713 and 614 HRUs were acquired for the 1992 and 2011 digitized satellite imageries, respectively. These HRUs were defined using the threshold values of 8%, 8% and 10% for the dominant land use, soil and slope of individual subbasin areas, respectively. The characteristics of the upper Cahaba River watershed's SWAT model are summarized in Table II-2.

2.3. Model Calibration, Validation and Model Performance Evaluation

Many hydrological models contain parameters that cannot be determined directly from field measurements. SWAT has a large number of parameters. Therefore, identification of the most sensitive parameters can increase the calibration efficiency. In this study, the sensitivity analysis, calibration, and validation were conducted using the SWAT Calibration and Uncertainty Program (Abbaspour et al., 2007 - SWAT-CUP) using Sequential Uncertainty Fitting (SUFI-2) algorithm and involved a total of 16 SWAT parameters (Table II-4.). SUFI-2 is the calibration algorithm

developed by Abbaspour et. al, 2007. In SUFI-2, parameter uncertainty accounts for all sources of uncertainties such as uncertainty in driving conceptual model, parameters, variables (e.g. precipitation), and measured data (e.g. observed flow data) (Abbaspour et. al, 2007). The model parameters were selected in the calibration procedure based on a literature review (Douglas-Mankin et al., 2010; Tuppad et al., 2011; Abbaspour et al., 2015), the preliminary sensitivity analysis results (Luo et al., 2008), study area conditions, and their functions on hydrologic processes.

Statistical measures such as the coefficient of determination (R^2), Nash-Sutcliffe Efficiency (*NSE*), percent bias (*PBIAS*), and ratio of the root mean square error to the standard deviation of measured data (*RSR*) are commonly used to evaluate model performance (Moriasi et al., 2007; Eckhardt and Arnold 2001; Krause et al., 2005). Our main purpose during the calibration process was to bracket most of measured data within the 95PPU band.

Coefficient of determination (R^2) indicates the strength of the linear relationship between the measured and simulated values (Santhi et al., 2001). R^2 ranges from 0 to 1, a score above 0.5 is considered acceptable (Santhi et al., 2001; Van Liew et al., 2003; Green et al., 2006). The equation for R^2 is:

$$R^2 = \frac{[\sum_i (Q_{m,i} - \bar{Q}_m)(Q_{s,i} - \bar{Q}_s)]^2}{\sum_i (Q_{m,i} - \bar{Q}_m)^2 \sum_i (Q_{s,i} - \bar{Q}_s)^2} \quad (2)$$

where Q is a variable of interest (e.g., discharge), $\bar{Q}$ is the average of variable Q over a specific period, m and s indexes represent the measured and simulated data, respectively, i is the i^{th} measured or simulated data.

Nash-Sutcliffe Efficiency (*NSE*) assesses how well the plot of measured versus simulated value fits the 1:1 line and measures the predictive power of the hydrological model (Nash and Sutcliffe 1970). *NSE* ranges from -∞ to 1, a score above 0.5 is considered satisfactory at monthly time step (Moriasi et al., 2007).

$$NSE = 1 - \frac{\sum_i (Q_m - Q_s)_i^2}{\sum_i (Q_{m,i} - \bar{Q}_m)^2} \quad (3)$$

Percent bias (*PBIAS*) evaluates the percent deviation between measured and simulated data. Positive values indicate that simulated values are lower than observed (underestimation), and negative values indicate that simulated values are higher than measured data (overestimation) (Grupta et al., 1999). The optimum value is zero, where low magnitude values indicate better simulations. A score of ±25 % is considered satisfactory at monthly time step (Moriasi et al., 2007).

$$PBIAS = 100 * \frac{\sum_{i=1}^{n} (Q_m - Q_s)_i}{\sum_{i=1}^{n} Q_{m,i}} \quad (4)$$

The ratio of the root mean square error to the standard deviation of measured data (*RSR*) is a commonly used error index. It is calculated as a ratio of the *RMSE* and standard deviation of the measured data. In other words, it combines a normalization factor with the error index so that the resulting *RSR* values can apply to various constituents. According to Moriasi et al., 2007; the better model performance is related to association of the lower the *RSR* and the lower the *RMSE*.

$$RSR = \frac{\sqrt{\sum_{i=1}^{n} (Q_m - Q_s)_i^2}}{\sqrt{\sum_{i=1}^{n} (Q_{m,i} - \bar{Q}_m)^2}} \quad (5)$$

Modified Nash-Sutcliffe efficiency factor (*MNS*) is a modified form of *NSE*. *NSE* is the most widely used performance indicator for hydrological model's flow simulation, however, it is not sensitive to low flows (Krause et al., 2005). *NSE* ignores lower values because of the use of square of difference between observed and simulated discharge (Legates and McCabe, 1999). In this study, the objective was to estimate changes in low, median and high flows. To overcome this, *MNS* objective function was used to evaluate low, median and high flow conditions (Krause et al., 2005; Oudin et al., 2006). For instance, if p=0.75, the overestimation of a peak is reduced significantly (p values between 0.5 and 2.0 was tested and then value of 0.75 was selected.).

$$MNS = 1 - \frac{\sum_i |Q_m - Q_s|_i^p}{\sum_i |Q_{m,i} - \bar{Q}_m|_i^p} \quad (6)$$

In general, according to the qualitative evaluations suggested by Moriasi et al., 2007, model simulation can be judged as satisfactory for monthly streamflow if *NSE* > 0.50, *RSR* ≤ 0.70, and *PBIAS* ±25 % for streamflow. Other studies have also suggested that an R^2 > 0.50 is considered acceptable (Van Liew et al., 2003; Green et al., 2006).

In order to calibrate and validate the model, daily measured discharge records from the USGS station for the period 1983-2013 (Station Number: 02423500) were split into two segments. The first 6 years (1/1/1988-12/31/1993 with 3 years warm-up (1/1/985-12/31/1987) records were used to calibrate and the second 6 years (1/1/2008-12/31/2013 with 3 years warm-up (1/1/2005-12/31/2007) were used to validate.

2.4. LULC Data Generation from Satellite Images

Because of the importance of LULC on hydrologic cycle, in addition to NLCD LULC dataset with 30-meter resolution, we utilized computer assisted land cover classification using digital remote

sensing technologies to examine the changes in land use/cover (LULC) in the Upper Cahaba River watershed by using Landsat 5 Thematic Mapper (TM) data (30-meter spatial resolution) for the years of 1992 and 2011. The images were processed at the USGS level.

The results indicated that during the last two decades, urban areas have increased by 20% (283 km^2) while agriculture and forest have been decreased by 8% (113 km^2) and 17% (240 km^2), respectively (Table II-1.). The preparation of data is described in the following sections.

2.4.1. Software and Data Source:

To identify urbanization increases in the study area, the latest version of ERDAS IMAGINE 2015 software was used. Two remotely sensed images (Landsat 5 TM Data) were selected for this study. The Landsat 5 TM images for 1992 and 2011 years, with a 30-meter resolution, covering the defined study area were obtained from USGS Earth Explorer website (http://earthexplorer.usgs.gov/ - Path: 20, Row: 37 - downloaded on October 29, 2015). The dates of both images were selected to be as closely as possible in the same vegetation season. Both of the images (1992 and 2011) were clear and nearly free of clouds (less than 10% cloud cover). The False Color composite of the Landsat TM scenes was used for the accuracy assessments. Furthermore, an aerial imagery of 2011 year, which is obtained from the National Agriculture Imagery Program (NAIP) (http://www.usda.gov/), was also used as a second reference data for the accuracy assessment of 2011 map.

2.4.2. Methods

Classification is the method of classifying dataset pixels into a number of classes basis of their spectral values (Singh, 1989). In this study, the common pixel-based classification method supervised classification (Jensen, 2005) was applied to evaluate changes in LULC for two periods,

1992 and 2011. Two maps were generated from the respective Landsat images. Then, accuracy assessment was performed for the evaluation of reliability of the generated LULC maps.

2.4.2.1. Layer Stack

The Landsat 5 TM Images obtained from USGS Earth Explorer includes seven bands as TIFF files. These seven layers needed to be combined to work with one image. ERDAS layer stack feature was used to combine the seven layers. As a result of this, one output file was created to use for the next steps.

2.4.2.2. Image Subset

The obtained data from USGS Earth Explorer are typically larger than the specific study area. Therefore, users usually have to create a subset of the image to be quick and focused on the determined study area. For this purpose, subset feature was used for the study area boundaries (Figure II-3.) to focus on the portion of the scene.

2.4.2.3. Supervised Classification

This study performed supervised classification in ERDAS IMAGINE 2015 software to identify LULC changes in the upper Cahaba River watershed using satellite images. Supervised classification methodology has been applied using maximum likelihood algorithm to obtain more reliable classification dataset. Because overall classification results in the supervised classification allow the user to pinpoint where differences need to be made and the statistics available for the study area.

Unlike unsupervised classification, which is used for the NLCD, supervised classification is based on the user idea that user needs to select sample pixels to represent specific classes. Supervised classification requires interact with a user who has knowledge about the area. In this

study, the created subset image is used to get for five classes (1) Water, (2) Urban, (3) Forest, (4) Agriculture, (5) Wetland. This step was performed by launching the signature editor and then drawing polygons overtop of relevant features within the specified study area. The new classes were created from the drawn polygons with "signature editor". For instance, pixels were collected for urban areas from many different parts of the image, not just from one or two area on the same side of the image. By doing this crucial step, the accuracy of representation of all features were increased. After all the study area data was gathered, the new classes were created within the signature editor. Then the names and colors were assigned. To overcome limitation of choosing vegetative areas in some regions, it is worth to note that the Normalized Difference Vegetation Index (NDVI) was also used to yield the image with pixel values ranging from -1 to +1. With the NDVI, the vegetative areas were analyzed successfully. For example, where Red reflectance exceeded NIR, the negative values occurred on the map. Therefore, the value range -1 to 0 in NDVI simply indicated no vegetative cover.

2.4.2.4. Classified Accuracy Assessment

After supervised classification, classified accuracy assessment was applied to data to evaluate the accuracy of the study. The False Color Composite of the Landsat TM scenes (1992 and 2011) were used for the accuracy assessment of both 1992 and 2011 data. Statistics for the study area were analyzed to detect the convenience and precision of data. An overall accuracy of 92 and 87% were acquired for the 1992 and 2011 LULC datasets, respectively.

3. RESULTS AND DISCUSSION

The results of this study provide information about impacts of changes in LULC and different LULC datasets on river streamflow in the upper Cahaba River watershed. Use of the calibrated model to explore the potential effects of continued LULC change show that any conversion of forest to urban will impact streamflow, especially in spring and fall seasons. The simulation results from the SWAT model with (1) NLCD dataset and (2) digitized Landsat 5 Images LULC datasets are described in detail in the following sections.

3.1. LULC change in the upper Cahaba River watershed

The land cover datasets within the five Anderson classes (water, urban, forest, agriculture, and wetland) were analyzed. It is observed that the LULC distribution in the two datasets was mostly represented by 3 major LULC classes (urban, forest, agriculture). Our results indicated that the watershed was dominated by forest for all data sets in 1992 and 2011 (1992: NLCD (78.4%) vs. Digitized (71.34%); 2011: NLCD (50.32%) vs. Digitized (55.01%), Table II-1.). Another difference among the land cover datasets was the amount of urban areas. The digitized Landsat images indicated that urban fraction in the watershed have increased from 10.08% (1992) to 30.97% (2011). On the other hand, the NLCD data showed that it has increased from 9.34% (1992) to 35.68% (2011) (Table II-1.). There were no significant differences in percentages of urban areas. However, it was realized that the distribution of urban areas was different in both LULC datasets that NLCD was not sensitive to the allocation of urban areas (Figure II-3.). The most significant differences between the two LULC datasets were observed in the forest, agriculture, and wetland areas. For example, the NLCD maps showed 7.06 % more forest areas and 5.38% fewer agriculture areas in 1992 (Table II-1.).

3.2. Model calibration and performance using NLCD versus Digitized Landsat 5 TM LULC datasets

Daily values of simulated streamflow were compared with observations to calibrate and validate the SWAT model. The sensitivity analysis was performed at daily time step. First, 24 hydrological parameters were tested for identifying the most sensitive parameters for the simulation of streamflow. After the first iteration of sensitivity analysis, the sensitivity analysis has pointed out the following 16 most sensitive parameters (mainly associated with surface, soil and groundwater parameters) for calibration of model: CANMX.hru, SOL_K.sol, CN2.mgt, GW_DELAY.gw, RCHRG_DP.gw, GWHT.gw, REVAPMN.gw, GWQMN.gw, GW_REVAP.gw, SOL_AWC.sol, ALPHA_BNK.rte, SOL_BD.sol, ALPHA_BF.gw, SURLAG.bsn, ESCO.hru, EPCO.hru. The parameters are presented in Table II-4 and 5, which shows the selected parameters with their calibration ranges, default values, final optimized values, sensitivity ranks, and p-values.

CN2 (initial curve number for moisture condition II) was found to be the most sensitive parameter for both NLCD and digitized Landsat 5 TM LULC datasets for the upper Cahaba River watershed at daily time step. This shows there is high runoff potential in the watershed. The maximum canopy storage (CANMX) was ranked 2nd for the NLCD data, but lowered to 4th for the digitized Landsat LULC data. Saturated hydraulic conductivity (SOL_K) and ground water delay (GW_DELAY) were found to be highly sensitive for both LULC datasets. Ranking of the sensitivity of the other parameters was found to be different for different LULC datasets (Table II-5.).

Figure II-4 and 5 present the time-series comparison of simulated and measured monthly streamflows for the upper Cahaba River watershed, AL, at Cahaba River near Acton (USGS Station Number: 02423500) over the 6 years calibration (1/1/1988-12/31/1993) and validation

(1/1/2008-12/312013) periods for both datasets. The predicted flows closely followed the measured flows with less underprediction of peak flow months, especially when the NLCD LULC dataset was used.

Table II-6. indicates the values of the statistical measures for the model performance for each LULC dataset at daily time scale. During the calibration period, the NSE values were greater than 0.70, which was within the good range (Moriasi et al., 2007). The values of R^2 between daily observed and measured streamflows were greater than 0.71. During the validation period, the NSE and R^2 were greater than 0.65 and 0.68, respectively. The average magnitude of simulated streamflow values was within very good range (Moriasi et al., 2007) with values smaller than 10% for both calibration and validation periods (PBIAS(%)$<\pm 10$) . In general, there was no significant difference between these two datasets and both NLCD and digitized LULC maps results were rated as good according to Moriasi et al. (2007).

It was expected that the digitized LULC maps for historical and current periods would be superior input data for the SWAT model for understanding impacts of LULC changes on watershed hydrology. The reason of this was that the classification processes were performed for a specific study area, not on big scale like NLCD, and all advantages of classification analyses, which were summarized in "*section 2.4. LULC Data Generation from Satellite Images*" part, were applied with information on the study area. The model accuracy was not significantly impacted by using different LULC datasets for simulating the streamflow from the upper Cahaba River watershed. However, the evaluation statistics (R^2, *NSE*, *PBIAS*, *RSR*) suggest that NLCD simulated the daily flow a little bit more accurately. It is also worth to note that the model missed only one peak during the six years calibration period, i.e. in July 1989.

Thus, the SWAT model accurately tracked the observed streamflows for the time period. These results recommend that the calibrated SWAT model using NLCD and digitized Landsat 5 TM images, and PRISM precipitation and temperature gridded dataset can represent the streamflow in the upper Cahaba River watershed, and validate that the calibrated model with optimized parameters can be applied to determine the responses of watershed's streamflow to LULC and climate changes.

3.3. Impacts of LULC Change on Hydrologic Responses

As mentioned in the introduction part, it has been widely reported that LULC changes, such as urbanization/deforestation, impact water quantity of water resources. The relationship of land use/cover (LULC) distributions between two datasets is a required procedure to analyze the impact of LULC datasets on the SWAT model outputs. The calibrated model was used to simulate hydrologic process of different LULC data with the historical/current climate (1988-2013).

In this study, model efficiency is evaluated through use of time-series of flow and flow duration curves (FDCs). Note that the discharge time series was actually implemented on a daily time scale and aggregated into monthly discharge. To describe the impacts of LULC changes on streamflow, we compared both 1992 and 2011 LULC maps. The distribution of LULC in 1992 and 2011 is given in Table II-1. Both LULC datasets showed urban cover has increased from 1992 to 2011. On the contrary, total forest areas has decreased during this period. For each year and LULC datasets, we assessed changes on mean monthly (Figure II-6.), annual and seasonal flows (Table II-7). It is observed that the changes on land-cover for both NLCD and digitized LULC maps did not have a strong impact on the SWAT outputs of water quantity. The differences between two simulated annual mean streamflows were 7.60 and 7.89 m^3/s with 1992 NLCD and

digitized LULC maps, respectively. The simulated mean annual streamflow with 2011 NLCD and digitized LULC were 8.05 and 8.31 m^3/s, respectively (Table II-7.)

Figure II-6. shows the time-series of mean monthly streamflows for each dataset. The changes in mean monthly flows due to LULC dataset show little variation. The LULC dataset did not have an important effect on mean monthly streamflow, however, the only slightly differences were observed in February and September. Table II-7. shows the changes in seasonal streamflows. With the NLCD dataset, a significant increasing trend was observed only for spring (11%), decreasing trend was observed in summer (-6%). As same as NLCD datasets, an important increasing trend was observed for spring (7%), decreasing trend was observed in fall (-5%) for digitized LULC datasets. Flow duration curves of daily streamflow simulations acquired with calibrated and validated for each LULC maps (Figure II-8). There were no significant differences in FDCs of different LULC datasets. In other words, FDCs with calibrated parameters of both NLCD and digitized Landsat 5 TM land-cover maps look similar to each other (Figure II-8.).

4. SUMMARY AND CONCLUSION

This chapter assessed the effects of LULC changes and different LULC datasets on water quantity using the watershed scale SWAT model in the Upper Cahaba River watershed. For this purpose, SWAT model was successfully calibrated and validated with both LULC datasets with "very good" for several of the model performance indicators. SWAT-CUP program was used for calibration and validation by using SUFI-2 algorithms. The results suggest that both LULC datasets simulated the daily flow accurately according to the R^2, *NSE*, *RSR* and *PBIAS* statistics. The model with NLCD dataset resulted in a slightly better model performance than the model with

digitized Landsat 5 TM dataset. However, there were insignificant differences observed in the model evaluation statistics (±3%). Thus, both of the calibrated models were able to simulate both high and low flows with sufficient accuracy. The calibrated model can be used for further analysis including land use and climate changes and their effects on streamflow of the watershed.

As a LULC data for the years 1992 and 2011, we used two different datasets (NLCD and digitized Landsat 5 TM images). According to the NLCD and digitized LULC data results, the major land cover type for the watershed was forest for the years 1992 and 2011. Our study investigated that both NLCD and digitized Landsat 5 TM data provided very similar land cover information for the upper Cahaba River watershed. However, the NLCD LULC data showed more rapid urban growth than did the digitized Landsat 5 TM scenes. Hence, the study results exhibited that discrepancy between the NLCD and digitized Landsat 5 TM scenes did not have a significant impact on the model outputs of annual streamflows. Furthermore, these datasets did not have strong impacts on monthly streamflows for the watershed. However, important impacts of these datasets were observed in seasons, especially in spring and winter. Our study analysis concluded that any additional forest conversion to urban may have large impacts on spring and fall streamflows in the Upper Cahaba River.

5. REFERENCES

Abbaspour, K.C., Rouholahnejad, E., Vaghefi, S., Srinivasan, R., Yang, H., Kløve, B. (2015). A Continental-Scale Hydrology and Water Quality Model for Europe: Calibration and uncertainty of a high-resolution large-scale SWAT model. Environmental Modelling & Software, 524: 48–65. http://doi.org/10.1016/j.jhydrol.2015.03.027.

Abbaspour, K.C., Vejdani, M., Haghighat, S. (2007). SWAT-CUP calibration and uncertainty programs for SWAT. In: Oxley, L., Kulasiri, D. (Eds.), Proc.Intl. Congress on Modelling and Simulation (MODSIM'07). Modelling and Simulation Society of Australia and New Zealand, Melbourne, Australia, pp. 1603-1609.

ADEM Upper Cahaba River Watershed TMDL. (2013). Available at: http://adem.alabama.gov/programs/water/wquality/tmdls/FinalCahabaRiverSiltationTMDL.pdf

Anderson, J. R., Hardy, E. E., Roach, J. T., Witmer, R. E. (1976). A land use and land cover classification system for use with remote sensor data. U.S. Geological Survey, Reston, VA, U.S. Geological Survey Professional Paper 964, 28 p.

Archer, D.R., Climent-Soler, D., Holman, I.P. (2010). Changes in discharge rise and fall rates applied to impact assessment of catchment land use. Hydrol. Res., 41:13–26.

Arnold, J.G., Srinivasan, R., Muttiah, R.S., Williams, J.R. (1998). Large area hydrologic modeling and assessment: Part I. Model development. JAWRA, 34(1):73–89.

Brath A., Montanari A., Moretti G. (2006). Assessing the effect on flood frequency of land use change via hydrological simulation (with uncertainty). Journal of Hydrology, 324(1–4):141–153.

Chen, J., Li, X. (2004). Simulation of hydrological response to land-cover changes. Chin. J. Appl. Ecol., 15:833–836.

Chen, P., Arnold, J. G. (2005). Impact of Two Land-Cover Data Sets on Stream Flow and Total Nitrogen Simulations Using a Spatially Distributed. Global Priorities in Land Remote Sensing.

Costa, M.H., Botta, A., Cardille, J.A. (2003). Effects of large-scale changes in land cover on the discharge of the Tocantins River, Southeastern Amazonia. J. Hydrol., 283:206–217.

Davenport, L.J. (1996). The cahaba lily: its distribution and status in Alabama. Journal of the Alabama Academy of Science, 67:222–233.

Debele, B., R. Srinivasan, and J. Y. Parlange. (2008). Coupling upland watershed and downstream waterbody hydrodynamic and water quality models (SWAT and CE-QUAL-W2) for better water resources management in complex river basins. Environ. Modeling Assess. 13(1): 135-153.

Douglas-Mankin, K. R., Srinivasan R., and Arnold J. G. (2010). Soil and Water Assessment Tool (SWAT) model: Current development and applications. Trans. ASABE 53(5): 1423-1431.

Dudgeon, D., Arthington, A. H., Gessner, M. O., Kawabata Z.-I., Knowler, D. J., L´ evˆ eque, C., Naiman, R. J., Prieur-Richard, A.- H., Soto, D., Stiassny, M. L. J., and Sullivan, C. A.: Freshwater biodiversity: importance, threats, status and conservation chal- lenges, Biol. Rev., 81, 163–182, 2006.

Eckhardt, K., Arnold, J.G. (2001) Automatic calibration of a distributed catchment model. J. Hydrol., 251(1–2):103–109. doi:10.1016/ S0022-1694(01)00429-2.

El-Sadek, A., Irvem, A. (2014). Evaluating the impact of land use uncertainty on the simulated streamflow and sediment yield of the Seyhan River basin using the SWAT model. Turkish Journal of Agriculture and Forestry, 38(4):515–530.

Fohrer, N., Haverkamp, S., Eckhardt, K., Frede, H.G. (2001). Hydrologic response to land use changes on the catchment scale. Phys. Chem. Earth Part B Hydrol. Oceans Atmos., 26:577–582.

Gassman, P.W., Reyes, M.R., Green, C.H., Arnold, J.G. (2007). The soil and water assessment tool: historical development applications, and future research directions. Trans ASABE 50(4):1211–1250.

Ghaffari, G., Keesstra, S., Ghodousi, J., Ahmadi, H. (2010). SWAT-simulated hydrological impact of land-use change in the Zan- janrood basin, Northwest Iran. Hydrol. Process. 24(7):892–903.

Green, C.H., Tomer, M.D., Di Luzio, M., Arnold, J.G. (2006) Hydrologic evaluation of the soil and water assessment tool for a large tile- drained watershed. Trans ASABE 49(2):413–422.

Guo, H., Hu, Q., Jiang, T. (2008). Annual and seasonal streamflow responses to climate and land cover changes in the Poyang lake basin, China. Journal of Hydrology 355(1-4): 106-122.

Gupta, H.V., Sorooshian, S., Yapo, P.O. (1999). Status of automatic calibration for hydrologic models: Comparison with multilevel expert calibration. J. Hydrologic Eng. 4(2): 135-143.

IPCC., 2007. Summary for policymakers. In: Solomon, S., Qin, D., Manning, M., Chen, Z., Marquis, M., Averyt, K.B., Ignor, M.T., Miller, H.L. (Eds.), Contribution of Working Group I to the Fourth Assessment Report of the Intergovernmental Panel on Climate Change, 2007. Cambridge University Press, Cambridge, United Kingdom and New York, NY, USA.

Jensen, J. R. (2005). Introductory digital image processing: a remote sensing perspective (3rd ed.). Upper Saddle River, NJ: Prentice Hall.

Jha, M., Arnold, J.G., Gassman, P.W., Giorgi, F., Gu, R.R. (2006). Climate change sensitivity assessment on Upper Mississippi River Basin streamflows using SWAT. J. Am. Water Resour. Assoc. 42(4):997–1015.

Jha, M., Gassman, P.W., Secchi, S.S., Gu, R., Arnold, J.G. (2004). Effect of watershed subdivision on SWAT flow, sediment, and nutrient predictions J. Am. Water Resour. Assoc., 40 (3):811–825.

Jin, C., Zhang, B., Song, K., Wang, Z., Yang, G. (2009). RS-based analysis on the effects of land use/cover change on regional evapotranspiration: A case study in Qian'an County, Jilin Province. Arid Zone Res., 26:734–743.

Kirsch, K., Kirsch, A., Arnold, J., (2002). Predicting sediment and phosphorus loads in the Rock River basin using SWAT. Forest 971, 10.

Krause, P., Boyle, D.P., Base, F. (2005) Comparison of different efficiency criteria for hydrological model assessment. Adv Geosci 5:89–97. doi:10.5194/adgeo-5-89-2005

Legates, D.R., McCabe, G.J. (1999) Evaluating the use of ''goodness-of- fit'' measures in hydrologic and hydroclimatic model validation. Water Resour Res 35(1):233–241. doi:10.1029/1998wr900018

Leopold, L. (1968), Hydrology for urban land planning—A guidebook on the hydrologic effects of urban land use, U.S. Geol. Surv. Circ.,554, 18 pp.

Li, L.J., Jiang, D.J., Li, J.Y. (2007a). A summary and perspective of forest vegetation impacts on water yield. J Nat Resour, 22(2): 211–224.

Li, L., Li, B., Liang, L., Li, J., Liu, Y. (2010). Effect of climate change and land use on stream flow in the upper and middle reaches of the Taoer River, northeastern China. Forestry Studies in China, 12(3), 107–115.

Li, Z., Liu, W.Z., Zhang, X.C., Zheng, F.L. (2009) Impacts of land use change and climate variability on hydrology in an agricultural catchment on the Loess Plateau of China. J Hydrol 377:35–42.

Liu, Y., Zhang, X., Xia, D., You, J., Rong, Y., Bakir, M. (2013). Impacts of land-use and climate changes on hydrologic processes in the Qingyi River watershed, China. J. Hydrol. Eng., 18:1495–1512.

Luo, Y., Gerten, D., LE Maire, G., Parton, W.J., Weng, E., Zhou, X., Keough, C., Beier, C., Ciais, P., Cramer, W., Dukes, J.S., Emmett, B., Hanson P.J., Knapp, A., Linder, S. , Nepstad, D., Rustad, L. (2008). Modeled interactive effects of precipitation, temperature, and [CO2] on ecosystem carbon and water dynamics in different climatic zones. Global Change Biology, 14, 1986–1999.

Luo, Y., He, C., Sophocleous, M., Yin, Z., Hongrui, R., Ouyang, Z. (2008) Assessment of crop growth and soil water modules in SWAT2000 using extensive field experiment data in an irrigation district of the Yellow River Basin. J. Hydrol., 352(1):139–156.

Luo, Y., Zhang, X., Liu, X., Ficklin, D., Zhang, M. (2008). Dynamicmodeling of organophosphate pesti- cide load in surfacewater in the northern San Joaquin Valleywatershed of California. Environ. Pollut., 156:1171–81.

Ma, X., Xu, J.C., Luo, Y., Aggarwal, S.P., Li, J.T. (2009). Response of hydrological processes to land-cover and climate changes in Kejie watershed, south-west China. Hydrol. Process. 23:1179–1191.

Mango, L. M., Melesse, A. M., McClain, M. E., Gann, D., and Setegn, S. G., (2011). Land Use and Climate Change Impacts on the Hydrology of the Upper Mara River Basin, Kenya: Results of a Modeling Study to Support Better Resource Management. Hydrology and Earth System Sciences 15(7): 2245–58. doi:10.5194/hess-15-2245-2011.

Mao, D.Z., Cherkauer, K.A. (2009). Impacts of land-use change on hydrologic responses in the Great Lakes region. J. Hydrol., 374, 71–82.

Moriasi, D.N., Arnold, J.G., Van Liew, M.W., Bingner, R.L., Harmel, R.D., Veith, T.L. (2007). Model evaluation guidelines for systematic quantification of accuracy in watershed simulations. Trans. ASABE, 50(3):885–900.

Nash, J.E., Sutcliffe, J.V. (1970). River flow forecasting through conceptual models part I—a discussion of principles. J Hydrol 10(3):282–290. doi:10.1016/0022-1694(70)90255-6

Neitsch, S.L., Arnold, J.G., Kiniry, J.R., Williams, J.R. (2011). Soil and water assessment tool theoretical documentation: version 2009, Texas Water Resources Institute Technical Report No. 406. Texas Water Resources Institute, USA.

Oudin, L., Andreassian, V., Mathevet, T., Perrin, C., Michel, C., (2006). Dynamic averaging of rainfall-runoff model simulations from complementary model parameterizations. Water Resour Res 42(7):W07410. doi:10.1029/2005wr004636

Pervez, M.S., Henebry, G.M., (2015). Assessing the impacts of climate and land use and land cover change on the freshwater availability in the Brahmaputra River basin. J. Hydrol. Reg. Stud., 3:285–311.

Rahman, K., Maringanti, C., Beniston, M., Widmer, F., Abbaspour, K., Lehmann, A., (2013). Streamflow modeling in a highly managed mountainous glacier watershed using SWAT: the Upper Rhone River watershed case in Switzerland. Water Resour. Manage. 27(2):323–339.

Santhi, C., Arnold, J.G., Williams, J.R., Dugas, W.A., Srinivasan, R., Hauck, L.M., (2001). Validation of the SWAT model on a large river basin with point and nonpoint sources. JAWRA, 37(5):1169–1188.

Schulze R E. 2000. Hydrological responses to land use and climate change: a southern African perspective. AMBIO, 29(1): 12–22.

Shi, P.J., Gong, P., Li, X.B., (2000). Methods and Practice of Land Use and Land Cover Change. Beijing: Science Press.

Singh, A., (1989). Digital change detection techniques using remotely-sensed data. International Journal of Remote Sensing, 10(6):989-1003.

Tibebe, D., Bewket, W., 2011. Surface runoff and soil erosion estimation using the SWAT model in the Keleta watershed, Ethiopia. Land Degrad. Dev. 22 (6), 551–564.

Tuppad, P., K. R. Douglas-Mankin, T. Lee, R. Srinivasan, and J. G. Arnold. (2011). Soil and Water Assessment Tool (SWAT) hydrologic/water quality model: Extended capability and wider adoption. Trans. ASABE 54(5): 1677-1684.

Van Liew, M.W., Arnold, J.G., Garbrecht, J.D. (2003). Hydrologic simulation on agricultural watersheds: Choosing between two models. T. ASAE 46: 1539–1551.

Vorosmarty, C.J., Green, P., Salisbury, J., Lammers, R.B. (2000). Global water resources: vulnerability from climate change and population growth. Science 289:284–288.

Wang, G.X., Zhang, Y., Liu, G.M., Chen, L. (2006). Impact of land-use change on hydrological processes in the Maying River basin, China. Sci China Ser D Earth Sci 49(10):1098–1110.

Xu, H., Taylor, R.G., Xu, Y., 2011. Quantifying uncertainty in the impacts of climate change on river discharge in sub- catchments of the Yangtze and Yellow River Basins, China. Hydrol. Earth Syst. Sci. 15, 333–344, http://dx.doi.org/ 10.5194/hess-15-333-2011.

Yang, T., Zhang, Q., Chen, D.Y., Tao, X., Xu, C.Y., Chen, X. (2008). A spatial assessment of hydrologic alteration caused by dam construction in the middle and lower Yellow River, China. Hydrol Process 22:3829–3843.

Table II-1. Land use/cover classes and changes in the Upper Cahaba River watershed.

Modified land cover classes of Anderson level 1	1992		2011		2045
	NLCD (%)	DIGITIZED (%)	NLCD (%)	DIGITIZED (%)	USGS-EROS (A1B) (%)
Water	1.13	0.93	1.43	1.02	0.95
Urban	9.34	10.08	35.68	30.97	47.94
Forest	78.40	71.34	50.32	55.01	45.41
Agriculture	9.01	14.39	10.29	6.26	4.48
Wetland	1.27	3.03	1.94	6.73	0.74

Table II-2. Characteristics of the Upper Cahaba River watershed.

Variables	
Maximum Elevation	440.72 meters
Minimum Elevation	91.86 meters
Area (km^2)	1416 km^2
Dominated land use/cover type (%)	Forest (50.32 - 2011 NLCD)
Soil Clay (% wt.)	17.5
Soil Silt (% wt.)	15.3
Soil Sand (% wt.)	67.2
Mean Slope	13.22
Mean Annual Precipitation (1950-2014)	142.98 cm
Mean Annual Max Temperature (1950-2014)	23.44 °C
Mean Annual Average Temperature (1950-2014)	16.89 °C
Mean Annual Min Temperature (1950-2014)	10.34 °C

Table II-3. Input data used in the SWAT model and data sources.

Input data	Data source	References
LULC map	NLCD and Digitized Landsat 5 TM (30 m)	National Land Cover Database (NLCD): http://www.mrlc.gov/ Landsat Images: http://earthexplorer.usgs.gov/
Soil map (SSURGO)	USDA	USDA The Geospatial Data Gateway: https://gdg.sc.egov.usda.gov/
DEM	USDA (10 m)	USDA The Geospatial Data Gateway: https://gdg.sc.egov.usda.gov/
Measured Streamflow	USGS	USGS National Water Information System: http://waterdata.usgs.gov/
Historical Climate data	PRISM and CFRS	PRISM Climate Group: http://prism.oregonstate.edu/ NCEP Climate Forecast System Reanalysis (CFRS): http://rda.ucar.edu/

Table II-4. Calibrated model parameters and fitted values for each LULC datasets.

Variation*	Parameter	Parameter Definition	Absolute Ranges	Default SWAT Values	Fitted value	
					NLCD	Digitized Map
(r)	*CN2*	Initial SCS CN II Value	35-98	Varies**	-0.22	-0.19
(v)	*CANMX*	Maximum canopy storage	0-100	0	64.42	53.18
(v)	*GW_REVAP*	Groundwater "revap" coefficient	0.02-2	0.02	0.033	0.052
(r)	*SOL_K*	Saturated hydraulic conductivity	0-2000	100.8	-0.29	-0.44
(v)	*GW_DELAY*	Groundwater delay (days)	0-500	31	26.83	12.56
(r)	*RCHRG_DP*	Deep aquifer percolation fraction	0-1	0.05	0.28	0.24
(v)	*GWQMN*	Treshold depth of water in the shallow aquifer (mm)	0-5000	1000	387.25	374.61
(r)	*SOL_BD*	Moist bulk density	0.9-2.5	1.45	0.14	0.08
(v)	*GWHT*	Initial groundwater height (m)	0-25	1	3.11	3.68
(v)	*ALPHA_BNK*	Baseflow alpha factor for bank storage	0-1	0	0.50	0.56
(v)	*SURLAG*	Surface runoff lag time	0.05-24	4	15.34	15.43
(v)	*ESCO*	Soil evaporation compensation factor	0-1	0.95	0.30	0.21
(v)	*REVAPMN*	Threshold depth of water in the shallow aquifer for "revap" (mm)	0-500	1	299.10	219.46
(r)	*SOL_AWC*	Available water capacity of the soil layer	0-1	0.15	0.16	0.31
(v)	*EPCO*	Plant uptake compensation factor	0-1	1	0.58	0.52
(v)	*ALPHA_BF*	Baseflow alpha factor (days)	0-1	0.048	0.37	0.44

(*(r) means an existing parameter value is multiplied by (1+ a given value), and (v) means the existing parameter value is to be replaced by given value. **varies: varies by soil type.)

Table II-5. Sensitivity ranks and *p*-values of two different LULC datasets.

Ranks	Parameters - NLCD LULC	*p*-values	Parameter ranges	Parameters- Digitized LULC	*p*-values	Parameter ranges
1	*CN2 (r)*	0	[-0.26_-0.19]	*CN2 (r)*	0	[-0.23_-0.16]
2	*CANMX (v)*	0	[36.3_68.9]	*SOL_K (r)*	0	[-0.62_-0.27]
3	*GW_REVAP (v)*	0	[0.01_0.07]	*GW_DELAY (v)*	0	[-18.32_20.06]
4	*SOL_K (r)*	0	[-0.44_-0.15]	*CANMX (v)*	0	[44.67_64.3]
5	*GW_DELAY (v)*	0	[18.41_35.25]	*SOL_BD (r)*	0	[0.01_0.17]
6	*RCHRG_DP (v)*	0	[0.22_0.35]	*RCHRG_DP (v)*	0	[0.17_0.31]
7	*GWQMN (v)*	0.01	[281_494]	*GWHT (v)*	0.15	[1.04_6.33]
8	*SOL_BD (r)*	0.02	[0.07_0.22]	*ALPHA_BNK (v)*	0.18	[0.49_0.64]
9	*GWHT (v)*	0.08	[0.17_6.06]	*REVAPMN (v)*	0.18	[188_251]
10	*ALPHA_BNK (v)*	0.09	[0.43_0.58]	*SOL_AWC (r)*	0.21	[0.25_0.39]
11	*SURLAG (v)*	0.09	[12.7_18.0]	*GW_REVAP (v)*	0.22	[0.02_0.09]
12	*ESCO (v)*	0.14	[0.23_0.38]	*EPCO (v)*	0.22	[0.46_0.59]
13	*REVAPMN (v)*	0.29	[259_339]	*ALPHA_BF (v)*	0.38	[0.37_0.52]
14	*SOL_AWC (r)*	0.53	[0.1_0.2]	*ESCO (v)*	0.42	[0.13_0.27]
15	*EPCO (v)*	0.55	[0.49_0.67]	*SURLAG (v)*	0.73	[12.22_18.66]
16	*ALPHA_BF (v)*	0.59	[0.31_0.44]	*GWQMN (v)*	0.78	[302_447]

Table II-6. Calibration and validation results.

Daily Calibration and validation results - LULC dataset	Evaluation Statistics			
	R^2	***NSE***	***PBIAS***	***RSR***
Calibration (1988-1993) – NLCD LULC	0.72	0.71	6.5	0.53
Validation (2008-2013) – NLCD LULC	0.68	0.65	9.3	0.59
Calibration (1988-1993) – Digitized LULC	0.71	0.70	9.6	0.55
Validation (2008-2013) – Digitized LULC	0.70	0.67	8.2	0.58

R^2: Coefficient of determination, *NSE*: Nash-Sutcliffe Efficiency, *PBIAS*: Percent bias, *RSR*: RMSE-SR

Table II-7. Differences in mean and seasonal streamflows for the datasets.

	1992 NLCD	1992 Digitized	2011 NLCD	2011 Digitized
Mean annual streamflow (m^3/s)	7.60	7.89	8.05	8.31
Spring (m^3/s)	9.64	9.96	10.71	10.74
Summer (m^3/s)	3.21	2.77	3.02	2.97
Fall (m^3/s)	5.54	6.74	5.59	6.38
Winter (m^3/s)	12.15	12.24	13.03	13.33

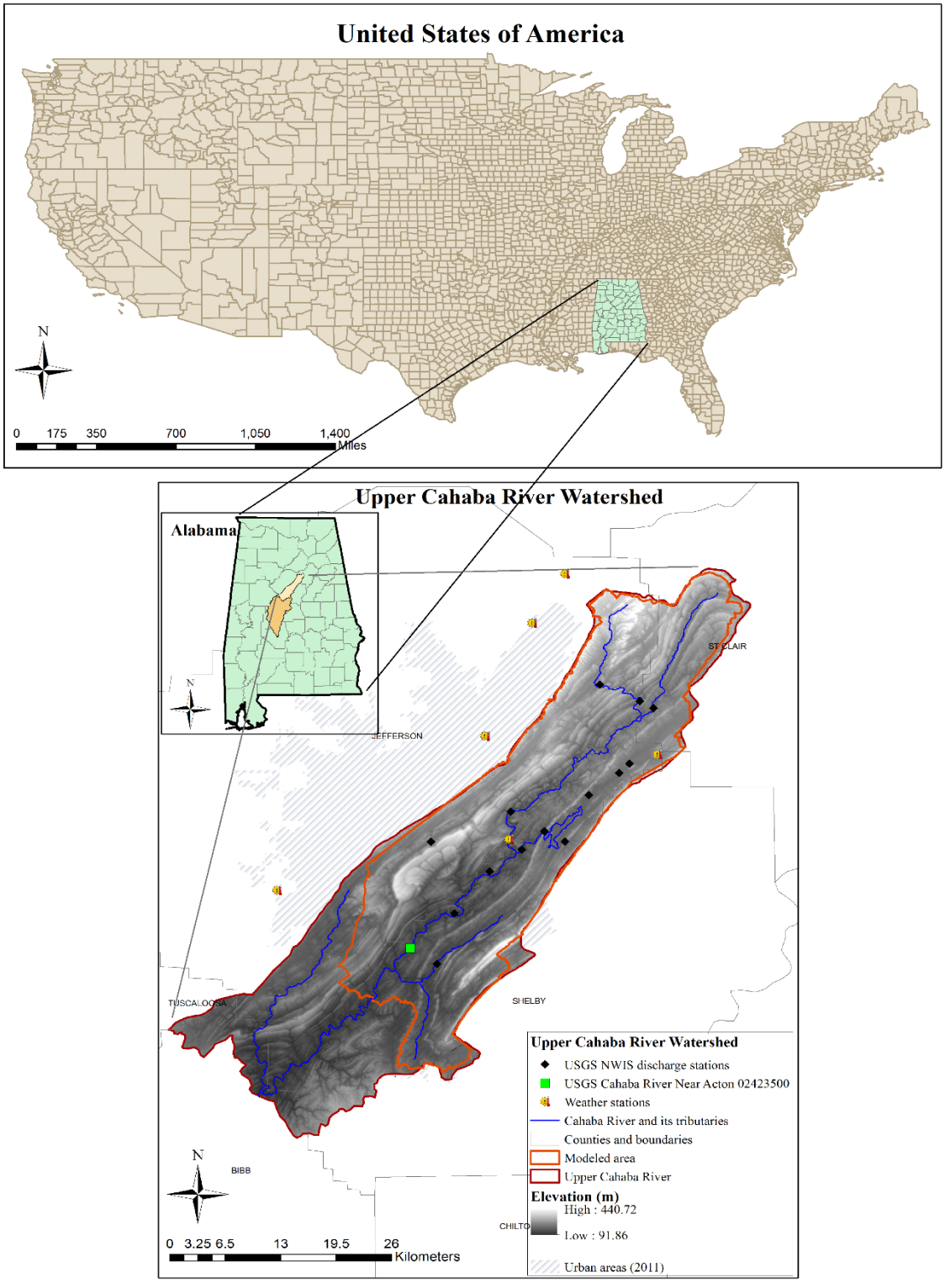

Figure II-1. Study area.

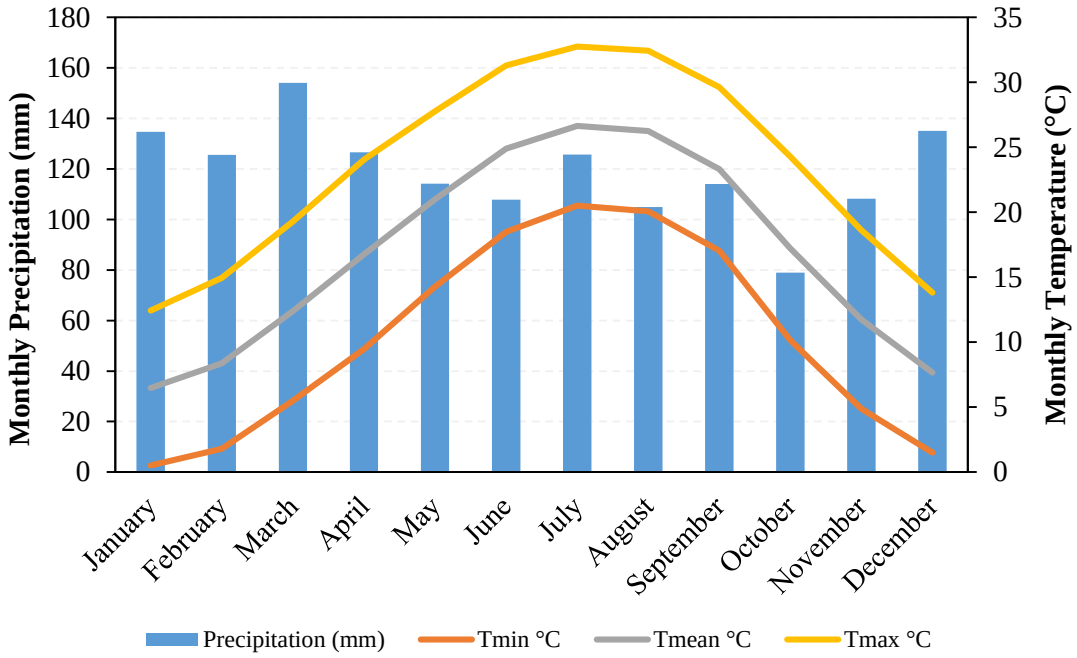

Figure II-2. 1950-2014 Upper Cahaba River watershed climate averages (NOAA).

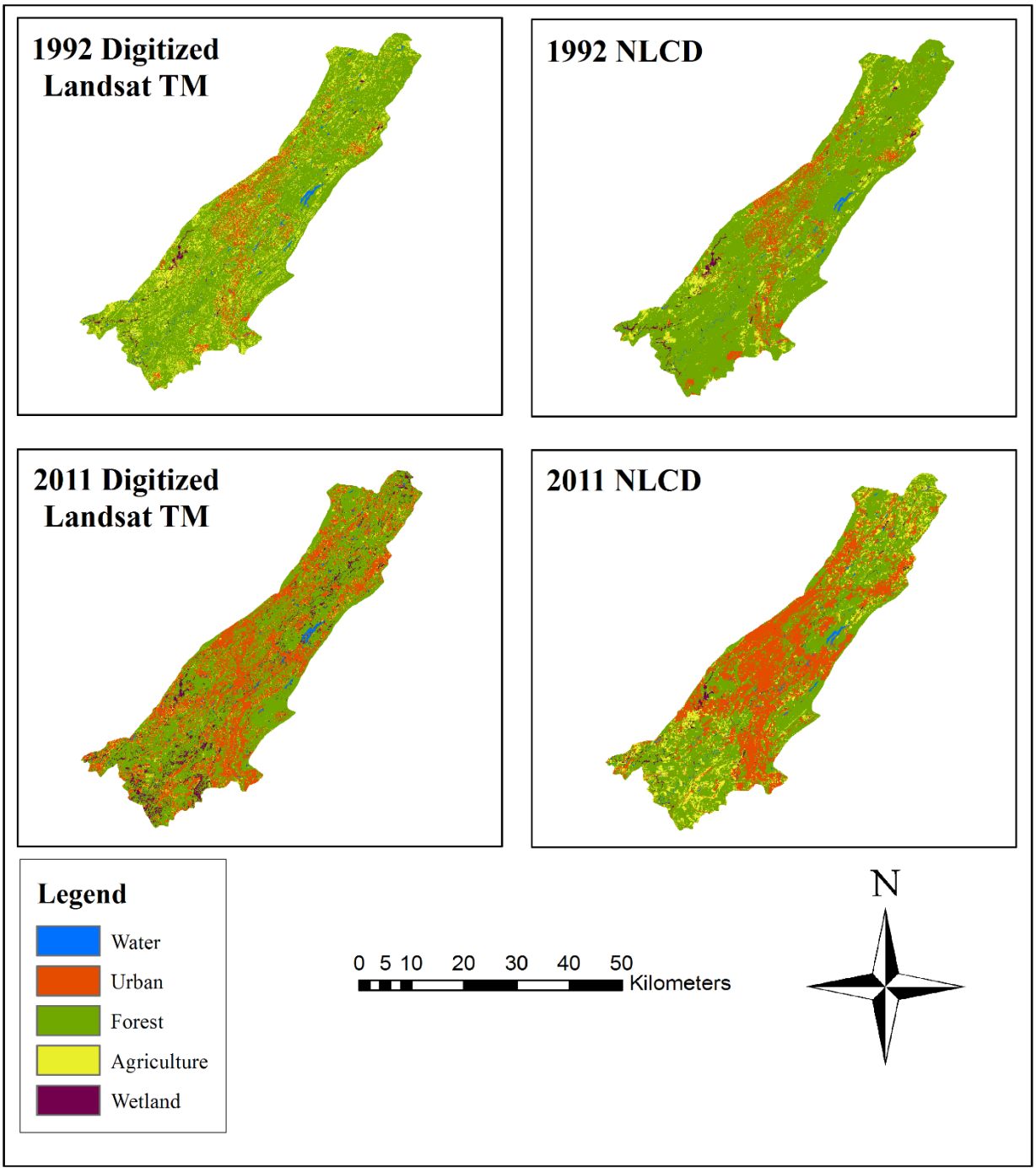

Figure II-3. LULC datasets used in this study.

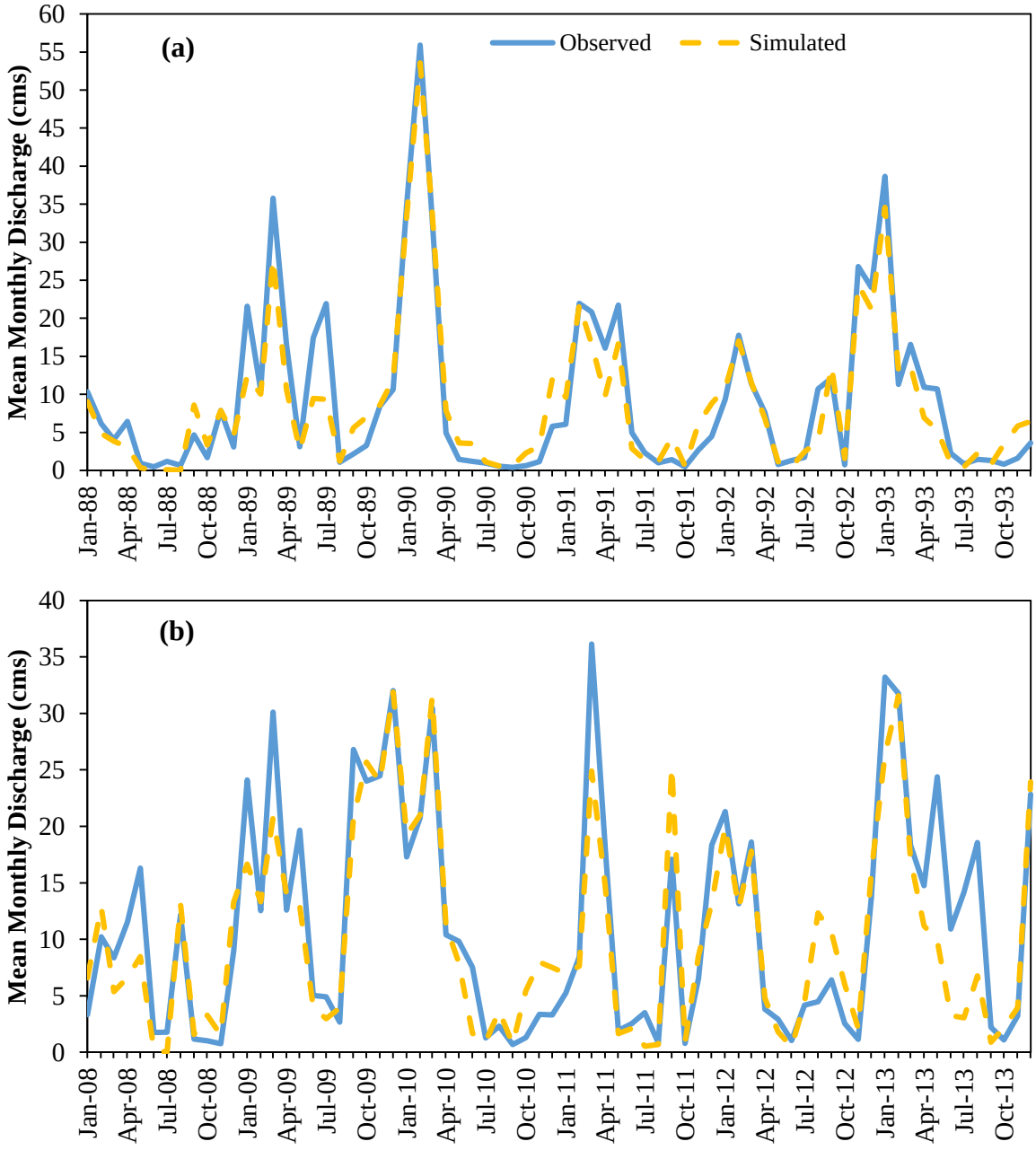

Figure II-4. Observed and simulated mean monthly streamflows based on the NLCD land use map for the calibration (a) and validation (b) periods.

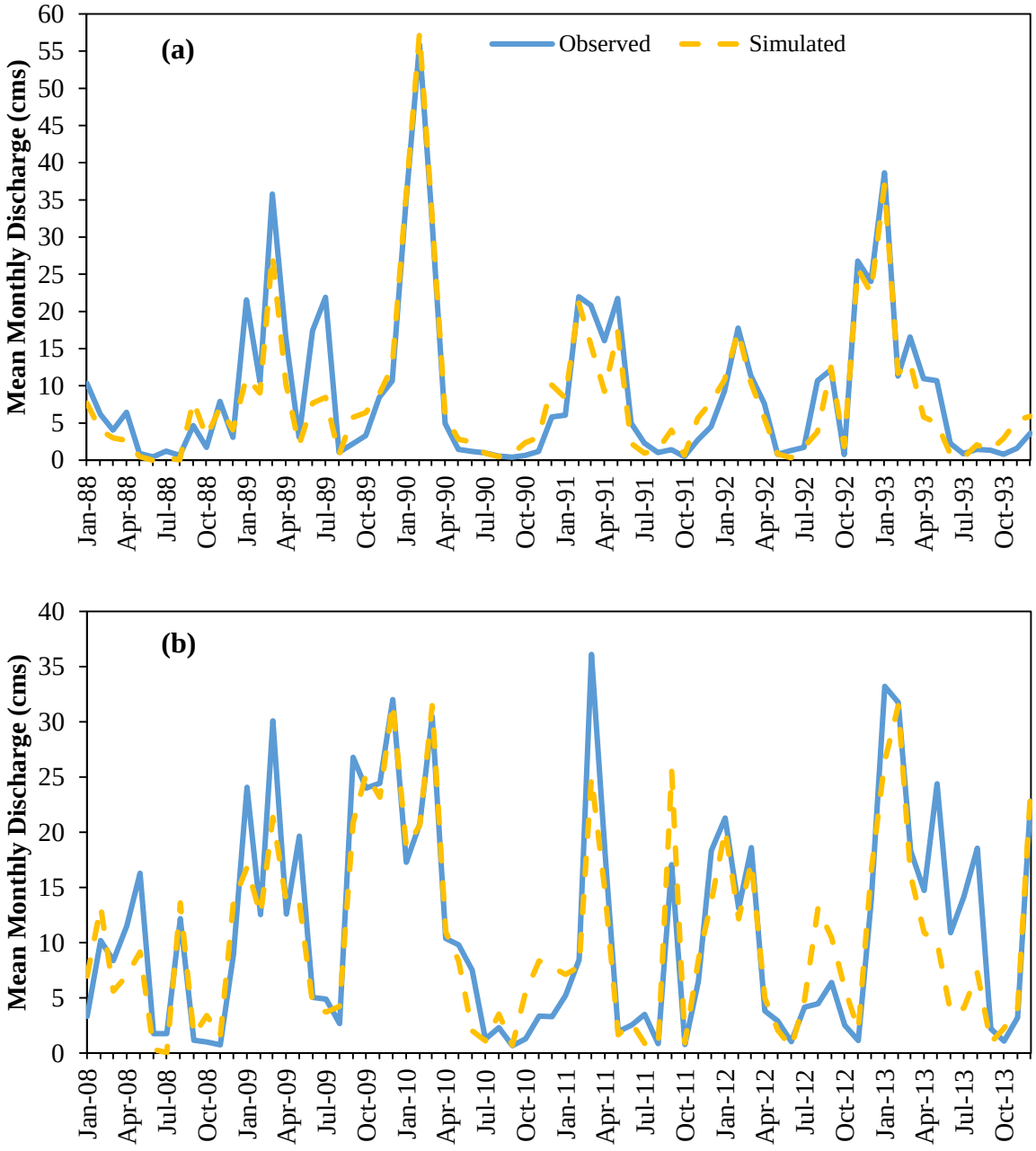

Figure II-5. Observed and simulated mean monthly streamflows based on the digitized Landsat 5 TM imageries land use map for the calibration (a) and validation (b) periods.

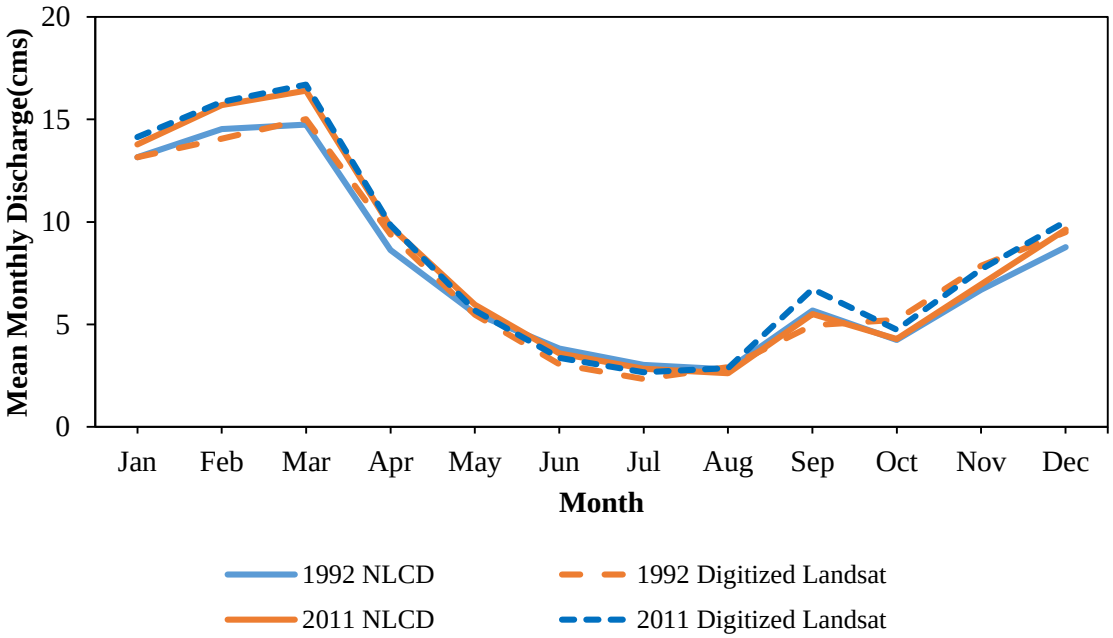

Figure II-6. Mean monthly streamflow changes due to LULC changes (1988-2013).

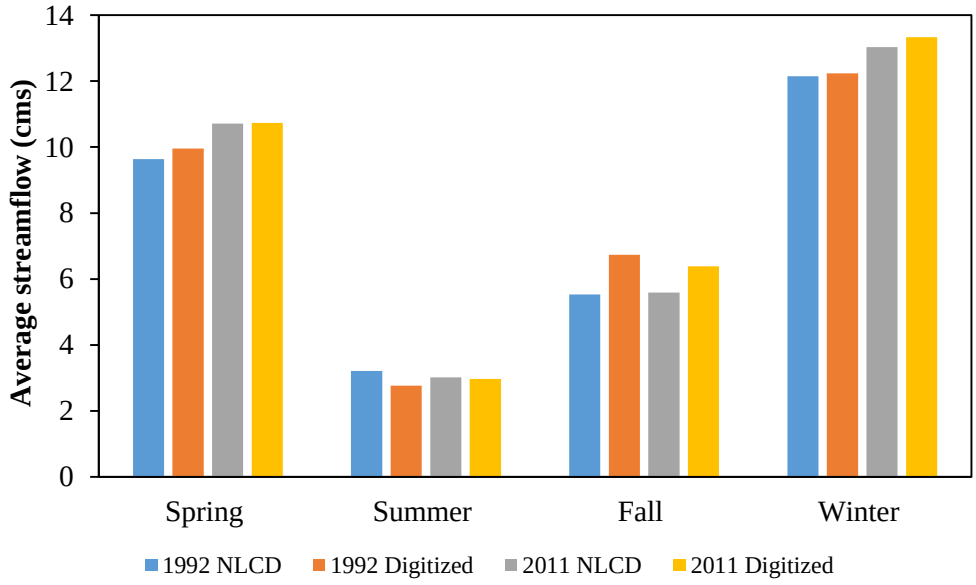

Figure II-7. Changes in average seasonal streamflows.

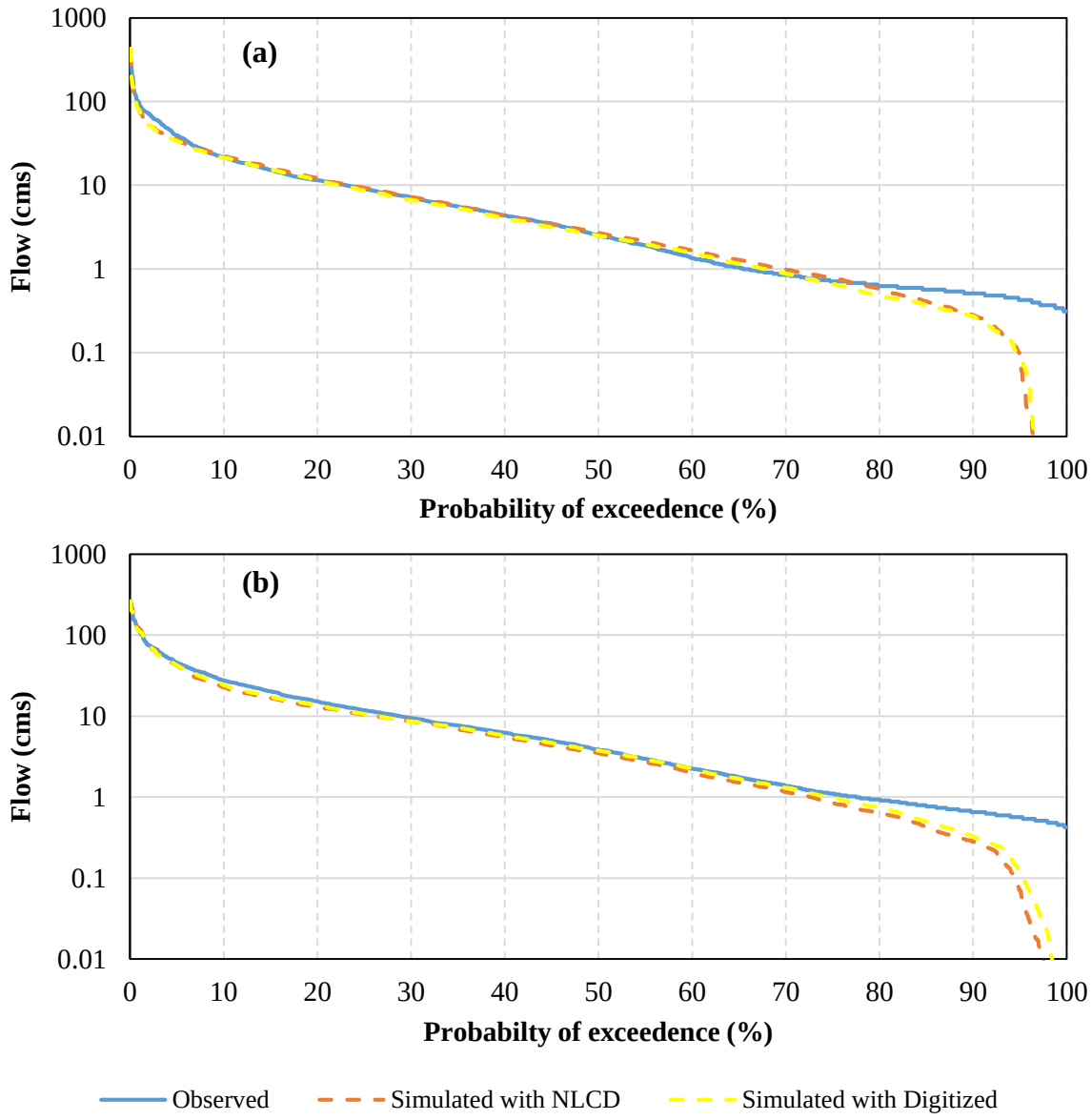

Figure II-8. Exceedence probability of calibration (a) and validation (b) periods for both LULC datasets.

Chapter III - Individual, Combined and Synergistic Impacts of Land Use/Cover and Climate Change on the Ecologically Relevant Flow Metrics

Abstract

This chapter explored the impacts of land use/cover (LULC) and climate change on hydrological responses, particularly on ecologically sensitive flow, in the rapidly urbanizing Upper Cahaba River basin in north-central Alabama. The Cahaba River is identified as the longest free-flowing river in the state of Alabama, and The Nature Conservancy noted it as one of the only eight "Hotspot of Biodiversity" in the contiguous United States. Past, present, and future potential streamflow responses to climate and LULC change were analyzed based on ecologically relevant flow metrics. We used 38 key flow metrics that capture high, low, and median flow, as well as flashiness, which are known to have significant impacts on flora and fauna. These flow metrics, thus the ecology, will certainly be affected by LULC and climate change. Daily streamflow was produced from 1988 to 2013 using historical climate and LULC data with the Soil and Water Assessment Tool (SWAT). Streamflow data from the periods of 1988-1993 and 2008-2013 were used for model calibration and validation, respectively. The SWAT-CUP calibration and uncertainty program was used for this purpose. Future daily streamflows were generated with SWAT by using bias corrected and downscaled CMIP5 climate data for the years 2035 to 2060 with eleven climate models under two different representative concentration pathways (RCP 2.6 and RCP 8.5). For the future land use/cover data, USGS EROS future projected dataset (250-meter resolution) was used. The daily streamflow from each period were fed into the Indicators of

Hydrological Alterations (IHA) software to calculate the 38 flow metrics in each period. Differences in the metrics were assessed, which may hint for increase/decrease in native species' density that may have occurred in the past or might occur in the future.

Keywords: Climate change, Land use/cover change, SWAT, CMIP5, Ecologically relevant flow metrics, Indicators of Hydrologic Alterations

1. INRODUCTION

Understanding impacts of alterations in climate and land use on eco-hydrologic processes in a watershed is crucial to sustaining water resources for multiple uses. With the continuous augmentation of human development, dramatic changes have taken place in climate and land use patterns in watersheds on a global scale. The effects of such changes on ecosystems and sustainable development have gained considerable concern (Vorosmarty et al. 2000; Yang et al. 2008; Li et al. 2009; Ma et al. 2009). Impacts on hydrological processes, such as recharge of groundwater, runoff, and infiltration are reflected in the balance of supply/demand of water sources, which in turn can significantly influence the economy, environment, and ecosystems. While climate variability can change the flow routing time, peak flows and volume (Prowse 2006), LULC change can result in alteration of flood frequency (Brath et al. 2006), base-flow (Wang et al., 2006) and average annual discharge (Costa et al., 2003). Therefore, comprehensive assessment at the watershed system scale is crucial for understanding impacts of climate and LULC changes on hydrological cycles, especially ecologically relevant flows, for effective planning, management and sustainable development of watersheds. This study performs a local scale assessment using simulation and statistical modeling to investigate ecologically relevant flow metrics within the Upper Cahaba River watershed under the past, present and future conditions.

Climate change has numerous direct and indirect impacts on the hydrological processes and water resources of basins (Schulze, 2000; Li et al., 2007a). Increasing concentrations of atmospheric greenhouse gasses, and consistent global warming are almost certainly responsible for important changes in global climatic patterns (IPCC, 2007; Xu et al., 2011). Alterations in the availability of water resources are expected to be among the most significant results of projected climate changes (IPCC, 2007; Kingston and Taylor, 2010). Concerns about the hydrological

system will have implications for discharge quantity and timing, as well as on ecosystem dynamics. Therefore, quantifying current and future freshwater availability is a critical aspect of adapting to changing and variable climate because the availability of water is linked to ecosystem health, LULC change and regional conflicts (Schuol et al., 2008).

Apart from climate change, human activities also play important roles in hydrology and water resources. The impacts of urbanization on watershed hydrology has been known since the late sixties (Leopold, 1968). Human-induced land use change can affect water circulation and spatio-temporal variations in the distribution of water resources. Freshwater systems are under stress due to increasing population and urbanizing landscapes. A number of studies have shown that changes in vegetation cover (i.e. deforestation or afforestation) can decrease or increase water yield and these kinds of changes have been observed in catchments ranging from less than 1 km^2 to over 1000 km^2 (Shi et al., 2000). Besides this, to satisfy the water demand of industrial and agricultural development, irrigation and drainage will greatly impact hydrological cycles both over time and space.

Many studies have investigated the combined impacts of LULC and climate change on water quantity (Guo et al. 2008, Li et al. 2010, Mango et al. 2011, Sample et al. 2012, Kim et al. 2013, Pervez and Henebry 2015). The studies differ in their study area, hydrological models, and climate and land use/cover data. Each of these studies used a calibrated hydrological model with climatic inputs representing one or several global warming scenarios and current or projected land use maps. For instance, Pervez and Henebry (2015) used SWAT model to explore sensitivities and patterns in freshwater availability due to projected LULC and climate changes in the Brahmaputra basin in South Asia. They found that streamflow, groundwater recharge, and total water yield were sensitive to changes in precipitation while average annual ET was sensitive to changes in CO2

concentration and temperature. They also observed strong increasing trends for total water yield, groundwater recharge, and streamflow, indicating increasing flooding potential during August-October. Conversely, strong decreasing trends were predicted for exacerbation of potential drought during May-July periods of the 21st century. Kim et al. (2013) simulated separate and combined impacts of future changes in LULC and climate change on streamflow in the Hoeya River basin, South Korea by using SWAT model and representative concentration pathway (RCPs) 4.5 and 8.5 scenarios of the Fifth Assessment Report (AR5) of the Intergovernmental Panel on Climate Change (IPCC) under three scenarios (LULC only, climate change only, and combined LULC and climate change). They found that under climate change streamflow increased only in spring, low flow decreased in summer and fall. On the other hand, LULC change decreased low flow in dry periods but increased high flow during wet periods. Their study claimed that LULC had a smaller effect than climate change on the changes in streamflow. However, both LULC and climate change were shown to influence seasonal variation in streamflow, significantly. Likewise, Wang et al. (2014) investigated LULC changes only causing higher surface runoff, but the changes did not have a significant impact on monthly mean streamflow under future LULC scenarios. However, they stated that combined impacts of LULC and climate, or only climate change, lead to dramatic increases in monthly average streamflow, especially during the fall season.

Mango et al. (2011) and Guo et al. (2008) also used the SWAT model to explore combined impacts of climate and LULC change on hydrological processes. Their simulation results indicated that deforestation, urbanization and climate change strongly influence seasonal variation in streamflow that LULC and climate changes reduce dry season flows and intensify peak flows, while increasing temperature and precipitation had a more predictable effect on the water balance components and discharge. El-Khoury et al. (2015) also used SWAT model to estimate combined

impacts of future LULC and climate changes on discharge in South Nation River basin in eastern Ontario Canada using historical and projected climate (SRES scenarios - A2) and LULC data. Contrasting to the results of Kim et al. (2013) and Mango et al. (2011), they found climate and LULC will drive the same variables in the same direction that both of them will increase monthly streamflow. The key finding of this study was that LULC changes can have a notable impact on the future hydrological cycle of South Nation River. The study results of Li et al. (2010) also supports this. They found that LULC and climate change in the upper and middle reaches of the Taoer River in northeastern China were responsible for approximately 55% and 45% increases in mean annual discharge, respectively.

As mentioned above, there are several studies in the literature focusing on the effects of LULC and climate change on hydrology. However, to date, questions still exist in hydrological responses to multiple environmental and ecological changes (Piao et al., 2007; Tomer and Schilling, 2009; Cui et al., 2009). Influences of LULC and climate changes and their interactions are still hot topics (Zhang and Schilling, 2006b; Zhang et al., 2010; Wang et al., 2010). Most analyses of climate impacts on river ecosystem focus on the effects of temperature changes (Millenium Ecosystem Assessment, 2005; Fischlin et al., 2007) and some of them only consider average precipitation changes (Lasalle and Rochard, 2009).

Wiley et al. (2010) assessed how changes in both climate and LULC may interact to form the habitat suitability of river segments for altering patterns of biological integrity in the North American Great Lakes basin. They observed both climate and LULC change altered ecosystem properties, in particular, changes in water temperature has a controlling effect on species distribution. Dyer et al. (2013) used ecologically relevant flow metrics to determine the effects of climate change and regulation on streamflow in the Upper Murrumbidgee River Catchment,

Australia. The study results have shown that the projected hydrological alterations for the catchment for 1 and 2 °C temperature rise are important for a range of ecologically relevant flow characteristics but not as significant as the impacts of river regulation, to supply water for human needs. Zhang et al. (2015) in studying the impacts of regulation of reservoirs in the East River Basin, China. They showed that water reservoirs increase the magnitude and frequency of low flows but decrease the magnitude and frequency of high flows.

The significance of flow regimes for river ecosystem has been well documented (Richter et al., 2003). According to Dudgeon et al. (2006), river biodiversity is associated with low flow events that restrict overall habitat availability and quality and high flow events that affect the river channel shape and allow access to differently disconnected floodplain habitats. Many characteristics of the flow regime, especially seasonality, interannual variability and timing of specific flow events, influence life history patterns like recruiting and spawning (Dudgeon et al., 2006). However, there is an enormous gap in the literature that studies generally explored combined and/or individual impacts of LULC and climate change on hydrological regime of rivers. It is a necessity that the effects of these changes on ecologically relevant hydrologic characteristics should be assessed for understanding and efficient planning, management and sustainable development of watersheds.

In this chapter, the Soil and Water Assessment Tool (SWAT) was utilized to explore changes in flow regimes under the past, present, and future LULC and climate conditions in the Upper Cahaba River Watershed, which eventually drains into the Mobile River. Indicators of Hydrologic Alterations software (IHA) with 38 key flow metrics was used to evaluate the alterations in ecologically relevant flow metrics. The main objectives are:

1. To explore how the hydrologic regime of the Upper Cahaba River responds to climate, and land use/cover (LULC) changes, mainly urbanization.
2. To examine how changes in flow in the Upper Cahaba River system will affect or have affected the ecologically-relevant flow metrics.

Observed streamflow data was used first to explore the pre-urbanized and post-urbanized period. SWAT model was then utilized to generate streamflows corresponding to future climate and LULC scenarios.

2. METHODOLOGY

2.1. Study Area

The study area used in this study is the Upper Cahaba River watershed (Figure II-1). The drainage area in our study area extends upstream from St. Clair County and encompasses in Jefferson, Shelby, and Bibb counties. The basin covers an area of 1416 km^2. The dominant soil type is sand (67.2%, Table II-2.). The climate of the area is mainly humid (Figure II-2.). The watershed receives a mean annual precipitation of 142.98 cm with annual mean maximum and minimum temperatures of 23.44 °C and 10.34 °C, respectively. More detail on the study area was provided in Chapter II., thus will not be repeated here.

2.2. Watershed Model

The latest version of the Soil and Water Assessment Tool (SWAT 2012.10.18) that runs on ArcGIS was used for preparing the input data and processing the output files (http://swat.tamu.edu/software/arcswat/). The SWAT model is a semi-physically based,

continuous-time, hydrological, and agricultural management practice simulation model that assesses impacts of land management practices on water quantity and quality in complex watersheds (Arnold et al., 1998). The main components of ArcSWAT (ArcGIS-ArcView extension and graphical user input interface for SWAT) are weather, hydrology, sedimentation, soil properties, loads and flows of nutrients, crop growth, pesticides, land management, stream routing, and agricultural management. The ArcSWAT model utilizes geographic information system (GIS) and digital elevation model (DEM) to delineate watersheds and extract the stream network.

SWAT runs on daily step and is capable of continuous simulation over a long time period (Gassman et al., 2007). It is suitable to evaluate the long-term influence of land management practices on water, sediment and agricultural chemical yields in heterogeneous watersheds with varying land use, soils and management conditions (Arnold et al., 1998; Neitsch et al., 2011). Therefore, the SWAT model, a process-based hydrology and water quality model, is one of the most commonly applied watershed models worldwide. SWAT has been applied in a variety of studies around the world. Some example applications are; plant growth in the Yellow River , China (Luo et al., 2008); erosion in the Keleta watershed, Ethiopia (Tibebe et al. 2011); nutrient transport and transformation in Iowa watersheds (ranging size from 2,000 to 18,000 km^2), IA, USA (Jha et al., 2004a); pesticide transport in Orestimba Creek, CA, USA (Luo and Zhang, 2009); sediment transport in the Rock River, WI, USA (Kirsch et al., 2002); water management in the Cedar Creek Reservoir, TX, USA (Debele et al., 2008); snowmelt in the Upper Rhone River watershed, Switzerland (Rahman et al., 2013); land use change in the Zanjanrood basin, Northwest Iran (Ghaffari et al., 2010); climate change impact assessment in the upper Mississippi River Basin,

MS, USA (Jha et al., 2006); and combined impacts of LULC and climate change in the Brahmaputra basin, South Asia (Pervez and Henebry 2015).

In order to characterize spatial heterogeneity, ArcSWAT divides a basin into multiple sub-basin based on drainage areas of tributaries. Depending on the homogeneity and combination of land use, soils and slope characteristics, each sub-basins are split into multiple hydrological response units (HRUs). Each HRU is expected to be spatially uniform in climate, LULC, soil, and topography. The ArcSWAT model simulates surface runoff, infiltration, percolation, evapotranspiration (ET), and deep and shallow aquifer flow (Arnold et al. 1998). SWAT simulates the hydrological cycle based on the following water balance equation in the soil profile:

$$SW_t = SW_0 + \sum_{i=1}^{t}(R_{day} - Q_{surf} - E_a - w_{seep} - Q_{gw}) \quad (7)$$

where SW_t is the final soil water content (mm H_20), SW_0 is the initial soil water content (mm H_20), t is the time (days), R_{day} is the amount of precipitation on day i (mm H_20), Q_{surf} is the amount of surface runoff on day i (mm H_20), E_a is the amount of evapotranspiration on day i (mm H_20), w_{seep} is the amount of percolation and bypass flow exiting the soil profile bottom on day i (mm H_20), Q_{gw} is the amount of return flow on day i (mm H_20).

2.2.1. Model Setup and Input Data

The geographic information system interface ArcSWAT was used to parametrize the model for the Upper Cahaba River watershed. The watershed was delineated from a 10-meter DEM (available at https://gdg.sc.egov.usda.gov – downloaded at 9/27/2015). The basin was subdivided into 45 sub-basins with a threshold area of 600 ha. The outlet near to USGS discharge station was selected to be the final outlet of the Upper Cahaba River watershed (Figure II-1.). To further

characterize the sub-basins for dominant soil types and land use, the multiple Hydrological Response Unit (HRU) option was performed. The detailed model setup process and input data are described in the following sections.

2.2.1.1. Weather Data

SWAT requires daily precipitation (*pcp*), maximum and minimum air temperature (T_{min} and T_{max}), solar radiation (*slr*), wind speed (*wnd*), and relative humidity (*hmd*) as meteorological inputs. The daily precipitation and maximum/minimum air temperature data were obtained from the highest-quality spatial climate gridded dataset (4 km cell size) of PRISM (PRISM Climate Group, Oregon State University, http://prism.oregonstate.edu, accessed on 8/20/2015). The other input data (solar radiation, wind speed, and relative humidity) were obtained from the National Centers for Environmental Prediction (NCEP) Climate Forecast System Reanalysis (CFSR) database (http://rda.ucar.edu/ accessed on 8/21/2015).

Bias corrected and spatially downscaled future daily (2035-2060) *pcp*, T_{max}, and T_{min} data under two different representative concentration pathways (RCP 2.6 and RCP 8.5) were acquired from the World Climate Research Programme's (WCRP) Coupled Model Intercomparison Project Phase 5 database (CMIP5, http://gdo-dcp.ucllnl.org/downscaled_cmip_projections/dcpInterface.html - accessed on 8/25/2015). Through that, the following three various datasets were downloaded and prepared: (1) observed historical data (*pcp*, T_{max} and T_{min}) from National Oceanic and Atmospheric Administration (NOAA) Birmingham Airport, AL US (ID: USW00013876) from 1950 to 1999 which is the nearest climatic station with 86 years (since 1930) historical data available; (2) simulated historical conditions from a given GCM which comes under the name "1/8 degree Observed data (1950-1999); and (3) the GCMs simulated future projections (2035-2060). Available CMIP5 projections

in daily scale were precipitation (mm/day), air temperature (°C), which were utilized in this study. For bias-identification of CMIP5 projections, it is recommended to select 1950-1999 period (Reclamation, 2013). The focus of this step is on datasets (1) and (2) which are observed historical from a gage station and simulated historical GCMs, respectively. After identifying the bias of dataset (2) from dataset (1), it is then used to guide bias correction of dataset (3). Bias-identification proceeds on a variable (*pcp*, T_{max} and T_{min}) and month basis meaning quantile mapping is used for all daily values within each month. For instance, all daily precipitation observations for all the months of September during the 50-year "observed" period are lumped into one pool to create a distribution of daily precipitation observation for September (n=50*30=1500 days). The pool of n daily observed precipitation values is then sorted, and each day is ranked, with a quantile of rank (n+1), and assembled into a cumulative distribution (Maurer et al., 2010). Similar pairs of distributions are prepared for all 12 months both datasets (1) and (2). The paired CDFs (Figure III-2 and 3) are combined to form a "quantile map" where at each rank probability, or percentile, one can access the bias between dataset (1) and (2) (observations and historical GCMs). To do so, utilizing polynomial fitting function can help as suggested by Drusch et al. (2005) for CDF matching. The polynomial fit is on the scaled GCM data and the differences (biases) for each month. Hence, by utilizing the derived coefficients for the polynomial fit, the bias corrected GCM is directly derived in its original time series. This procedure was performed for all 22 projections (11 climate model under two representative concentration pathways (RCPs)– Table III-2.) within the MATLAB software.

SWAT calculates actual evaporation (ET) from potential evapotranspiration (PET). In this study, the Penman-Monteith method was selected to estimate PET. The Penman-Monteith method requires air temperature, solar radiation, relative humidity and wind speed. As mentioned earlier,

downscaled future daily (2035-2060) precipitation and air temperature were obtained from the CMIP5 database. Other climate variables (solar radiation, relative humidity and wind speed) were individually generated by the WXGEN weather generator model in SWAT (Sharpley and Williams 1990). This stochastic weather generator is widely used for climate change studies (Ficklin et al. 2009, Zhang et al. 2011, Kim et al. 2013, Fan and Shibata 2015, Cousino et al. 2015).

2.2.1.2. Observed Streamflow

The daily measured discharge data for the period 1983-2013 was obtained from the United States Geological Survey National Water Information System website (USGS Station Name: Cahaba River near Acton AL, Station Number: 02423500, http://waterdata.usgs.gov/nwis accessed on 8/21/2015). This station is located in Jefferson County, AL (Figure II-1 - Drainage area: 595.65 km^2, Latitude 33°21'48" Longitude 86°48'47" NAD27). Daily discharge data in that station have been collected for over 78 years (since 1938) and are operated in cooperation with the Alabama Department of Environmental Management (ADEM). Daily observed streamflow averages 10.23 m^3/sec, although it can vary from 0.07 m^3/sec to 385.11 m^3/sec, during late summer flow conditions and at peak flow conditions during late fall and winter, respectively. The daily discharges were used for model calibration and validation in the SWAT Calibration and Uncertainty Program (SWAT-CUP).

2.2.1.3. Digital Elevation Model (DEM)

The model utilized a 10-meter digital elevation model (DEM), which was downloaded from the USDA Geospatial Data Gateway (available at https://gdg.sc.egov.usda.gov – downloaded on 9/17/2015). The DEM was used to delineate the surface drainage of the watershed, along with 45 subwatersheds.

2.2.1.4. LULC Data

LULC changes impact various components of the hydrologic cycle, such as surface runoff, erosion, recharge, and evapotranspiration either directly or indirectly. To examine LULC change, two sources of LULC data was used (NLCD and USGS-EROS) in this study. The National Land Cover Database (NLCD) is a publicly available dataset at 30-meter resolution (available at http://www.mrlc.gov/ - accessed on 6/12/2015). USGS-EROS projected future land cover map (250-meter resolution, available at http://landcover-modeling.cr.usgs.gov/projects.php - accessed on 8/20/2015) was used for the future scenarios. Since these historical and future maps had different LULC classifications, reclassification process were applied to all LULC maps that the original categories were classified into five classes to make them consistent with SWAT's own database. The classes are water (1), urban (2), forest (3), agriculture (4), and wetland (5).

2.2.1.5. Soil Data

The model incorporated soil types obtained from SSURGO database, certified database by United States Department of Agriculture – Natural Resources Conservation Service Soils (USDA-NRCS, available at https://gdg.sc.egov.usda.gov - accessed on 9/17/2015), was used as the soil data source. The dominant soil types in the Upper Cahaba River watershed are sand (67.2%), clay (17.5%) and silt (15.3%) (Table II-2.).

2.2.1.6. Sub-basins and Hydrological Response Units (HRUs)

The model with 45 sub-basins was obtained at the end of the process. The sub-basins were then divided into hydrologic response units (HRUs), which are unique combinations of soil and land cover. As a result, the watershed was discretized into 557 and 540 HRUs for the 1992 and 2011 NLCD LULC datasets, respectively. On the contrary, 604 HRUs were acquired for the 2045

USGS-EROS LULC dataset. These HRUs were defined using the threshold values of 8%, 8% and 10% for land use, soil and slope, respectively.

2.3. Ecologically relevant flow metrics

Rivers are a source of water for agriculture, domestic, and industrial purposes. Besides, river flow regimes are crucial parts of the ecological integrity of river systems (Poff et al., 1997; Hart and Finelli, 1999). Flow variability and river discharge changes are well recognized by ecologists as the primary driver of many major ecological processes in riverine ecosystem function and structure (Poff et al., 1997). Therefore, it is a necessity that the effects of climate and LULC changes on ecologically relevant hydrologic characteristics should be explored for understanding and efficient planning, management and sustainable development of watersheds.

The US Nature Conservancy (http://www.nature.org/), the developer of IHA, has identified 67 parameters to compare and assess natural discharge characteristics, flow regime, and environmental flow components. These parameters are subdivided into 2 groups: (1) IHA, (2) Environmental Flow Component (EFC). There are 33 IHA and 34 EFC parameters. In this study, 38 (26 IHA and 12 EFC) of these 67 parameters, which are sensitive to ecosystem influences, were used to characterize the ecologically relevant flow regime changes in the Upper Cahaba River watershed. The parameters are selected based on their ecological relevance and their use in published ecological studies. The 38 key index can be divided into five groups: (1) magnitude of monthly discharge - 12 parameters, (2) magnitude and duration of peak discharge - 10 parameters, (3) timing of annual extreme discharge - 2 parameters, (4) rate and frequency of discharge changes- 2 parameters, and (5) EFC monthly low flows – 12 parameters. The list of groups, the hydrologic

parameters, and their ecosystem influences are given in Table III-3 (The Nature Conservancy, 2009).

2.4. Model Experiment Setup

In this study, three different experiments (LULC change only, climate change only, combined climate and LULC change) were set up to assess the separate and combined the impacts of LULC change and climate variability on hydrological processes. Two 25-year time periods (baseline period: 1988-2013 and future period: 2035-2060) were selected. The climate change only experiments were based on bias corrected and downscaled CMIP5 database (the World Climate Research Programme's (WCRP) Coupled Model Intercomparison Project Phase 5 database - http://cmip-pcmdi.llnl.gov/cmip5/) with 11 climate models under the RCP 2.6 and 8.5 scenarios (22 models in total, Table III-2.).

To assess the sensitivity of model outputs to LULC changes, the following two LULC data were used (Table III-1 and Figure III-1). The LULC data for the year 2011 (NLCD) was used to represent the baseline period. For future LULC data, 2045 USGS EROS data under the IPCC-SRES A1B scenario, which was developed by U.S. Geological Survey Earth Resources Observation and Science Center, were utilized (Table III-1.). The IPCC-SRES A1B Emission Scenario (a scenario in A1 family) describes "a future world of very rapid economic growth, global population that peaks in mid-century and declines thereafter, and rapid introduction of new and more efficient technologies" (IPCC, 2007).

The simulated streamflow for the baseline period under each scenario was compared to the corresponding values for the future period. To assess only climate change impacts on discharge, it was assumed that the future LULC would be the same as the current LULC (2011). Then, eleven

climate models under two representative concentration pathways (RCP 2.6 and 8.5, Table III-2.) for the future period were applied to 2011 LULC. To analyze only LULC change effects on streamflow, the climate in the future period was assumed to be the same as that in the baseline period (1988-2013). Then, the model was simulated under projected future LULC (2045 – A1B) with historical climate data (1988-2013). To evaluate the combined impacts of LULC and climate changes, one projected LULC map (2045 – A1B) and bias corrected and spatially downscaled future daily eleven climate model data (2035-2060) under two representative concentration pathways (RCP 2.6 and 8.5) were performed (Table III-2.). As mentioned in the introduction, the main objective of this study is to assess the flow regime changes under LULC and climate changes. In this regard, the Indicators of Hydrological Alterations (IHA) statistical software package, suggested by Richter et al. 1996, was used to assess the changes in ecologically relevant flow metrics from the 46 SWAT model outputs (all with a 25-year period of simulation, Appendix A, B and C.), which were generated under different scenarios (Table III-4.) for the past, present and future periods. Below is a summary of the experiments conducted:

a. *Baseline period (1988-2013):* The model is calibrated and validated with 1992 and 2011 land use/cover maps, respectively (see Chapter II.). The LULC map for the year 2011 and historical climate data (1988-2013) were used as SWAT input.
b. *Only climate change (1988-2013):* The LULC map for the year 2011 and bias corrected/downscaled eleven future climate model under two different RCPs (11 RCP 2.6 and 11 RCP8.5 scenarios) were performed. (1 LULC map * 22 climate model = 22 scenarios.)
c. *Only LULC change impact (2035-2060):* Projected 2045 A1B LULC map with historical climate data (1988-2013) were performed. (1 LULC map * 1 climate data = 1 scenario.)

d. *Combined impacts of LULC and climate change (2035-2060):* Projected 2045 A1B LULC map with eleven future climate model under two RCPs (11 RCP 2.6 and 11 RCP 8.5 scenarios) were performed. (1 LULC map * 22 climate model = 22 scenarios.)

3. RESULTS AND DISCUSSION

3.1. Evaluating changes in precipitation and temperature

Figure III-4. indicates general information about the potential changes in temperature and precipitation in the future (2035-2060) in the Upper Cahaba River watershed (i.e., seasonal and annual changes). An analysis of the precipitation and temperature pattern from 2035 to 2060 derived using CMIP5 shows that precipitation and temperature in the Upper Cahaba River watershed increases in spring, summer and winter. The eleven model under both RCP 2.6 and 8.5 emission scenarios predict increases in annual temperatures (ensemble mean from the 22 climate models) of 1.9 °C (0.7 to 2.8 °C, RCP 2.6 emission scenarios) to 3.3 °C (1.8 to 4.5 °C, RCP 8.5 emission scenarios) by the 2050s, relative to the baseline period (1988-2013). Annual precipitation is projected to increase (ensemble mean from 22 climate models) between 1.9% (-2.7~6.9%, RCP 2.6) and 2.3% (-1.5~3.7%, RCP 8.5) by the 2050s.

It is also observed that all future climate models indicate a rising trend in temperature in all seasons. For winter and spring, the range is from 0.7 to 3.7 °C. On the contrary, the range is from 0.6 to 6.9 °C for the summer and fall. Thus, there is higher uncertainty in these months. For seasonal changes in precipitation, there is no clear trend of increase or decrease. For example, 5 of the 22 climate projections show a decrease in spring precipitation with an average of -3.4%, while other 17 climate projections show an increase about 5.7%. Moreover, 16 of the 22 climate

projections show a decrease trend in precipitation for fall season approximately -4.4%. In general, the Upper Cahaba River watershed will more likely experience increased temperature, especially in summer and fall. Precipitation is also expected to increase in spring, summer, and winter. Thus, the Upper Cahaba River watershed could experience moderate to significant changes in climate by 2050s, especially under RCP 8.5 scenarios.

3.2. Changes in LULC

Figure III-1 shows the historical and future LULC maps for each scenario. In the current LULC (2011 NLCD), forests cover more than 50% of the area, while urban and agriculture land account for 35% and 10% of the whole area, respectively (Table II-1). Thus, forest areas are currently larger than the areas of urban and agriculture. Compared to the baseline LULC map (2011), there is a trend of urban sprawl in the future. Based on the projected future LULC map (2045 USGS-EROS A1B), percentage of urban areas within the watershed will increase from 35 to 47% over the 30 years. This urban area growth reduced the proportions of the other LULC types (water, forest, agriculture and wetland). For instance, the areas of forest was predicted to be 5% smaller than the area in 2011 (Table II-1), which does not represent a significant deforestation trend in the future (IPCC-SRES A1B Scenario). Other changes in land use are insignificant.

3.3. Impacts of climate change on the ecologically relevant flow metrics

The simulated streamflows for the future period under 22 climate models (11 RCP 2.6 and 11 RCP 8.5) were compared to the corresponding values in the baseline period. The projected annual average daily streamflow for the future period was observed as 8.97 and 8.79 m^3/s under RCP 2.6 and 8.5 emission scenarios, respectively. Compared to the average daily streamflow in the baseline period (8.04 m^3/s), annual average trends show that the annual streamflow will increase by 11.4%

(RCP2.6) and 9.2% (RCP 8.5) in the future period (Appendix B.). The difference of the mean value for each IHA metrics (38 metrics in total) between the two RCP scenarios was calculated and showed in between Figure III-5 and Figure III-15 (also see Appendix B.). The following sections describe the changes in each groups separately.

3.3.1. Group 1: Magnitude of monthly water conditions

This group includes 12 parameters, each of measures the mean of the daily water conditions for a given month. On average, the magnitude of mean monthly flows under future climate scenarios is higher than the baseline period, particularly from May to September. Figure III-5. shows relative changes in monthly streamflows as box and whisker plots, in which the median values illustrated, during the future period (2035-2060) under RCP 2.6 and 8.5 scenarios compared with the baseline period (1988-2013). The sensitivity of monthly streamflow to climate change differed between the emission scenarios.

The relative changes in monthly streamflow in June and July had greater uncertainty than those in other months. The changes in monthly median streamflows for the future RCP 2.6 and 8.5 climate change scenarios were predicted to decrease in October (-13%) and November (-11%) (RCP 2.6) and April (-9%) and May (-5%) (RCP 8.5). This finding indicates a significant decrease in the fall flow under RCP 2.6 scenarios. On the contrary, significant increases were observed in May-September and June-September periods under RCP 2.6 and 8.5 scenarios, respectively. Although there were some variations among the RCP 2.6 and 8.5 results, the general pattern indicated increases in June-September flow. In particular, the monthly median flow increased by 24% and 11% in June under RCP 2.6 and 8.5 scenarios, respectively. Correspondingly, the maximum increases are observed as 55% and 74% in July under RCP 2.6 and 8.5 scenarios,

respectively, and this changes contributed to the increase of summer streamflow. This suggests that changes in streamflow were mainly caused by the changes in precipitation.

3.3.2. Group 2: Magnitude and duration of annual extreme water conditions

The 10 parameters in this group measure the magnitude of extreme (min-max) annual water conditions of various duration and ranging from daily (1-3-7 days) to seasonal (30-90 days). Significant differences were observed in the annual minimum-maximum flows under future climate scenarios. Figure III-6 shows changes in the annual minimum maximum flows under RCP 2.6 and 8.5 scenarios. The results of RCP 2.6 scenarios indicated that the minimum flows of 1-3-7 days increased about 7%, and the 30 and 90 days minimums also increased about 30% and 42%, respectively. Moreover, the maximum flows of 1-3-7-30-90 days increased about 69, 49, 43, 34, and 15%, respectively. The RCP 8.5 scenarios also showed similar patterns for annual minimum and maximum flows, except 1-3-7 day minimums. The RCP 8.5 scenarios indicated that the minimum flows of 1-3-7 days decreased about -8%.

3.3.3. Group 3: Timing of annual extreme water conditions

This group includes two parameters. These parameters are critical for the seasonal feature of the hydrological conditions. The first parameter group is measuring the Julian date of the annual 1-day maximum water condition and the second parameter group is measuring the Julian date of the annual 1-day minimum water condition. For example, reproduction, which is a key life cycle phase, maybe linked to timing of annual extremes that changes in timing may cause reproductive stress, or failure. The timing of the annual extreme flows for RCP 2.6 and RCP 8.5 were similar to the baseline period. In general, the Julian date of each annual 1-day maximum for both RCP scenarios were 9 days (RCP 2.6) and 7 days (RCP 8.5) later than the baseline period, whereas the

Julian dates of 1-day minimum were 10 days (RCP 2.6) and 6 days (RCP 8.5) earlier than the baseline period (Figure III-7).

3.3.4. Group4: Rate and frequency of water conditions changes

The two parameters in this group measure the mean rate and number for both negative and positive changes in water conditions. It is investigated that the rise and fall rates will be much faster under future climate conditions (Figure III-8). In this group, the parameters were generally high, particularly for the fall rates. For instance, the median of the rise rate for both RCP 2.6 and 8.5 emission scenarios were 14 and 9%, respectively. Similarly, the median of fall rate for both RCP 2.6 and 8.5 emission scenarios were about 15%.

3.3.5. Group5: Monthly low flows (EFCs)

Figure III-9 shows the impact of 22 climate change scenarios on monthly low flows. In RCP 8.5 scenarios, the monthly low flows are predicted to decrease more often than they are predicted to increase. The monthly median low flows were increased by RCP 8.5 in July (18%), August (13%), September (22%) and October (9%) and decreased in other months about 2-14%. On the contrary, the monthly low flows are predicted to increase between May and October under RCP 2.6 emission scenarios in the percentage range from 5 to 19%. This group is very important for plants. For example, if the monthly low flows are extremely low during the growing season, the water temperature and water chemistry would probably be effected significantly that it can increase stress in plants.

3.4. Impacts of only LULC change on the ecologically relevant flow metrics

3.4.1. Group 1: Magnitude of monthly water conditions

LULC change impacts on the hydrologic regime of the Upper Cahaba River watershed were analyzed by using 2045 USGS – EROS (A1B) LULC map with historical climate data (1988-2013). It is observed that there is an increasing trend in mean annual streamflow under future LULC conditions. Compared to the 2011 LULC map results, the projected future mean annual flow increased from 8.04 m^3/s to 8.75 m^3/s under 2045 LULC map (Appendix A). This can be explained by urban growth in the watershed. Figure III-16 shows monthly mean streamflows simulated by SWAT under future land use conditions in the Upper Cahaba River watershed. Changes in monthly streamflow are slightly affected by LULC changes. Monthly streamflow decreased from April to July (about -5%), but increased in other months (about 17%). Due to LULC, the maximum increases and maximum decreases are observed as 27% in October, -8% in June, respectively. Thus, LULC change had a smaller impact on streamflow compared to climate change impact.

3.4.2. Group 2: Magnitude and duration of annual extreme water conditions

The annual minimum and maximum daily averages are presented in Figure III-10. Due to urbanization, significant differences are expected in daily minimum flows. 1-, 3-, 7-, and 30-day minimum daily flows decreased approximately 60% under the 2045 LULC data. On the other hand, for the case of extremely high flows, approximately 21% increases were observed. Compared to only climate change impacts (Section 3.3.2.), it is observed that magnitude and duration of annual extreme water conditions are more sensitive to LULC changes than to changes in climate.

3.4.3. Group 3 and 4: Timing of annual extreme water conditions and Rate and frequency of water conditions changes

The Julian dates of annual 1-day maximum and minimum significantly changed under changes in LULC. In particular, we observed annual 1-day minimum was 28 days earlier than the baseline period, whereas 1-day maximum was 23 days later than the baseline period (Figure III-7.) The means of fall and rise rate increased about %29 (Appendix A), while the mean differences of fall and rise rate was lower in scenario *b* ((impacts of only climate change - Table III-4), and Figure III-8.).

3.4.4. Group5: Monthly low flows (EFCs)

Figure III-11 shows the impact of only LULC change on monthly low flows. The results indicated that the monthly low streamflow decreased in all months due to urbanization and the ranges of change were -24% in February and -54% in June. Monthly low flows in this scenario are very close to scenario *d* (combined impacts of LULC and climate). Therefore, it can be stated that urbanization results in lower streamflow.

3.5. Combined and synergistic impacts of future climate and LULC change on the ecologically relevant flow metrics

In addition to the assessment of the individual impacts of LULC and climate change, the combined and synergistic effects of these changes on the ecologically relevant flow metrics were evaluated (Appendix C.). The following sections describe the changes in each IHA group separately.

3.5.1. Group 1: Magnitude of monthly water conditions

The first IHA group presents the monthly water conditions. The changes in monthly hydrological conditions for the period of January through December are presented in Figure III-12. According

to this figure, the average streamflow significantly increased from July to September approximately 63% under RCP 2.6 and 42% under RCP 8.5. The ranges of change from October to May were 1% to 16% for RCP 2.6, and -32% to 3% for RCP 8.5 (Figure III-12). The mean streamflow only decreased in April and May under RCP 8.5 scenarios. Streamflow decreases ranged from -32% to -17% under RCP 8.5. It is also worth to note that the ranges of relative changes in monthly streamflow for the future periods were significantly larger in June and July than in other months. These results recommend that the availability of aquatic ecosystem habitat will be effected in future summers. Thus, it appears that streamflow in the Upper Cahaba River watershed is more sensitive to climate change than to changes in LULC.

3.5.2. Group 2: Magnitude and duration of annual extreme water conditions

The magnitudes and durations of annual extreme water conditions under future LULC and climate change are presented in Figure III-13. Important differences were observed in the annual minimum-maximum flows under future RCP 2.6 and 8.5 scenarios, especially under RCP 8.5. The magnitudes of annual minimum flows decreased in RCP 2.6 ranging from -56% to -21%. The magnitudes of annual maximum and 90-day minimum flows were increased under future conditions ranging from 26% to 55%. On the contrary, the annual minimums significantly decreased in RCP 8.5 ranging from -87% to -65%. As similar as RCP 2.6, annual maximum and 90-day minimum flows showed an increasing trend in RCP 8.5 ranging from 7% to 69% (Figure III-13).

3.5.3. Group 3: Timing of annual extreme water conditions

The Julian dates of annual 1-day maximum and minimum changed significantly in both RCP 2.6 and 8.5 scenarios (Figure III-7.). In particular, annual 1-day minimum was 51 days (RCP2.6) and

40 days (RCP8.5) earlier than the baseline period, whereas 1-day maximum was 34 days (RCP 2.6) and 48 days (RCP 8.5) later than that of the baseline period.

3.5.4. Group 4: Rate and frequency of water conditions changes

Changes in this group define the stress of the aquatic ecosystem and its frequency caused by a rapid decrease or increase in streamflow. The parameters in this group were generally high due to combined impacts of LULC and climate change. Therefore, the rise and fall rates will be much faster under future LULC and climate conditions (Figure III-14). For instance, the median of the rise rate for both RCP 2.6 and 8.5 scenarios were 24 and 33%, respectively. Similarly, the median of fall rate for both RCP 2.6 and 8.5 scenarios were 49 and 45%, respectively.

3.5.5. Group5: Monthly low flows (EFCs)

Figure III-15 presents the impact of 22 climate change scenarios on monthly low flows. Monthly low flows are predicted to decrease in all months under RCP 2.6 and 8.5 scenarios ranging from -3% to -61%. Most important decreases are observed in March-June period.

3.6. Synergistic impact

This study have shown both LULC and climate change impact on watershed hydrology. However, there is a crucial need to assess the synergistic effects of these changes on water quantity in a watershed system. Figure III-16 shows the separate and synergistic effects of climate, LULC and combined changes on mean monthly streamflow of Upper Cahaba River watershed. We assessed the synergistic impact based on the following equation:

$$\Delta Q_{synergistic} = \Delta Q_{combined} - \Delta Q_{climate} - \Delta Q_{LULC}$$

As seen in Figure III-16, the mean monthly percentage change in streamflow is mainly due to LULC in October-February period. Conversely, changes in May-September period are due to climate change. They also have opposite impacts in January, October, and November. The study results revealed that the synergistic impact has significant influences on streamflow in July-August period. In addition to monthly flows, substantial synergistic impacts were observed on magnitude and duration of annual extreme water conditions, and monthly low flows. Figure III-17 shows the relative importance of LULC and climate impact on magnitude and duration of annual extreme water conditions. Synergistic impact of LULC and climate change was explored for 1-3-90 day minimum and 1-3-7 day maximum flows under RCP 2.6 scenarios. Synergistic impact on these minimum flows exceeds climate change impact in 1- and 3-day minimum flows. Similarly, synergistic interaction between LULC and climate change was observed for 1-3-7-30-90 day minimum and maximum flows under RCP 8.5 scenarios. For monthly low flows (EFCs), LULC is the main driver while climate change slightly impacts monthly low flows. Important synergistic impacts were detected in September-December period (Figure III-18).

4. SUMMARY AND CONCLUSION

This chapter explored the individual and combined impacts of LULC and climate change on hydrological responses using the hydrological model SWAT in the Upper Cahaba River watershed. 46 experiments were established and streamflows under each experiment were simulated by the SWAT model. The results from each experiment were fed into the Indicators of Hydrological Alteration (IHA) software to analyze impacts of LULC and climate change on ecologically relevant flow metrics.

Historical (2011) and future (2045) LULC maps were obtained from National Land Cover Database (NLCD) and USGS Earth Resources Observation and Science (EROS) center, respectively. For the baseline period (1988-2013), climate data were obtained from PRISM and CFRS. For the future period (2035-2060), information on the climate and climate change provided by eleven climate models (GCMs) under two representative concentration pathways (RCP 2.6 and RCP 8.5) provided by the World Climate Research Programme's (WCRP) Coupled Model Intercomparison Project Phase 5 (CMIP5) database. In this study, eleven GCMs (BCC-CSM1-1, GFDL-ESM2G, GFDL-ESM2M, IPSL-CM5A-LR, IPSL-CM5A-MR, MIROC5, MIROC-ESM, MIROC-ESM-CHEM, MRI-CGCM3, and NORESM1-M) were applied under RCP 2.6 and RCP 8.5 scenarios, resulting in an additional 22 sets of climate change data. The bias-corrected and downscaled are input into the SWAT model. To assess the ecosystem influences of estimated future streamflows, 38 ecologically relevant flow metrics were calculated with Indicators of Hydrological Alteration (IHA) software.

Based on the climate change scenarios, the Upper Cahaba River watershed will experience increasing temperature, especially in summer. The watershed will also experience increasing precipitation in spring, summer and winter. Compared to baseline period for 2035-2060, the monthly variance ranges of daily precipitation are -17% though +43%. For temperature, the variance range is estimated as between -0.4 °C and 6.9 °C. Moreover, urbanization rates are expected to increase for the future. USGS-EROS LULC data showed that percentage of urban areas within the watershed will increase from 35 to 47% in 2045. As urban areas expand, the amount of forest and agriculture areas will decrease.

The study results revealed that LULC and climate changes will significantly impact the hydrologic regime of the Upper Cahaba River watershed. For example, climate change will be

driving maximum monthly streamflow, especially in June-September period. This can be explained by changes in the precipitation pattern. Our study results also suggest that climate change will have a stronger impact on magnitude and duration of annual extreme water conditions. It is predicted that 1-3-7-30 day maximum flows will be significantly affected by future climate conditions. On the other hand, we explored that LULC will cause significant decreases in 1-3-7-30 day minimum flows and increases in rise and fall rates. Another important impact of LULC change will be occurred on timing of annual extreme water conditions, such as annual 1-day maximum and minimum water conditions. The timing of 1-day maximum flow will be shifted by approximately 23 days later. LULC change does not have a substantial impact on monthly mean streamflow, however increasing trends are identified in September-January period. Thus, when LULC change is combined with climate change, it is observed that streamflow of the Upper Cahaba River watershed is predicted to increase in all months, except in April. Furthermore, more dramatic decreasing trends in 1-3-7-30 day minimum flows and monthly low flows, and increasing trend for timing of 1-day maximum flow (48 days later) were explored for combined impacts of LULC and climate changes, especially under RCP 8.5 scenarios.

5. REFERENCES

Arnold, J.G., Srinivasan, R., Muttiah, R.S., Williams, J.R. (1998). Large area hydrologic modeling and assessment: Part I. Model development. JAWRA, 34(1):73–89.

Brath A., Montanari A., Moretti G. (2006). Assessing the effect on flood frequency of land use change via hydrological simulation (with uncertainty). Journal of Hydrology, 324(1–4):141–153.

Costa, M.H., Botta, A., Cardille, J.A. (2003). Effects of large-scale changes in land cover on the discharge of the Tocantins River, Southeastern Amazonia. Journal of Hydrology, 283:206–217.

Cousino, L.K., Becker, R.H, Zmijewski, A.K. (2015). Modeling the Effects of Climate Change on Water, Sediment, and Nutrient Yields from the Maumee River Watershed. Journal of Hydrology: Regional Studies. Elsevier B.V. doi:10.1016/j.ejrh.2015.06.017.

Cui, B., Q. Yang, Z. Yang, and K. Zhang, (2009). Evaluating the Eco- logical Performance of Wetland Restoration in the Yellow River Delta, China. Ecological Engineering, 35:1090-1103.

Debele, B., R. Srinivasan, and J. Y. Parlange. (2008). Coupling upland watershed and downstream waterbody hydrodynamic and water quality models (SWAT and CE-QUAL-W2) for better water resources management in complex river basins. Environ. Modeling Assess., 13(1): 135-153.

Drusch, M., Wood, E. F., Gao, H. (2005). Observation operators for the direct assimilation of TRMM microwave imager retrieves soil moisture. Geophysical Research Letters, 32, L15403, doi:10.1029/2005GL023623.

Dudgeon, D., Arthington, A.H., Gessner, M.O., Kawabata Z.I., Knowler, D.J., Leveque, C., Naiman, R.J., Prieur-Richard, A.H., Soto, D., Stiassny, M. L. J., Sullivan, C.A. (2006). Freshwater biodiversity: importance, threats, status and conservation challenges, Biol. Rev., 81:163–182.

Dyer, F., ElSawah, S., Croke, B., Griffiths, R., Harrison, E., Lucena-Moya, P., & Jakeman, A. (2013). The effects of climate change on ecologically-relevant flow regime and water quality attributes. Stochastic Environmental Research and Risk Assessment, 28(1):67–82. http://doi.org/10.1007/s00477-013-0744-8

El-Khoury, A., Seidou, O., Lapen, D.R., Que, Z., Mohammadian, M., Sunohara, M., Bahram, D. (2015). Combined impacts of future climate and land use changes on discharge, nitrogen and phosphorus loads for a Canadian river basin. Journal of Environmental Management, 151:76–86. http://doi.org/10.1016/j.jenvman.2014.12.012.

Ficklin, D.L., Luo, Y., Luedeling, E., Zhang, M. (2009). Climate change sensitivity assessment of a highly agricultural watershed using SWAT model. J. Hydrol., 374:16–29.

Fischlin, A., Midgley, G. F., Price, J. T., Leemans, R., Gopal, B., Turley, C., Rounsevell, M. D. A., Dube, O. P., Tarazona, J., and Velichko, A. A. (2007). Ecosystems, their properties, goods, and services. Climate Change 2007: Impacts, Adaptation and Vulnerability. Contribution of Working Group II to the Fourth Assessment Report of the Intergovernmental Panel on Climate Change, edited by: Parry, M. L., Canziani, O. F., Palutikof, J. P., van der Linden, P. J., and Hanson, C. E., Cambridge University Press, Cambridge, 211–272.

Gassman, P.W., Reyes, M.R., Green, C.H., Arnold, J.G. (2007). The soil and water assessment tool: historical development applications, and future research directions. Trans. ASABE, 50(4):1211–1250.

Ghaffari, G., S. Keesstra, J. Ghodousi, and H. Ahmadi. (2010). SWAT-simulated hydrological impact of land-use change in the Zanjanrood basin, northwest Iran. Hydrol. Proc., 24(7):892-903.

Guo, H., Hu, Q., Jiang, T. (2008). Annual and seasonal streamflow responses to climate and land cover changes in the Poyang lake basin, China. Journal of Hydrology, 355(1-4):106-122.

Hart, D.D., Finelli, C.M. (1999). Physical–biological coupling in streams: the pervasive effects of flow on benthic organisms. Annu. Rev. Ecol. Syst., 30:363–395.

IPCC. (2007). Summary for policymakers. In: Solomon, S., Qin, D., Manning, M., Chen, Z., Marquis, M., Averyt, K.B., Ignor, M.T., Miller, H.L. (Eds.), Contribution of Working Group I to the Fourth Assessment Report of the Intergovernmental Panel on Climate Change, 2007. Cambridge University Press, Cambridge, United Kingdom and New York, NY, USA.

Jha, M., Arnold, J.G., Gassman, P.W., Giorgi, F., Gu, R.R. (2006). Climate change sensitivity assessment on Upper Mississippi River Basin streamflows using SWAT. J. Am. Water Resour. Assoc., 42(4):997–1015.

Jha, M., Gassman, P.W., Secchi, S.S., Gu, R., Arnold, J.G. (2004). Effect of watershed subdivision on SWAT flow, sediment, and nutrient predictions J. Am. Water Resour. Assoc., 40(3):811–825.

Kim, J., Choi, J., Choi, C., Park, S. (2013). Impacts of changes in climate and land use/land cover under IPCC RCP scenarios on streamflow in the Hoeya River Basin, Korea. Sci Total Environ., 452-453:181-195. doi:10.1016/j.scitotenv.2013.02.005.

Kingston, D.G., Taylor, R.G. (2010). Sources of uncertainty in climate change impacts on river discharge and groundwaterin a headwater catchment of the Upper Nile Basin. Uganda Hydrol. Earth Syst. Sci., 14:1297–1308, http://dx.doi.org/10.5194/hess-14-1297-2010.

Kirsch, K., Kirsch, A., Arnold, J., (2002). Predicting sediment and phosphorus loads in the Rock River basin using SWAT. Forest 971, 10.

Lasalle, G. and Rochard, E. (2009). Impact of twenty-first century climate change on diadromous fish spread over Europe, North Africa and the Middle East, Glob. Change Biol., 15:1072–1089.

Leopold, L. (1968). Hydrology for urban land planning—A guidebook on the hydrologic effects of urban land use, U.S. Geol. Surv. Circ.,554, 18 pp.

Li, L., Li, B., Liang, L., Li, J., Liu, Y. (2010). Effect of climate change and land use on stream flow in the upper and middle reaches of the Taoer River, northeastern China. Forestry Studies in China, 12(3):107–115.

Li, L.J., Jiang, D.J., Li, J.Y. (2007a). A summary and perspective of forest vegetation impacts on water yield. J Nat Resour, 22(2): 211–224.

Li, Z., Liu, W.Z., Zhang, X.C., Zheng, F.L. (2009) Impacts of land use change and climate variability on hydrology in an agricultural catchment on the Loess Plateau of China. J. Hydrol., 377:35–42.

Luo, Y., Gerten, D., LE Maire, G., Parton, W.J., Weng, E., Zhou, X., Keough, C., Beier, C., Ciais, P., Cramer, W., Dukes, J.S., Emmett, B., Hanson P.J., Knapp, A., Linder, S. , Nepstad, D., Rustad, L. (2008). Modeled interactive effects of precipitation, temperature, and [CO2] on ecosystem carbon and water dynamics in different climatic zones. Global Change Biology, 14:1986–1999.

Luo, Y., He, C., Sophocleous, M., Yin, Z., Hongrui, R., Ouyang, Z. (2008) Assessment of crop growth and soil water modules in SWAT2000 using extensive field experiment data in an irrigation district of the Yellow River Basin. J. Hydrol., 352(1):139–156.

Ma, X., Xu, J.C., Luo, Y., Aggarwal, S.P., Li, J.T. (2009). Response of hydrological processes to land-cover and climate changes in Kejie watershed, south-west China. Hydrol. Process., 23:1179–1191.

Mango, L. M., Melesse, A. M., McClain, M. E., Gann, D., and Setegn, S. G., (2011). Land Use and Climate Change Impacts on the Hydrology of the Upper Mara River Basin, Kenya: Results of a Modeling Study to Support Better Resource Management. Hydrology and Earth System Sciences, 15(7):2245–58. doi:10.5194/hess-15-2245-2011.

Maurer, E. P., Hidalgo, H. G., Das, T., Dettinger, M. D., Cayan, D. R. (2010). The utility of daily large-scale climate data in the assessment of climate change impacts on daily streamflow in California, Hydrol. Earth Syst. Sci., 14, 1125-1138.

Millennium Ecosystem Assessment: Ecosystems and human well-being: wetlands and water synthesis.World Resources Institute, Washington, DC, 2005.

Min, F., Shibata, H. (2015). Simulation of Watershed Hydrology and Stream Water Quality under Land Use and Climate Change Scenarios in Teshio River Watershed, Northern Japan. Ecological Indicators 50:79–89. doi:10.1016/j.ecolind.2014.11.003.

Moss, R. H., Edmonds, J. A., Hibbard, K. A., Manning, M. R., Rose, S. K., Van Vuuren, D. P., Carter, T. R., Emori, S., Kainuma, M., Kram, T., Meehl, G. A., Mitchell, J. F. B., Nakicenovic, N., Riahi, K., Smith, S. J., Stouffer, R. J., Thomson, A. M., Weyant, J. P., Wilbanks, T. J. (2010). The next generation of scenarios for climate change research and assessment. Nature, 463, 747–756.

Neitsch, S.L., Arnold, J.G., Kiniry, J.R., Williams, J.R. (2011). Soil and water assessment tool theoretical documentation: version 2009, Texas Water Resources Institute Technical Report No. 406. Texas Water Resources Institute, USA.

Pervez, M.S., Henebry, G.M., (2015). Assessing the impacts of climate and land use and land cover change on the freshwater availability in the Brahmaputra River basin. J. Hydrol. Reg. Stud., 3:285–311.

Piao, S., Friedlingstein, P., Ciais, P., de Noblet-Ducoudré, N., Labat, D., Zaehle, S. (2007). Changes in climate and land use have a larger direct impact than rising CO2 on global river runoff trends. Proceedings of the National Academy of Sciences of the United States of America, 104(39), 15242–7. http://doi.org/10.1073/pnas.0707213104

Poff, N.L., Allan, J.D., Bain, M.B., Karr, J.R., Prestegaard, K.L., Richter, B.D., Sparks, R.E., Stromberg, J.C., (1997). The natural flow regime: a paradigm for river conservation and restoration. Bioscience, 47:769–784.

Prowse, T.D. (2006). Climate change, flow regulation and land-use effects on the hydrology of the Peace-Athabasca-Slave system: findings from the northern rivers ecosystem initiative. Environ. Monit. Assess., 113:167–197.

Rahman, K., Maringanti, C., Beniston, M., Widmer, F., Abbaspour, K., Lehmann, A., (2013). Streamflow modeling in a highly managed mountainous glacier watershed using SWAT: the Upper Rhone River watershed case in Switzerland. Water Resour. Manage., 27(2):323–339.

Reclamation, (2013). 'Downscaled CMIP3 and CMIP5 Climate and Hydrology Projections: Release of Downscaled CMIP5 Climate Projections, Comparison with preceding Information, and Summary of User Needs', prepared by the U.S. Department of the Interior, Bureau of Reclamation, Technical Services Center, Denver, Colorado. 47pp.

Richter, B.D., Baumgartner, J.F., Powell, J., Braun, D.P. (1996). A method for assessing hydrologic alterations within ecosystems. Conservation Biology 10(4): 1163–1174.

Richter, B.D., Matthew, R., Harrison, D.L., and Wigington, R. (2003). Ecologically sustainable water management: managing river flows for ecological integrity, Ecol. Appl., 13: 206–224.

Sample, J., Dunn, S., Brown, I., Towers, W. (2012). Scotland's Water Resources: Impacts of Land Use and Climate.

Schulze, R.E. (2000). Hydrological responses to land use and climate change. A southern African perspective. AMBIO, 29(1):12–22.

Schuol, J., Abbaspour, K.C., Srinivasan, R., Yang, H. (2008). Estimation of freshwater availability in the West African sub-continent using the SWAT hydrologic model. J. Hydrol., 352 (1–2):30–49.

Sharpley, A.N., Williams, J.R. (1990). EPIC-Erosion Productivity Impact Calculator, I. Model Documentation; U.S. Department of Agriculture, Agricultural Research Service: Washington, DC, USA, p. 235.

Shi, P.J., Gong, P., Li, X.B., (2000). Methods and Practice of Land Use and Land Cover Change. Beijing: Science Press.

The Nature Conservancy, 2009. Indicators of Hydrologic Alteration Version 7.1 User's Manual. Available at: https://www.conservationgateway.org/Documents/IHAV7.pdf

Tibebe, D., Bewket, W. (2011). Surface runoff and soil erosion estimation using the SWAT model in the Keleta watershed, Ethiopia. Land Degrad. Dev., 22(6):551–564.

Tomer, M.D., Schilling, K.E. (2009). A Simple Approach to Distinguish Land-Use and Climate Change Effects on Watershed Hydrology. Journal of Hydrology, 376:24-33.

Vorosmarty, C.J., Green, P., Salisbury, J., Lammers, R.B. (2000). Global water resources: vulnerability from climate change and population growth. Science, 289:284–288.

Wang, G.X., Zhang, Y., Liu, G.M., Chen, L. (2006). Impact of land-use change on hydrological processes in the Maying River basin, China. Sci China Ser D Earth Sci, 49(10):1098–1110.

Wang, K., Dickinson, R.E., Wild, M., Liang, S. (2010). Evidence for Decadal Variation in Global Terrestrial Evapotranspiration Between 1982 and 2002: 2. Results. Journal of Geophysical Research 115:D20113.

Wang, R., Kalin, L., Kuang, W., Tian, H. (2014). Individual and combined effects of land use/cover and climate change on Wolf Bay watershed streamflow in southern Alabama. Hydrological Processes, 28(22):5530–5546. http://doi.org/10.1002/hyp.10057

Xu, H., Taylor, R.G., Xu, Y., (2011). Quantifying uncertainty in the impacts of climate change on river discharge in sub- catchments of the Yangtze and Yellow River Basins, China. Hydrol. Earth Syst. Sci., 15:333–344, http://dx.doi.org/ 10.5194/hess-15-333-2011.

Yang, T., Zhang, Q., Chen, D.Y., Tao, X., Xu, C.Y., Chen, X. (2008). A spatial assessment of hydrologic alteration caused by dam construction in the middle and lower Yellow River, China. Hydrol. Process., 22:3829–3843.

Zhang, H., Huang, G.H., Wang, D., Zhang, X. (2011). Uncertainty assessment of climate change impacts on the hydrology of small prairie wetlands. J. Hydrol., 396, 94–103.

Zhang, K., Kimball, J.S., Nemani, R.R, Running, S.W. (2010). A Continuous Satellite-Derived Global Record of Land Surface Evapotranspiration from 1983 to 2006. Water Resources Research, 46:W09522.

Zhang, Q., Gu, X., Singh, V. P., Chen, X. (2015). Evaluation of ecological instream flow using multiple ecological indicators with consideration of hydrological alterations. Journal of Hydrology, 529:711–722. http://doi.org/10.1016/j.jhydrol.2015.08.066

Zhang, Y.K., Schilling K.E, (2006b). Increasing Streamflow and Baseflow in Mississippi River Since the 1940s: Effect of Land Use Change. Journal of Hydrology 324:412-422.

Table III-1. Input data used in the SWAT model and data sources.

Input data	Data source	References
LULC map	NLCD and Digitized Landsat 5 TM, USGS-EROS (250m)	National Land Cover Database (NLCD): http://www.mrlc.gov/ Landsat images: http://earthexplorer.usgs.gov/ USGS-EROS: http://landcover-modeling.cr.usgs.gov/
Soil map	SSURGO	United States Department of Agriculture (USDA): https://gdg.sc.egov.usda.gov/
DEM	USDA (10 m)	United States Department of Agriculture (USDA): https://gdg.sc.egov.usda.gov/
Measured Streamflow	USGS	USGS National Water Information System: http://waterdata.usgs.gov/
Historical Climate data	PRISM and CFRS	PRISM Climate Group: http://prism.oregonstate.edu/ NCEP Climate Forecast System Reanalysis (CFRS): http://rda.ucar.edu/
Future Climate data	CMIP5	Coupled Model Intercomparison Project Phase 5 (CMIP5): http://cmip-pcmdi.llnl.gov/cmip5/

Table III-2. List of the CMIP5 climate models used in this study under RCP 2.6 and 8.5 scenarios.

Number	Model Name	Modeling Center (or Group)
1	BCC-CSM1-1	Beijing Climate Center, China Meteorological Administration, China
2	CCSM4	National Center of Atmospheric Research, USA
3	GFDL-ESM2G	NOAA Geophysical Fluid Dynamics Laboratory, USA
4	GFDL-ESM2M	NOAA Geophysical Fluid Dynamics Laboratory, USA
5	IPSL-CM5A-LR	Institut Pierre Simon Laplace, France
6	IPSL-CM5A-MR	Institut Pierre Simon Laplace, France
7	MIROC5	Atmosphere and Ocean Research Institute (The University of Tokyo), National Institute for Environmental Studies,and Japan Agency for Marine-Earth Science and Technology, Japan
8	MIROC-ESM	Japan Agency for Marine-Earth Science and Technology, Atmosphere and Ocean Research Institute (The University of Tokyo), and National Institute for Environmental Studies, Japan
9	MIROC-ESM-CHEM	Japan Agency for Marine-Earth Science and Technology, Atmosphere and Ocean Research Institute (The University of Tokyo), and National Institute for Environmental Studies, Japan
10	MRI-CGCM3	Meteorological Research Institute, Japan
11	NORESM1-M	Norwegian Climate Center, Norway

*Representative Concentration Pathways (RCPs) represent pathways of radiative forcing. RCP 2.6 (low emissions) and 8.5 (high emissions) lead to a radiative forcing of 2.6 and 8.5 W/m^2 by 2100, respectively (additional information can be found in Moss et al., 2010).

Table III-3. Summary of hydrological parameters used in the IHA to characterize flow regime and their ecosystem influences.

IHA Parameter Group	Hydrologic Parameters	Ecosystem Influences
1. Magnitude of monthly water conditions	Mean value for each calendar month	▪ Habitat availability for aquatic organisms ▪ Soil moisture availability for plants ▪ Availability of water for terrestrial animals ▪ Availability of food/cover for furbearing mammals ▪ Reliability of water supplies for terrestrial animals ▪ Access by predators to nesting sites ▪ Influences water temperature, oxygen levels, photosynthesis in water column
	Subtotal 12 parameters	
2. Magnitude and duration of annual extreme water conditions	Annual minima, 1-day mean Annual minima, 3-day means Annual minima, 7-day means Annual minima, 30-day means Annual minima, 90-day means Annual maxima, 1-day mean Annual maxima, 3-day means Annual maxima, 7-day means Annual maxima, 30-day means Annual maxima, 90-day means	▪ Balance of competitive, ruderal, and stress- tolerant organisms ▪ Creation of sites for plant colonization ▪ Structuring of aquatic ecosystems by abiotic vs. biotic factors ▪ Structuring of river channel morphology and physical habitat conditions ▪ Soil moisture stress in plants Dehydration in animals ▪ Anaerobic stress in plants ▪ Volume of nutrient exchanges between rivers and floodplains ▪ Duration of stressful conditions such as low oxygen and concentrated chemicals in aquatic environments ▪ Distribution of plant communities in lakes, ponds, floodplains ▪ Duration of high flows for waste disposal, aeration of spawning beds in channel sediments
	Subtotal 10 parameters	
3. Timing of annual extreme water conditions	Julian date of each annual 1-day maximum Julian date of each annual 1-day minimum	▪ Compatibility with life cycles of organisms Predictability/avoidability of stress for organisms ▪ Access to special habitats during reproduction or to avoid predation ▪ Spawning cues for migratory fish ▪ Evolution of life history strategies, behavioral mechanisms
	Subtotal 2 parameters	
4. Rate and frequency of water condition changes	Rise rates: Mean or median of all positive differences between consecutive daily values Fall rates: Mean or median of all negative differences between consecutive daily values	▪ Drought stress on plants (falling levels) ▪ Entrapment of organisms on islands, floodplains (rising levels) ▪ Desiccation stress on low-mobility streamedge (varial zone) organisms

	Subtotal 2 parameters	
5. Environmental Flow Components (EFCs) Parameters – Monthly low flows	Mean values of low flows during each calendar month	▪ Provide adequate habitat for aquatic organisms ▪ Maintain suitable water temperatures, dissolved oxygen, and water chemistry ▪ Maintain water table levels in floodplain, soil moisture for plants ▪ Provide drinking water for terrestrial animals ▪ Keep fish and amphibian eggs suspended ▪ Enable fish to move to feeding and spawning areas ▪ Support hyporheic organisms (living in saturated sediments)
	Subtotal 12 parameters	
	Ground total 38 parameters	

Table III-4. Model experiment setup.

	a	**b**	**c**	**d**
LULC	2011	2011	2045 A1B	2045 A1B
Weather	Historical climate	22 future climate model	Historical climate	22 future climate model
	(1*1= 1)	(**1*22= 22**)	(**1*1= 1**)	(**1*22= 22**)

The letters show the scenarios: (a) Baseline period, (b) only climate change, (c) only LULC change, (d) combined impact of LULC and climate change. A total simulation number is 46.

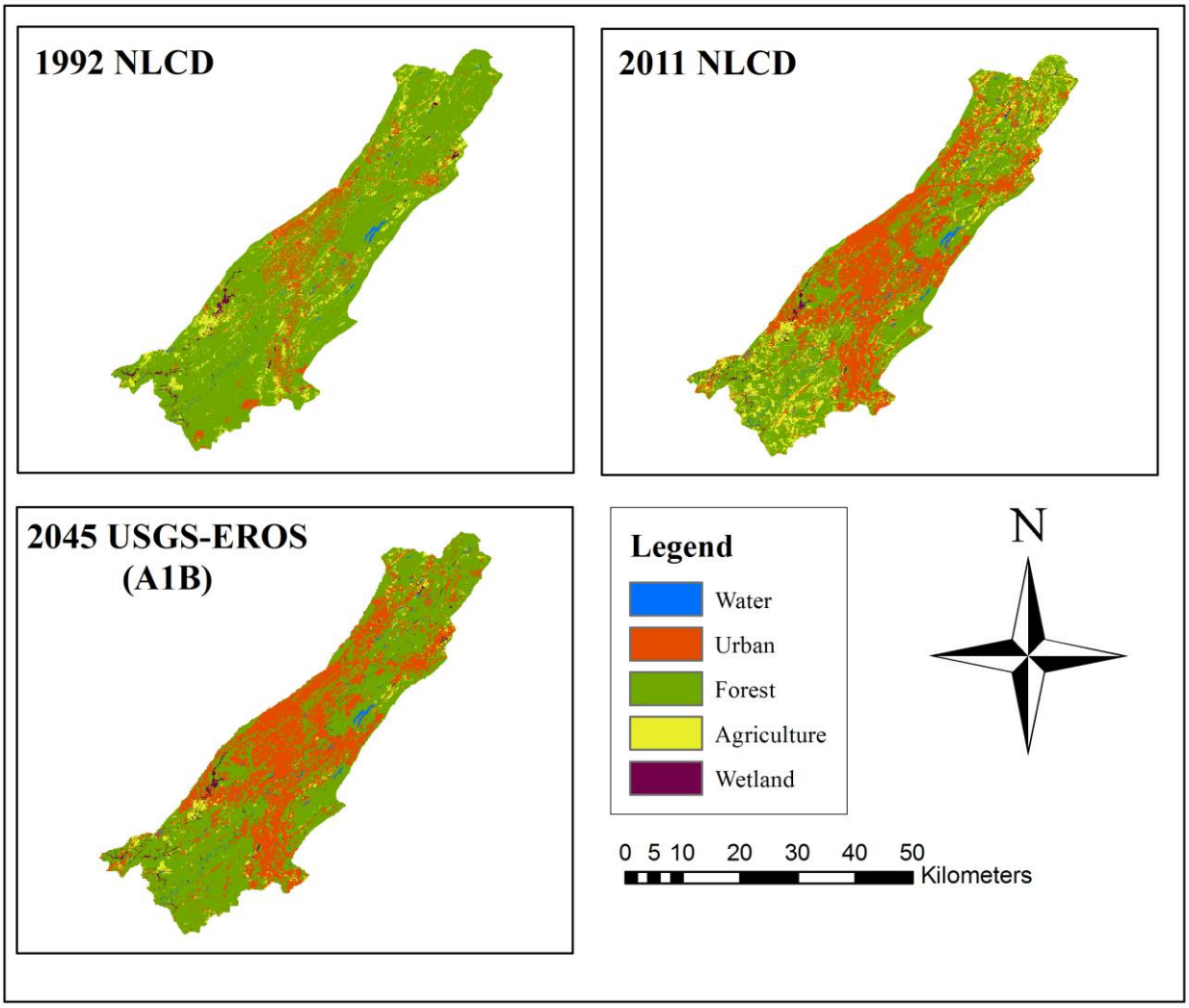

Figure III-1. LULC datasets used in this study.

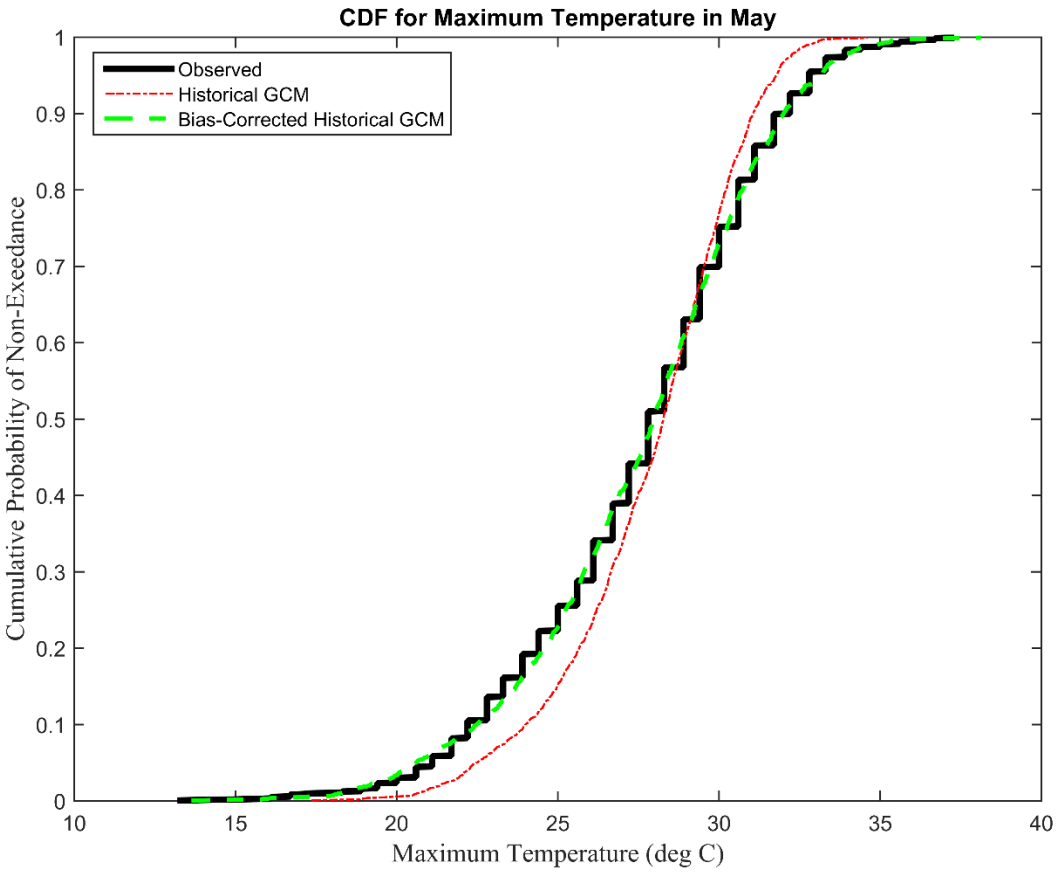

Figure III-2. Cumulative distribution functions (CDFs) for historical (observed) maximum temperature data, historical conditions of a GCM and the bias-corrected historical GCM. Note that this graph displays pool of the daily maximum temperature values for May from 1950 to 1999.

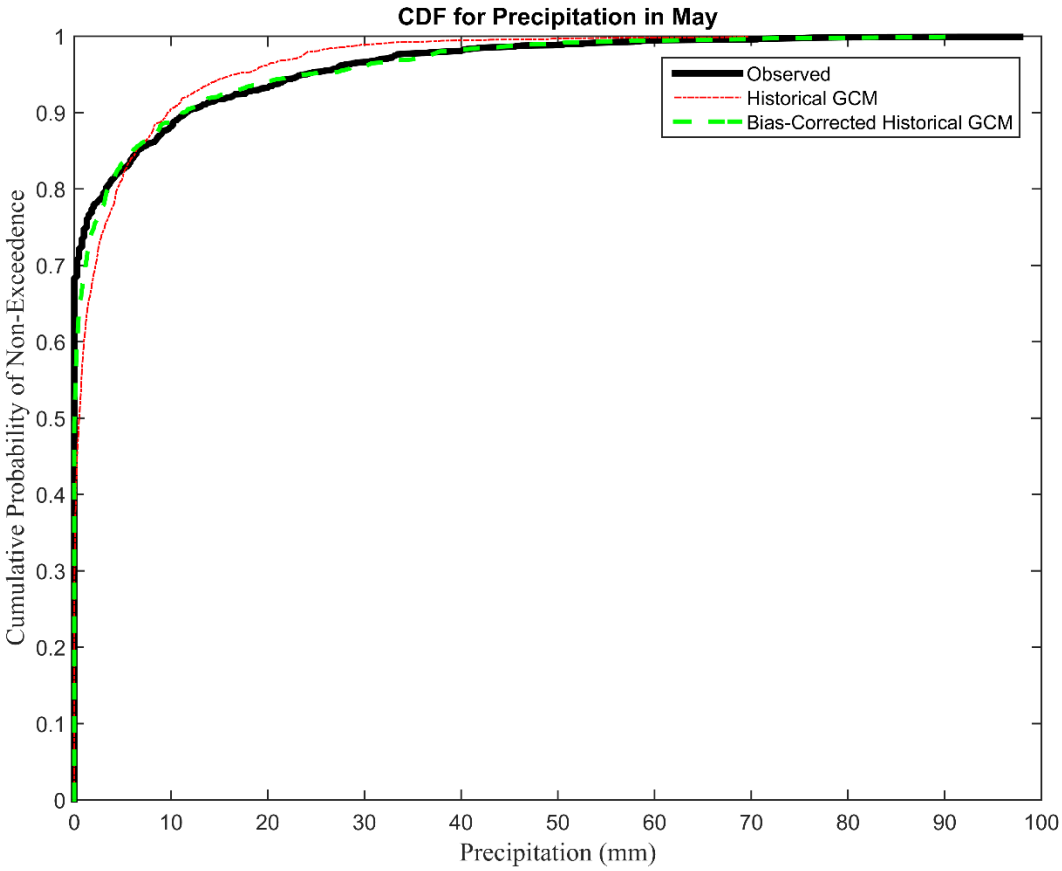

Figure III-3. Cumulative distribution functions (CDFs) for historical (observed) precipitation data, historical conditions of a GCM and the bias-corrected historical GCM. Note that this graph displays pool of the daily precipitation values for May from 1950 to 1999.

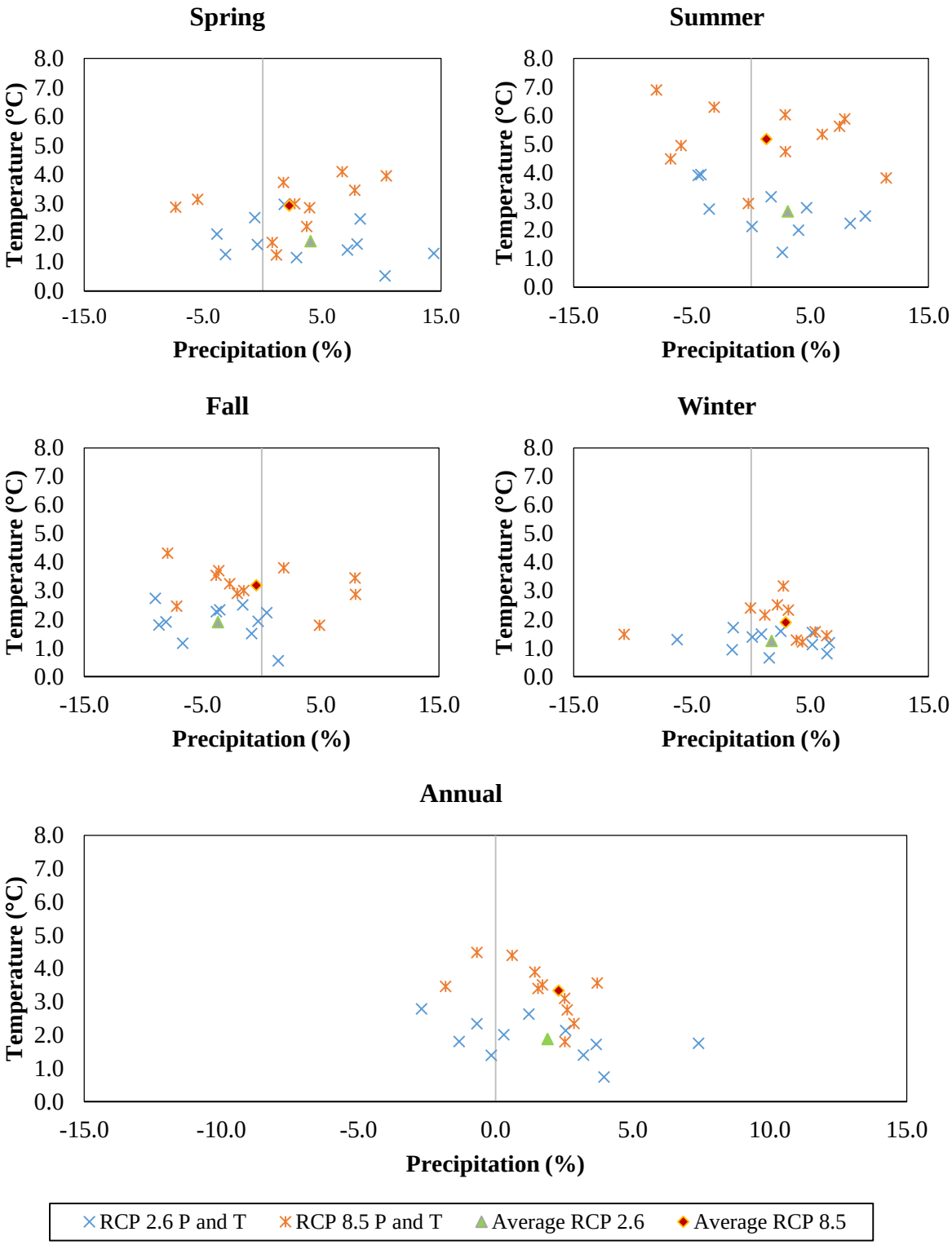

Figure III-4. Seasonal mean temperature and precipitation variation from the baseline period according to 11 climate models under RCP 2.6 and 8.5 emission scenarios. The 22 dots in each panel correspond to 22 future climate models under RCP 2.6 and 8.5 emissions scenarios.

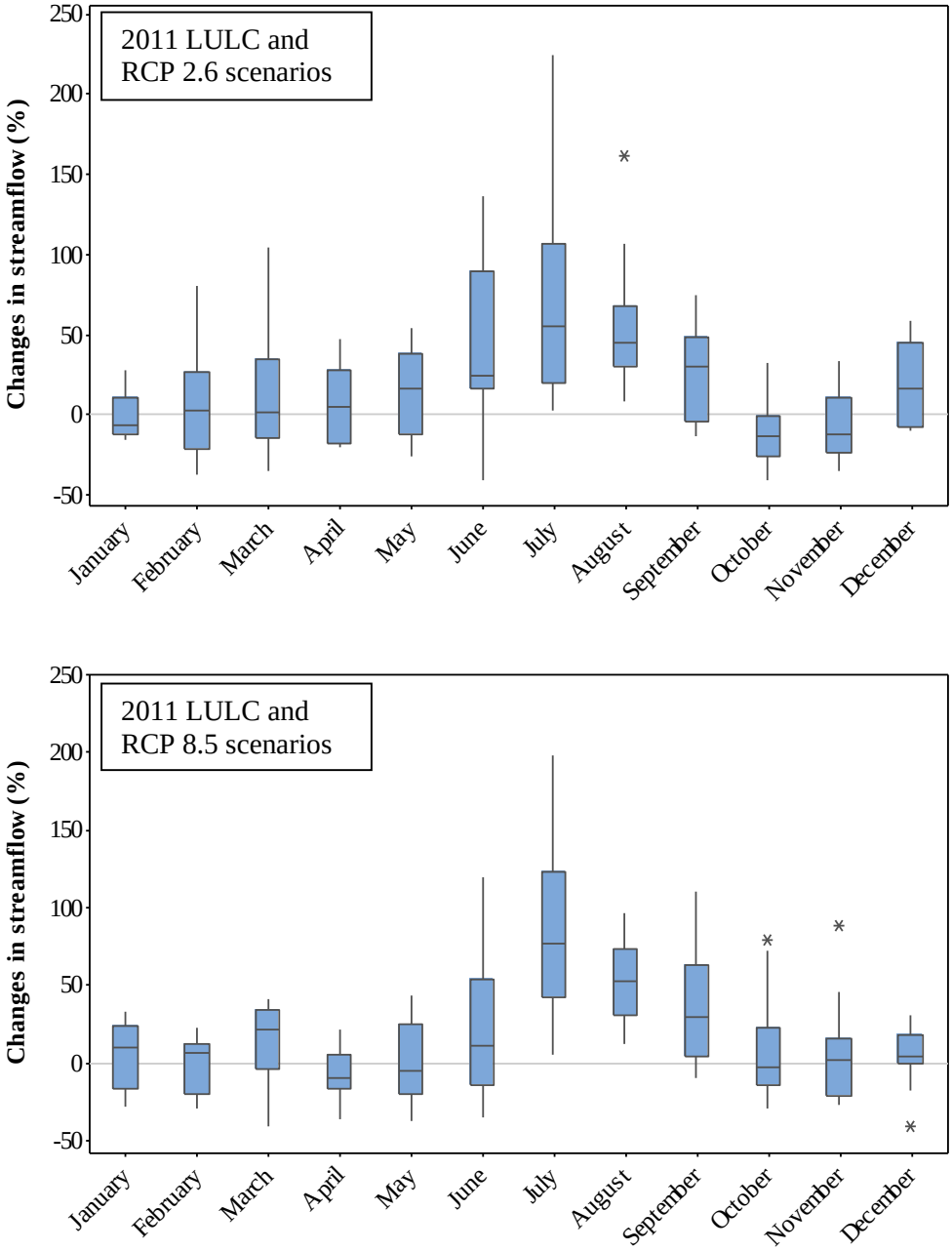

Figure III-5. Magnitude of monthly water conditions (Only climate change, group 1). The boxes define the median values (horizontal central line), the 25th, 50th and 75th percentile values, and the vertical bars (whiskers) define the 10th and 90th percentile values.

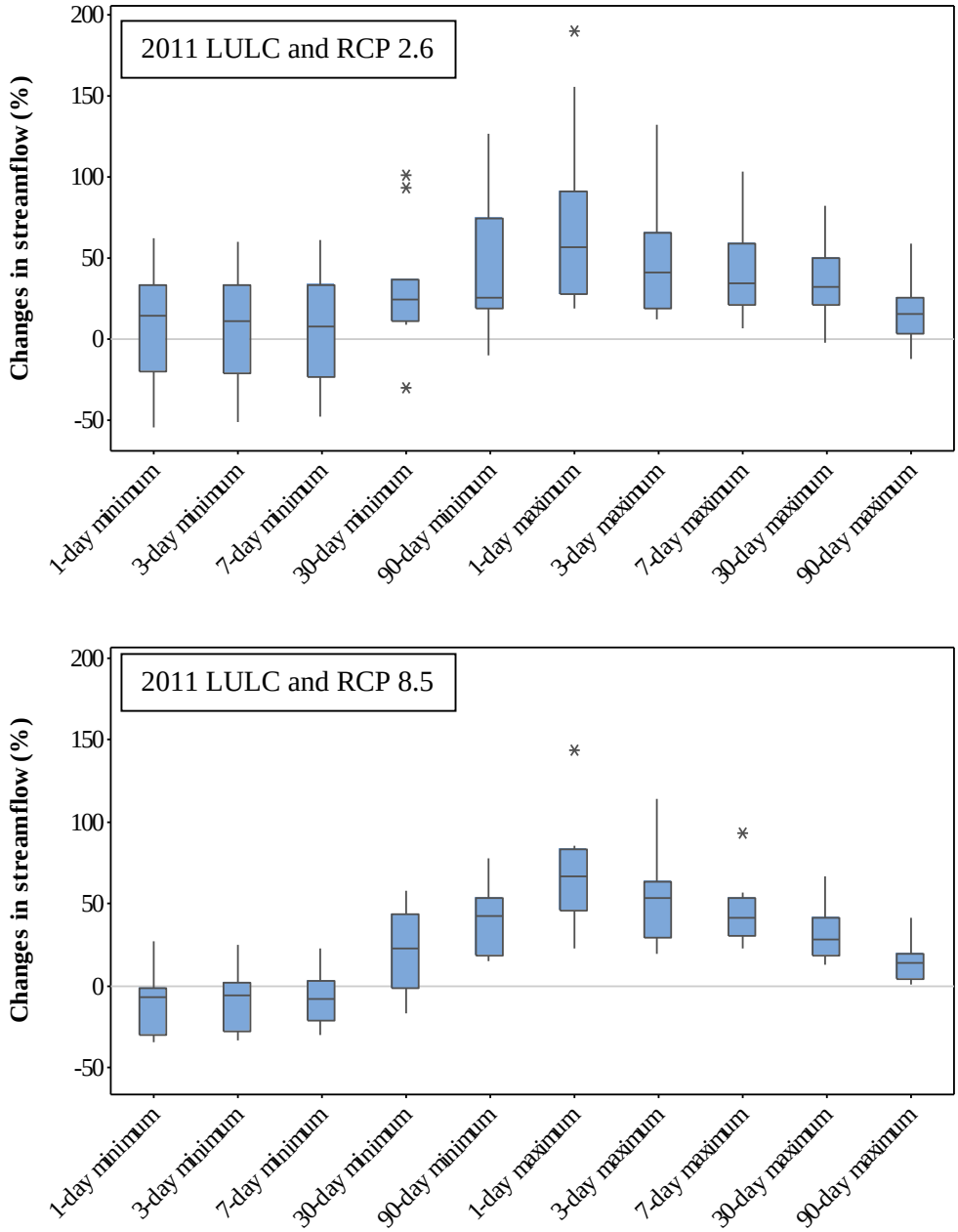

Figure III-6. Magnitude and duration of annual extreme water conditions (Only climate change, group 2). The boxes define the median values (horizontal central line), the 25th, 50th and 75th percentile values, and the vertical bars (whiskers) define the 10th and 90th percentile values.

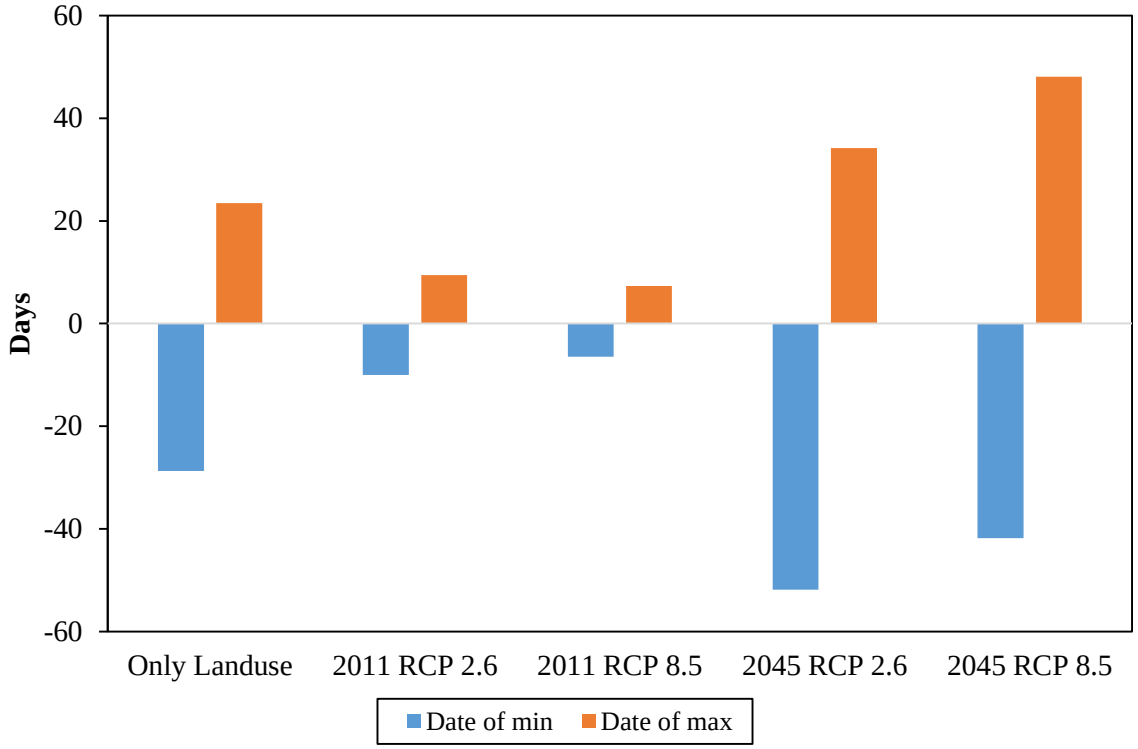

Figure III-7. Timing of annual extreme water conditions of all scenarios. Only land use/cover change (2045 LULC + historical climate), only climate change (2011 LULC + future climate), combined impacts (2045 LULC + future climate) (Group 3).

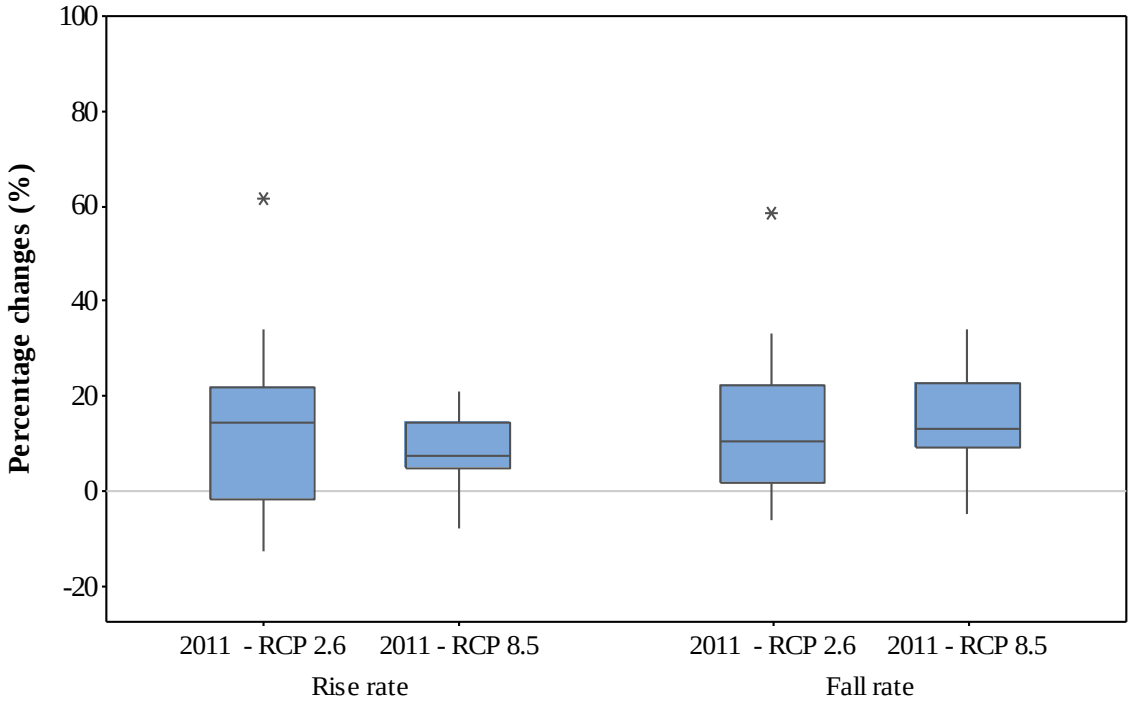

Figure III-8. Rate and frequency of water condition changes (Only climate change, group 4). The boxes define the median values (horizontal central line), the 25th, 50th and 75th percentile values, and the vertical bars (whiskers) define the 10th and 90th percentile values.

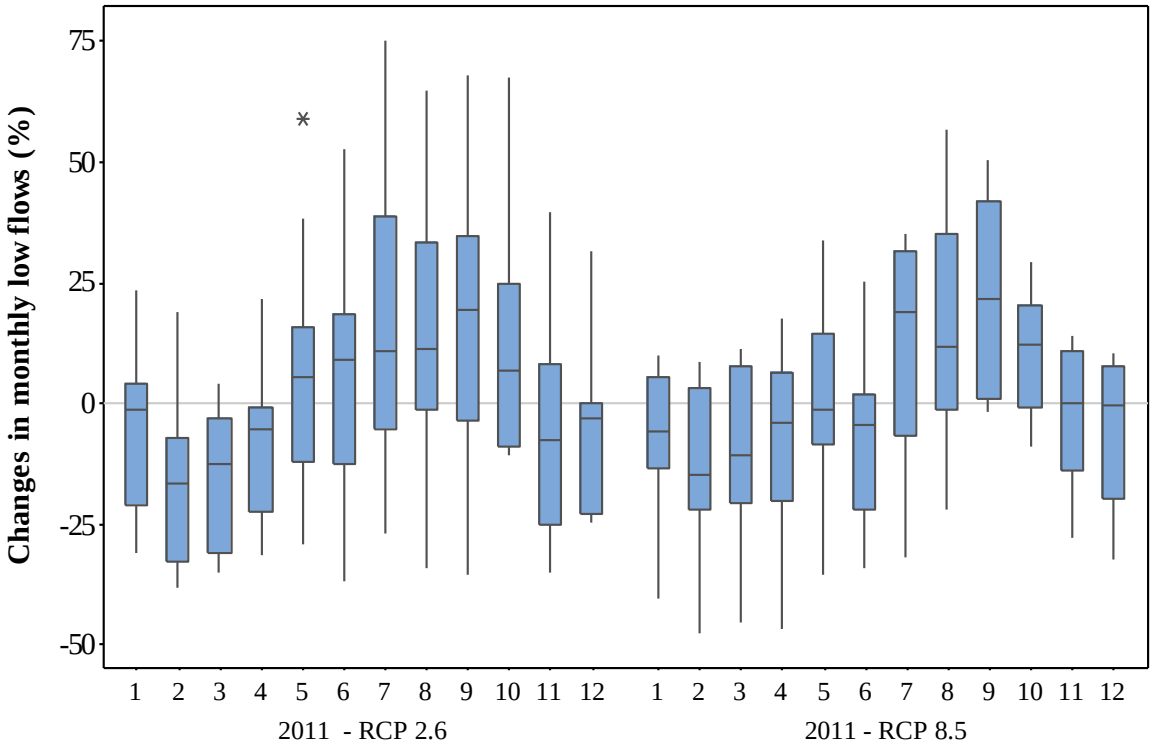

Figure III-9. Monthly low flows (Only climate change, group 5 - EFCs). The boxes define the median values (horizontal central line), the 25th, 50th and 75th percentile values, and the vertical bars (whiskers) define the 10th and 90th percentile values.

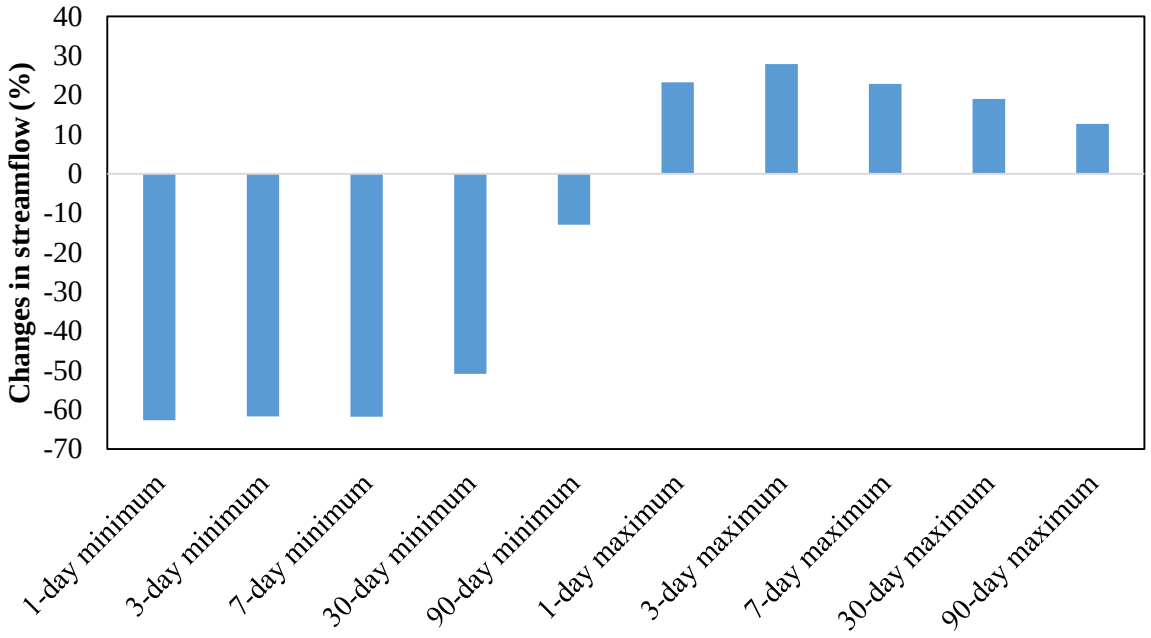

Figure III-10. Magnitude and duration of annual extreme water conditions (Only LULC, group 2.)

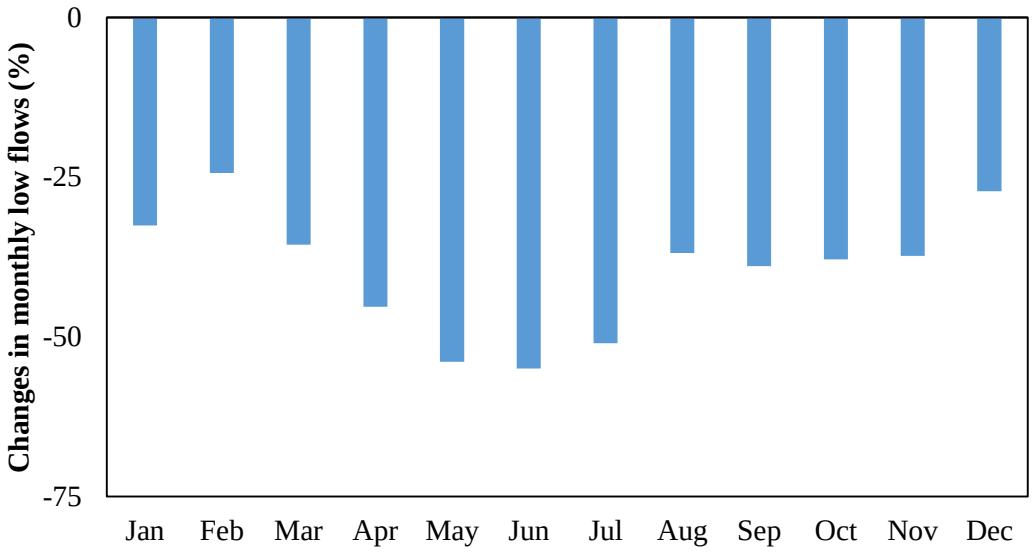

Figure III-11. Monthly low flows (Only LULC, group 5 - EFCs)

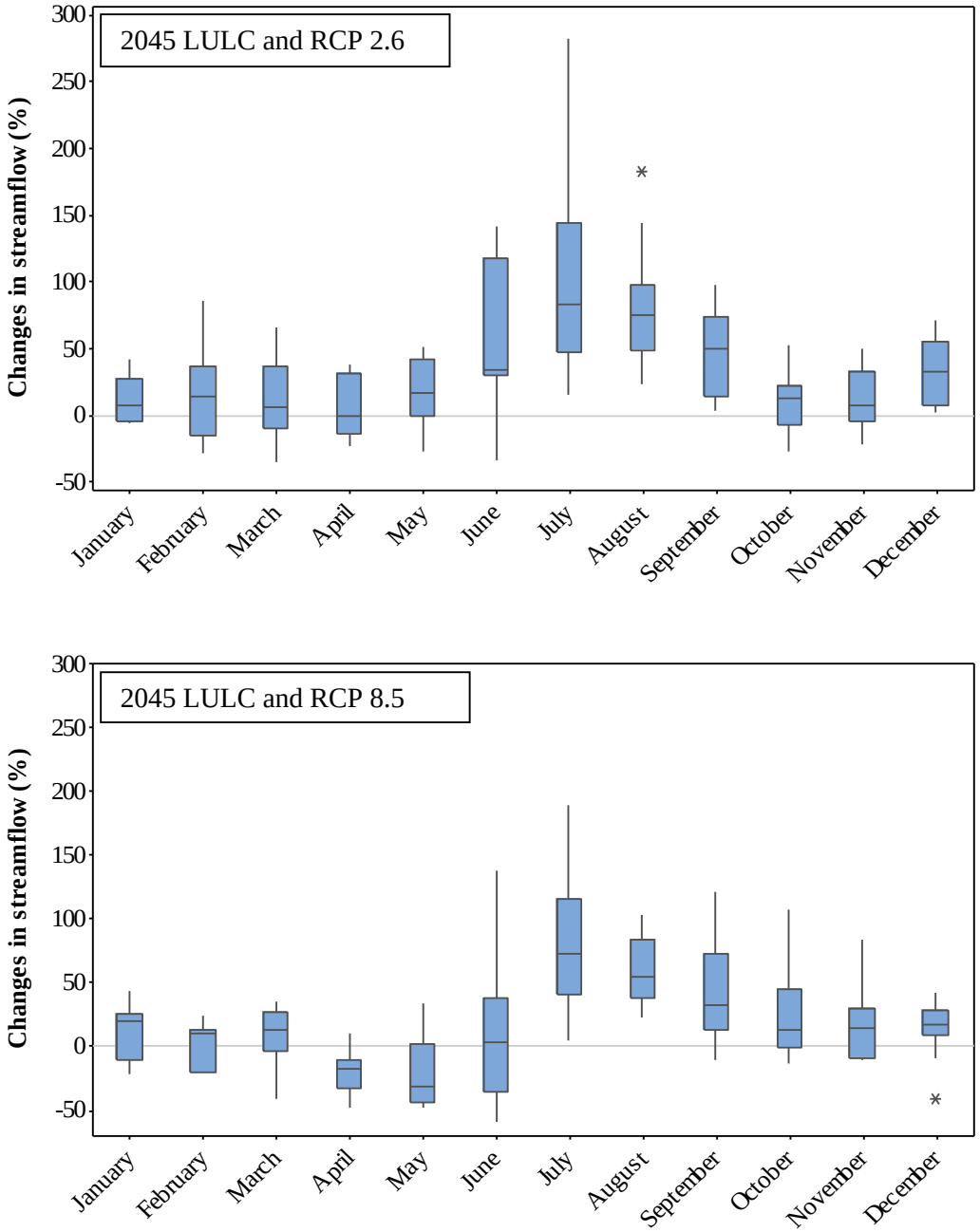

Figure III-12. Magnitude of monthly water conditions (Combined impacts – IHA group 1). The boxes define the median values (horizontal central line), the 25th, 50th and 75th percentile values, and the vertical bars (whiskers) define the 10th and 90th percentile values.

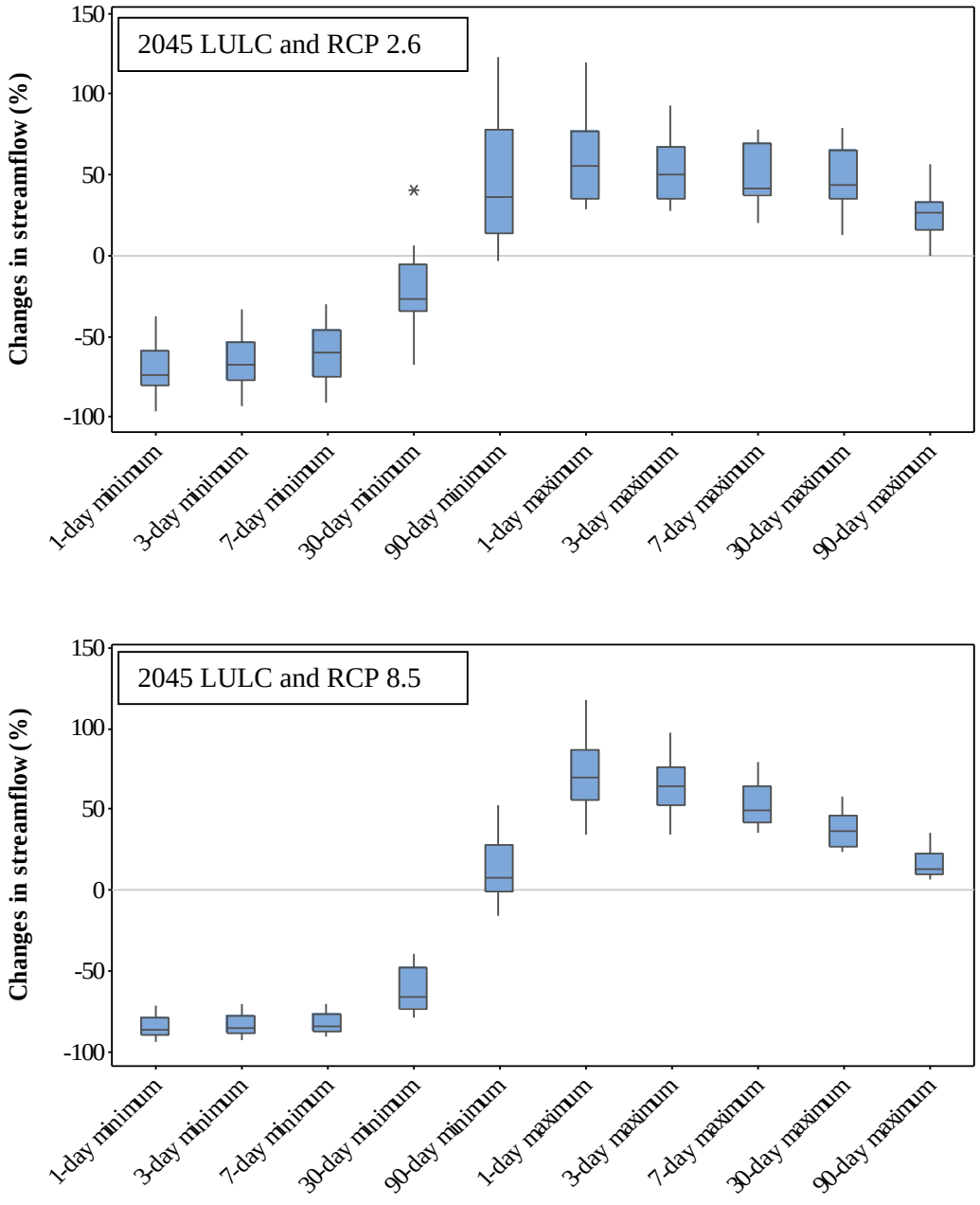

Figure III-13. Magnitude and duration of annual extreme water conditions (Combined impacts, IHA group 2). The boxes define the median values (horizontal central line), the 25th, 50th and 75th percentile values, and the vertical bars (whiskers) define the 10th and 90th percentile values.

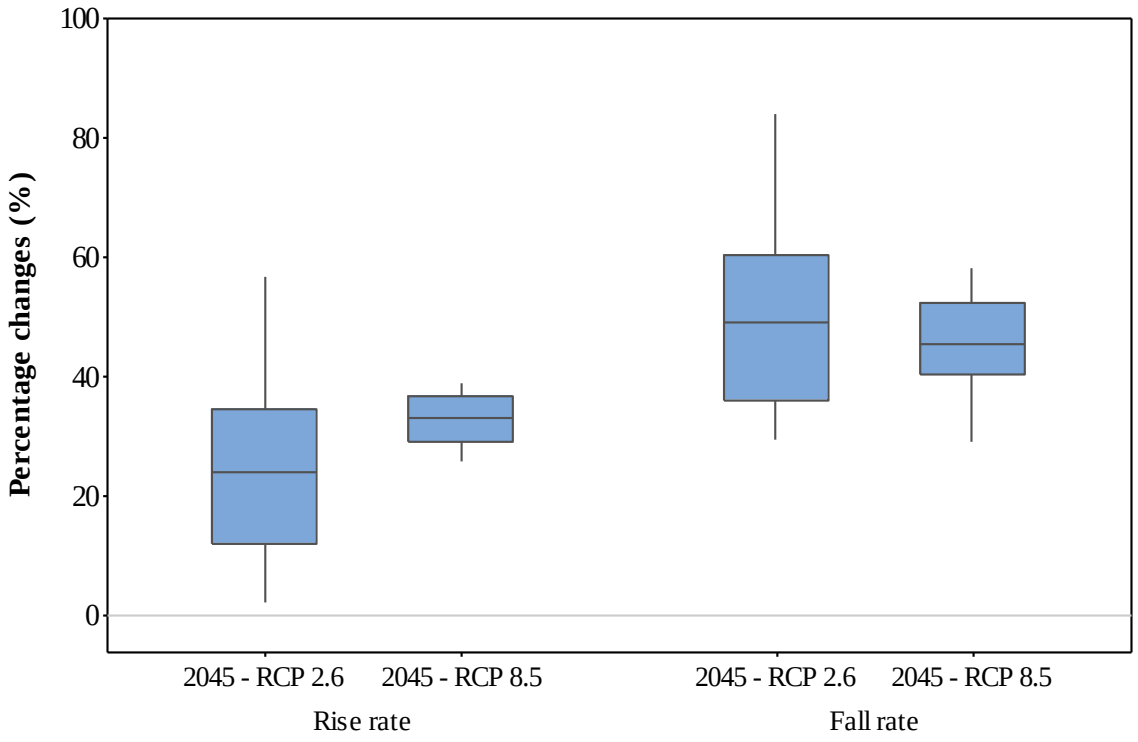

Figure III-14. Rate and frequency of water condition changes (Combined impacts – IHA group 4). The boxes define the median values (horizontal central line), the 25th, 50th and 75th percentile values, and the vertical bars (whiskers) define the 10th and 90th percentile values.

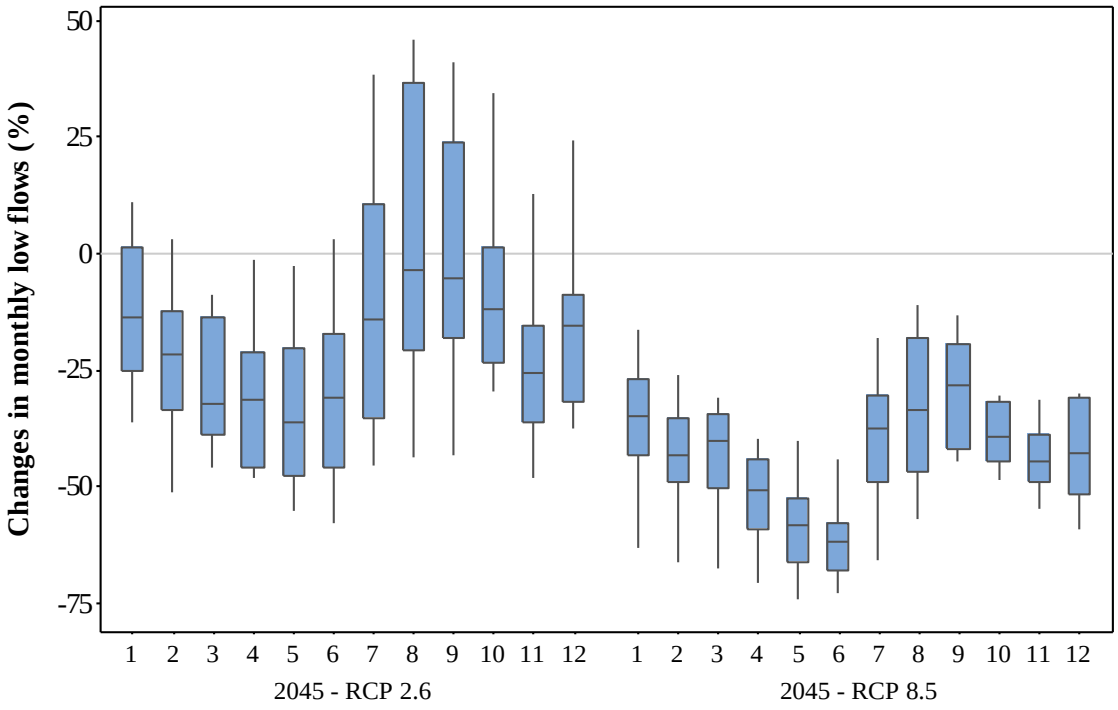

Figure III-15. Monthly low flows (Group 5 (EFC) - Combined impacts – IHA group 5 – EFC). The boxes define the median values (horizontal central line), the 25th, 50th and 75th percentile values, and the vertical bars (whiskers) define the 10th and 90th percentile values.

LULC, Cimate, Combined and Synergic Impact on Mean Monthly Percentage Changes (RCP 2.6 Emission Scenarios)

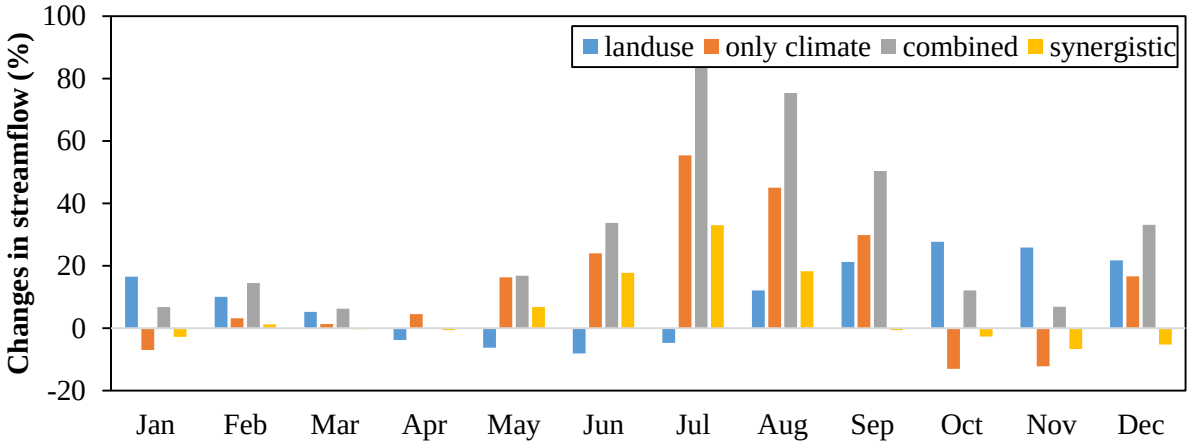

LULC, Climate, Combined and Synergistic impacts on Mean Monthly Percentage Changes (RCP 8.5 Emission Scenarios)

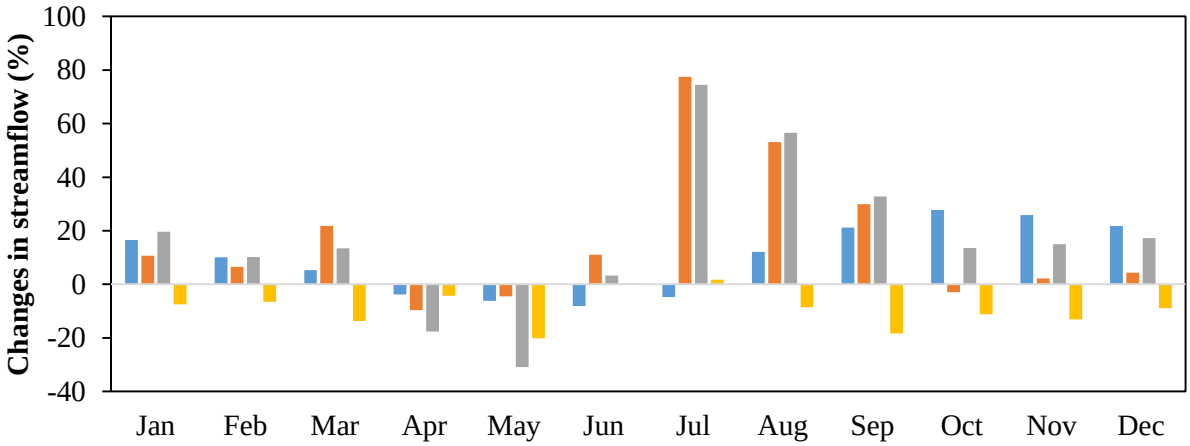

Figure III-16. LULC, climate, combined and synergic impacts on mean monthly percentage change of streamflow.

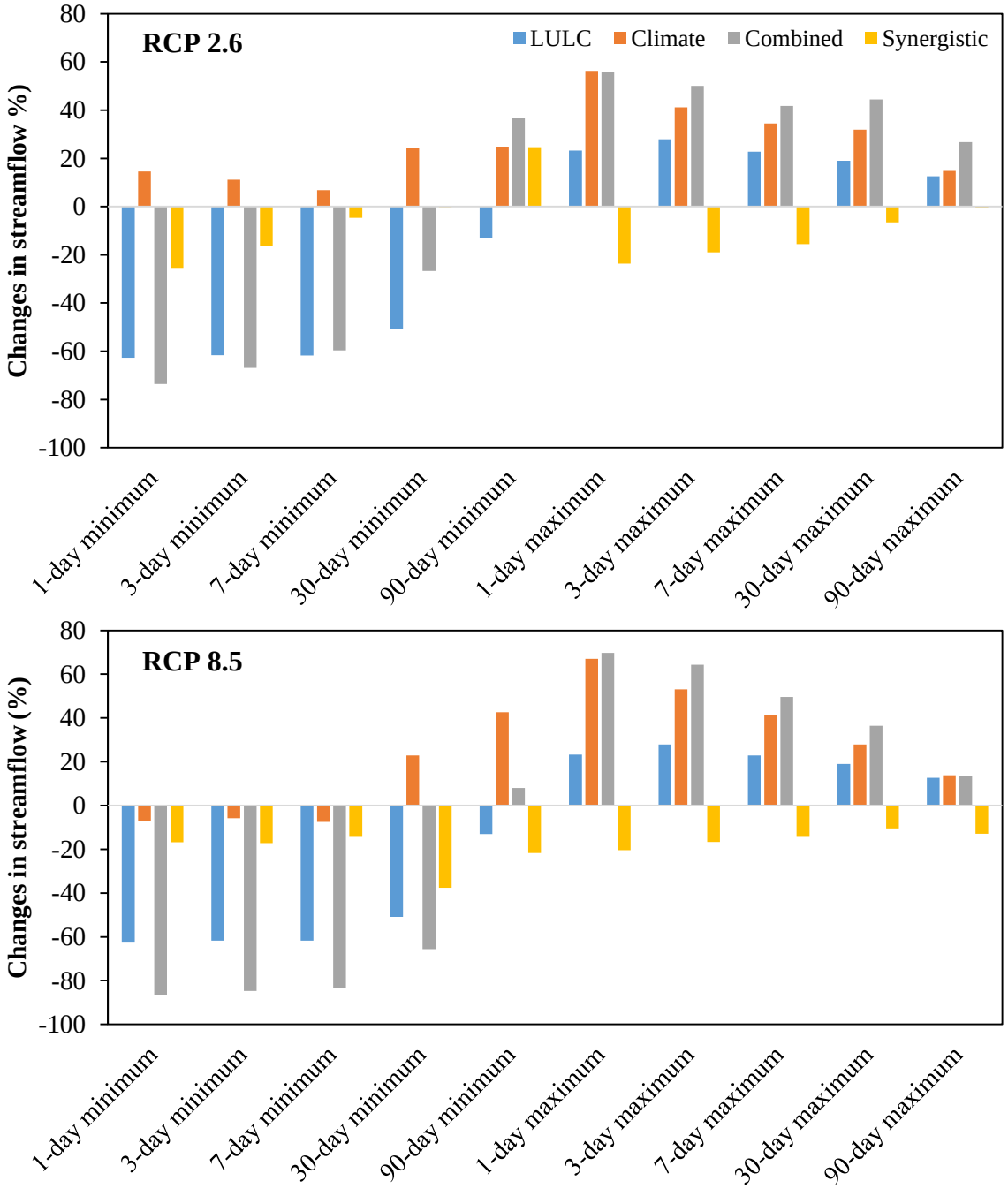

Figure III-17. Changes in magnitude and duration of annual extreme water conditions (Synergistic impact).

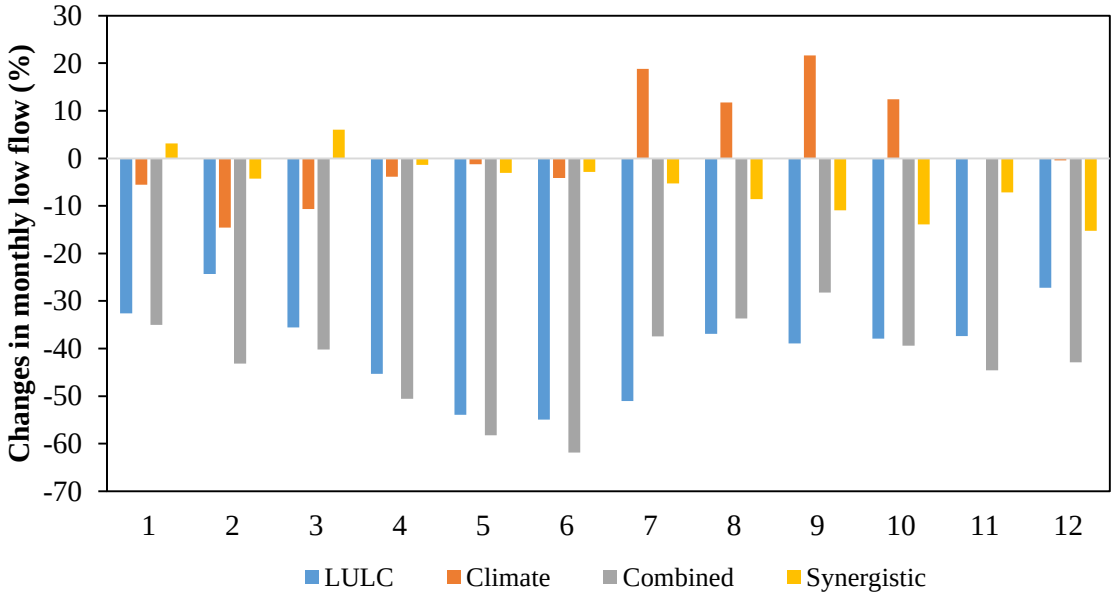

Figure III-18. LULC, climate, combined and synergistic impact on monthly low flows (Synergistic impact).

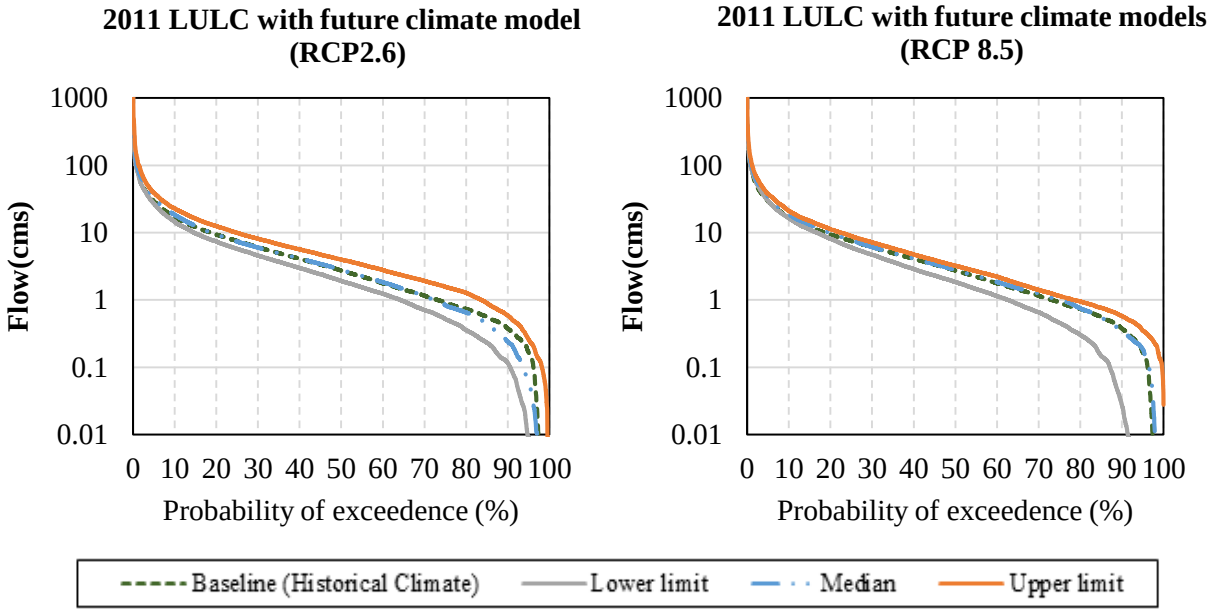

Figure III-19. 25-year flow duration curves (FDCs) under projected future climate and 2011 LULC data.

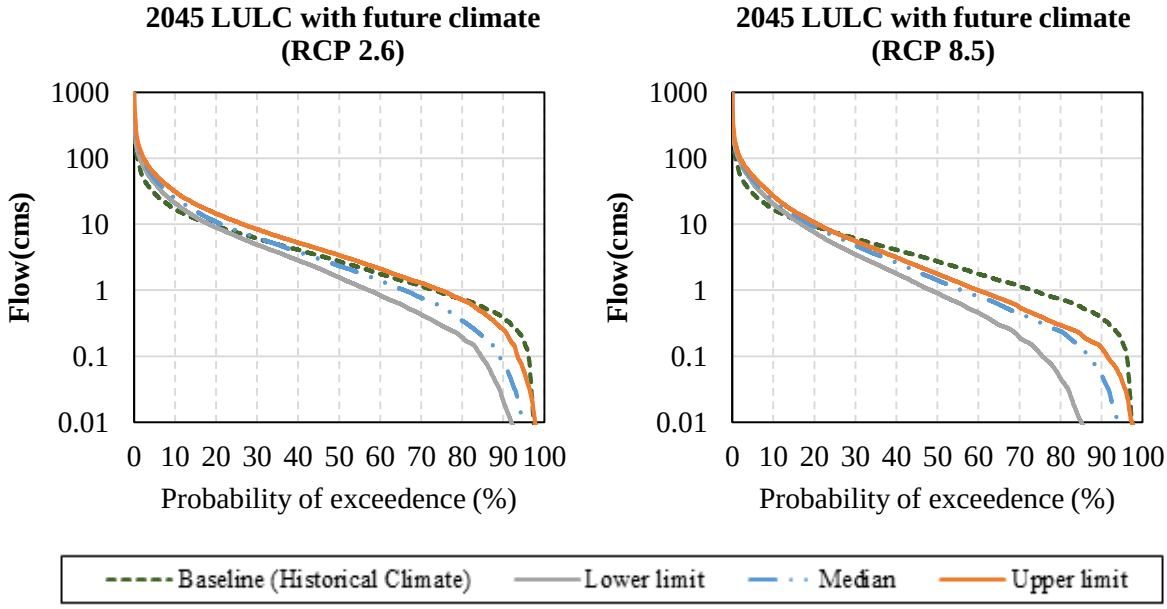

Figure III-20. 25-year flow duration curves (FDCs) under projected future climate and 2045 LULC data.

Chapter IV – Summary and Conclusions

LULC and climate change are both key drivers of significant changes in flow regimes. Flow regimes are crucial parts of the ecological integrity of river systems (Poff et al., 1997; Hart and Finelli, 1999). Understanding the changes in watershed hydrology due to separate and combined impacts of future LULC and climate changes is critical for sustainable water resource management, planning and ecological processes. The study area, Upper Cahaba River watershed, is a rapidly developed urban area (ADEM Upper Cahaba River Watershed TMDL, 2013) due to expansion of the Birmingham metropolitan area. Based on the USGS EROS projected future land cover data, it is also expected that the urban areas will continue to increase over the next 35 years.

In this study, past, present and future potential streamflow responses to climate and LULC changes were explored based on ecologically relevant flow metrics within the Upper Cahaba River watershed. For the baseline period (1988-2013), 1992 and 2011 LULC datasets (NLCD and digitized Landsat scenes), and historical climate data (PRISM and CFRS) were used. The model was successfully calibrated and validated for several of the model performance indicators, such as R^2, *NSE*, *RSR* and *PBIAS*. The SWAT-CUP program was used for calibration and validation by using the SUFI-2 algorithms. For the future period (2035-2060), eleven bias-corrected and downscaled GCMs data under two RCPs were used to represent the future climate, and two LULC maps (NLCD and USGS-EROS) were used to reflect the present and future LULC conditions. Hydrological simulations were performed using the SWAT hydrological model. The SWAT model

outputs were fed into to the Indicators of Hydrological (IHA) software to assess impacts of changes on ecologically relevant flow metrics.

Impacts of LULC datasets on streamflow for the baseline period were analyzed. Both NLCD and digitized Landsat 5 TM images for the years of 1992 and 2011 showed that any additional forest and agriculture conversion to urban may have significant influences on spring and fall streamflow. The study results also revealed that the source of LULC dataset did not substantially affect the SWAT model simulation of streamflows.

The annual distribution pattern of streamflow will be changed due to LULC and climate changes. These changes significantly affect the hydrologic conditions in the Upper Cahaba River watershed. They reduced monthly low flows, altered the timing of high and low flows, and changed the timing of annual extreme water conditions. The streamflow of the Upper Cahaba River watershed has a high probability of increasing in the future, while low flows were predicted to decrease. Results revealed the followings:

1. The stress on the aquatic ecosystem due to extremely low flow will increase. Low flows in the Upper Cahaba River watershed would be decreased in all months due to possible LULC and climate change.
2. The influence of hydrological alteration on the life cycle of the aquatic system will not be negligible, especially in summers.
3. The aquatic ecosystem stress due to rapid fall and rise rates in the streamflow will be more severe.
4. The RCP 2.6 scenarios generally led to increases in peak discharge while RCP 8.5 led to slight decreases in peak discharges.

5. Projected changes in hydrologic regimes simulated with different GCMs and RCPs can be subject to important uncertainties.
6. The uncertainty should be considered when water managers and planners establish water environment policies.

References

ADEM Upper Cahaba River Watershed TMDL. (2013). Available at: http://adem.alabama.gov/programs/water/wquality/tmdls/FinalCahabaRiverSiltationTMDL.pdf

Hart, D.D., Finelli, C.M. (1999). Physical–biological coupling in streams: the pervasive effects of flow on benthic organisms. Annu. Rev. Ecol. Syst., 30:363–395.

Poff, N.L., Allan, J.D., Bain, M.B., Karr, J.R., Prestegaard, K.L., Richter, B.D., Sparks, R.E., Stromberg, J.C., (1997). The natural flow regime: a paradigm for river conservation and restoration. Bioscience, 47:769–784.

APPENDIX A. ONLY LULC CHANGE IMPACTS

	ONLY LULC CHANGE IMPACTS	
Simulations	2011 LULC	2045 LULC
Mean annual flow	8.04	8.75
Group 1		
January	13.15	15.32
February	14.06	15.48
March	15.01	15.80
April	9.39	9.04
May	5.48	5.12
June	3.06	2.79
July	2.33	2.22
August	2.92	3.27
September	4.95	6.00
October	7.40	9.45
November	7.86	9.89
December	9.50	11.57
Group 2		
1-day minimum	0.338	0.124
3-day minimum	0.365	0.142
7-day minimum	0.409	0.153
30-day minimum	0.630	0.302
90-day minimum	1.534	1.352
1-day maximum	199.5	245.8
3-day maximum	101.1	129.3
7-day maximum	58.2	71.4
30-day maximum	24.9	29.7
90-day maximum	16.3	18.4
Group 3		
Date of minimum	279.0	250.3
Date of maximum	78.9	102.4
Group 4		
Rise rate	13.00	17.52
Fall rate	-4.28	-6.21
Group 5		
January Low Flow	4.128	3.123
February Low Flow	4.159	2.804
March Low Flow	4.995	3.218
April Low Flow	4.097	2.242
May Low Flow	2.870	1.323
June Low Flow	2.067	0.931
July Low Flow	1.741	0.853
August Low Flow	1.741	1.099
September Low Flow	1.904	1.163
October Low Flow	1.958	1.216
November Low Flow	2.576	1.614
December Low Flow	3.148	2.292

APPENDIX B. ONLY CLIMATE CHANGE IMPACTS (RCP 2.6 and RCP 8.5)

Appendix B.1. Only climate change impacts under RCP 2.6

*The climate models are listed in Table III-2.

	ONLY CLIMATE CHANGE IMPACTS (RCP 2.6)										
Simulations (Climate models)	1	2	3	4	5	6	7	8	9	10	11
Mean annual flow	8.43	11.91	9.82	8.76	7.36	9.79	7.83	6.86	8.42	9.47	10.1
Group 1											
January	11.33	16.76	11.97	12.88	11.12	12.23	11.60	12.04	12.62	14.49	15.20
February	11.12	15.67	25.42	20.38	8.85	11.79	13.38	9.96	14.88	14.51	17.85
March	16.56	30.77	13.55	15.21	12.32	9.69	14.00	12.80	19.00	24.11	20.29
April	12.02	13.80	12.43	10.25	7.64	7.55	7.76	8.77	9.41	9.82	10.46
May	7.44	7.98	7.59	4.80	5.77	6.24	4.80	4.08	6.37	6.64	8.47
June	3.79	7.23	3.67	3.66	3.16	5.81	5.85	1.81	3.55	5.42	5.15
July	3.91	5.68	3.44	3.19	4.84	7.67	3.68	2.78	2.40	2.50	4.59
August	4.56	4.52	4.30	6.04	4.18	7.59	3.76	3.11	4.21	3.72	5.04
September	4.51	7.37	6.85	4.73	6.65	8.63	5.20	4.32	8.16	6.38	6.43
October	4.94	7.42	6.84	7.32	6.44	9.84	6.57	4.38	5.93	5.92	5.45
November	7.94	8.59	9.91	6.20	6.21	8.72	6.91	6.05	5.10	10.46	5.68
December	11.08	13.77	11.59	8.61	8.70	15.04	9.54	11.76	8.84	9.08	14.08
Group 2											
1-day minimum	0.298	0.539	0.387	0.445	0.242	0.546	0.270	0.154	0.270	0.391	0.448
3-day minimum	0.318	0.580	0.406	0.486	0.263	0.581	0.287	0.178	0.297	0.429	0.477
7-day minimum	0.353	0.636	0.437	0.543	0.294	0.655	0.312	0.213	0.348	0.489	0.519
30-day minimum	0.779	1.218	0.786	0.855	0.680	1.262	0.748	0.440	0.699	0.784	0.860
90-day minimum	1.745	3.046	2.172	1.856	1.809	3.466	1.916	1.380	1.906	2.170	2.660
1-day maximum	263.9	576.2	311.9	253.1	245.8	379.5	334.9	236.3	316.5	508.0	303.1
3-day maximum	124.5	234.6	145.3	119.4	116.5	167.0	140.6	113.5	142.7	212.7	149.1
7-day maximum	72.4	118.0	88.4	70.1	65.6	92.3	75.1	61.8	78.2	106.1	91.5
30-day maximum	30.0	45.3	40.7	30.0	26.6	34.3	30.3	24.4	32.9	37.4	36.1
90-day maximum	17.4	25.9	22.6	18.2	14.7	18.7	16.8	14.3	19.1	20.5	19.8
Group 3											
Date of minimum	304.3	306.9	268.6	282.9	235.4	216.5	248.2	240.3	290.3	286.7	276.1

Date of maximum	61.0	68.2	42.8	87.5	54.7	306.2	84.5	60.0	81.7	62.5	63.0
Group 4											
Rise rate	12.83	21.00	14.88	13.79	11.39	15.89	14.33	11.44	14.89	17.43	15.27
Fall rate	-4.36	-6.79	-4.74	-4.49	-4.03	-5.13	-4.69	-4.11	-4.90	-5.71	-5.25
Group 5											
January Low Flow	3.795	5.091	4.082	4.228	2.847	4.611	3.258	3.046	3.884	4.232	4.307
February Low Flow	3.480	4.951	3.357	3.824	2.582	3.863	3.093	2.723	2.795	3.841	3.858
March Low Flow	3.881	5.209	4.006	4.434	3.349	4.382	3.263	3.447	4.390	4.842	4.838
April Low Flow	3.878	4.985	3.471	4.024	2.994	3.353	3.176	2.811	3.944	4.072	4.505
May Low Flow	3.085	4.568	3.029	2.964	2.034	2.554	2.523	2.099	3.031	3.327	3.966
June Low Flow	2.307	3.155	2.214	2.326	1.307	2.255	1.814	1.439	2.028	2.449	2.593
July Low Flow	2.096	3.048	2.040	1.932	1.728	2.420	1.647	1.278	1.616	1.677	2.743
August Low Flow	1.942	2.874	1.920	2.320	1.866	2.318	1.401	1.150	1.977	1.717	2.543
September Low Flow	2.040	3.071	2.563	2.273	1.842	3.201	1.761	1.234	1.851	2.296	2.383
October Low Flow	2.146	2.913	2.097	2.057	1.753	3.278	1.783	1.757	2.427	1.878	2.441
November Low Flow	1.866	3.597	2.223	2.464	1.929	3.387	2.251	1.681	2.384	2.411	2.791
December Low Flow	3.059	4.150	3.159	3.118	2.426	3.227	2.398	2.374	2.475	2.884	3.101

Appendix B.2. Only climate change impacts under RCP 8.5

*The climate models are listed in Table III-2.

	ONLY CLIMATE CHANGE IMPACTS (RCP 8.5)										
Simulations (Climate models)	1	2	3	4	5	6	7	8	9	10	11
Mean annual flow	9.98	8.91	8.33	9.94	9.55	7.74	8.01	8.55	8.04	9.2	9.59
Group 1											
January	16.32	12.50	16.32	17.50	15.58	9.57	13.59	10.98	10.83	14.80	14.55
February	15.41	14.14	11.22	15.87	17.24	9.92	10.90	15.30	14.98	16.65	14.39
March	20.66	16.39	11.30	21.28	16.42	9.00	14.40	20.18	18.28	18.28	19.12
April	9.60	11.48	8.50	9.95	6.95	6.08	8.23	10.25	7.90	8.14	9.89
May	5.23	4.98	7.86	4.97	4.38	3.48	3.65	6.87	5.60	6.08	7.32
June	2.19	4.75	2.64	3.87	3.56	3.40	6.73	2.87	1.99	2.74	4.72
July	3.37	4.18	2.45	6.99	5.31	5.83	4.28	3.90	3.39	2.87	4.11
August	4.49	3.91	3.90	5.89	5.22	4.76	4.52	4.22	3.24	3.75	5.76
September	7.72	6.01	8.07	4.51	5.53	10.45	4.63	5.16	6.43	9.08	6.71
October	7.16	6.41	7.18	7.86	12.76	13.29	9.13	5.61	5.26	6.66	7.57
November	14.82	8.71	7.39	6.15	9.10	8.28	6.24	5.77	8.04	11.47	7.64
December	11.21	12.11	12.43	9.77	9.86	5.67	7.84	9.91	9.96	9.49	10.39
Group 2											
1-day minimum	0.282	0.314	0.276	0.418	0.431	0.224	0.232	0.321	0.237	0.332	0.317
3-day minimum	0.303	0.348	0.303	0.458	0.457	0.243	0.265	0.344	0.263	0.371	0.361
7-day minimum	0.334	0.390	0.328	0.501	0.497	0.285	0.325	0.378	0.293	0.421	0.405
30-day minimum	0.624	0.840	0.638	0.903	0.996	0.525	0.623	0.774	0.576	0.815	0.998
90-day minimum	1.832	2.357	1.824	2.188	2.383	1.760	2.353	2.053	1.811	2.214	2.724
1-day maximum	485.5	320.5	353.1	359.5	333.2	245.8	304.1	290.5	365.8	369.6	251.9
3-day maximum	216.4	148.9	157.7	168.7	165.2	127.7	145.0	131.0	154.8	160.0	121.0
7-day maximum	112.3	80.8	82.1	91.1	89.0	76.2	76.1	73.5	82.8	83.6	71.6
30-day maximum	41.6	33.7	30.0	35.2	35.6	29.6	28.3	29.6	30.5	32.1	31.9
90-day maximum	23.0	18.6	17.3	20.9	19.4	16.5	16.4	17.5	16.9	18.8	19.6
Group 3											
Date of minimum	295.8	280.8	242.1	279.2	249.4	206.8	269.8	301.2	278.0	280.9	313.8

Date of maximum	41.7	39.4	321.6	95.7	79.4	92.8	83.0	63.2	42.2	21.7	67.9
Group 4											
Rise rate	15.76	13.66	13.46	14.92	13.75	11.99	13.84	14.75	14.21	15.62	14.02
Fall rate	-5.75	-4.64	-4.75	-5.32	-4.85	-4.09	-4.68	-4.91	-4.89	-5.25	-4.82
Group 5											
January Low Flow	4.548	4.022	3.590	4.867	4.109	2.467	3.827	4.105	3.570	4.905	4.889
February Low Flow	4.056	3.456	3.539	4.530	3.897	2.191	3.554	3.255	3.093	4.305	4.329
March Low Flow	5.376	3.829	3.999	5.427	4.464	2.734	3.999	4.704	3.961	5.575	5.133
April Low Flow	4.817	3.830	3.432	4.715	3.985	2.185	3.277	4.298	2.984	4.369	4.334
May Low Flow	3.186	2.828	2.834	3.294	2.629	1.852	2.202	3.312	2.629	3.210	3.842
June Low Flow	1.910	2.243	1.982	2.044	1.919	1.366	1.617	2.109	1.602	2.099	2.590
July Low Flow	2.077	2.069	1.486	2.291	2.290	1.185	1.910	2.094	1.625	1.790	2.356
August Low Flow	2.118	2.030	1.719	2.556	2.351	1.357	1.719	1.929	1.523	1.946	2.728
September Low Flow	2.304	2.451	1.871	2.867	2.703	2.144	2.316	1.885	1.927	2.343	2.807
October Low Flow	2.358	2.203	1.916	2.201	2.263	1.941	2.016	1.984	1.786	2.533	2.471
November Low Flow	2.575	2.705	2.338	2.670	2.937	2.218	2.213	2.250	1.861	2.921	2.854
December Low Flow	3.060	3.322	3.236	3.482	3.134	2.136	2.537	2.913	2.408	3.446	3.393

APPENDIX C. COMBINED IMPACTS (RCP 2.6 and RCP 8.5)

Appendix C.1. Combined impacts under RCP 2.6.

*The climate models are listed in Table III-2.

	COMBINED IMPACTS (RCP 2.6)										
Simulations (Climate models)	1	2	3	4	5	6	7	8	9	10	11
Mean annual flow	9.28	12.33	10.85	9.98	8.65	10.97	9.04	7.94	9.39	10.01	11.25
Group 1											
January	12.38	18.60	12.56	14.83	12.62	13.92	13.60	14.04	14.43	16.70	17.37
February	11.96	16.52	26.17	23.28	10.11	12.82	15.11	11.22	16.75	16.10	19.14
March	17.38	24.88	14.21	15.95	13.47	9.81	14.49	13.60	20.04	20.43	20.88
April	12.37	12.99	12.67	9.55	8.11	7.17	7.73	9.24	9.40	8.93	9.70
May	7.79	7.64	7.83	3.98	6.15	6.70	5.45	4.25	6.40	6.19	8.27
June	3.98	7.38	3.69	3.99	4.09	7.32	6.65	2.03	4.01	6.51	5.71
July	4.40	5.72	3.80	3.74	6.17	8.98	4.83	3.49	2.70	2.82	5.59
August	5.20	5.22	5.22	7.18	5.13	8.28	4.30	3.67	4.80	4.35	5.88
September	5.13	8.62	8.07	5.64	7.37	9.78	6.21	5.40	8.65	7.50	7.45
October	5.63	9.05	8.90	9.79	8.30	11.26	8.55	5.40	7.61	7.69	6.85
November	8.65	10.41	11.75	7.55	7.46	10.32	8.41	7.56	6.13	11.54	6.82
December	12.65	16.12	13.38	10.08	9.75	14.74	11.23	13.93	10.20	10.23	16.31
Group 2											
1-day minimum	0.068	0.179	0.113	0.135	0.089	0.212	0.060	0.013	0.066	0.088	0.140
3-day minimum	0.086	0.229	0.142	0.170	0.115	0.245	0.084	0.024	0.081	0.121	0.168
7-day minimum	0.104	0.264	0.176	0.220	0.130	0.287	0.106	0.037	0.104	0.165	0.197
30-day minimum	0.417	0.669	0.463	0.462	0.441	0.889	0.425	0.207	0.330	0.506	0.597
90-day minimum	1.751	2.739	2.255	1.682	2.187	3.428	2.018	1.493	1.954	2.095	2.867
1-day maximum	270.3	439.2	311.0	278.5	269.2	353.3	342.7	256.6	305.6	407.9	321.4
3-day maximum	136.9	195.1	162.2	138.5	134.9	169.6	151.7	129.7	146.6	187.6	168.0
7-day maximum	81.1	102.8	96.4	80.3	76.6	98.6	82.4	70.4	81.8	96.9	103.7
30-day maximum	33.8	42.4	44.9	34.9	31.5	39.5	34.0	28.0	36.0	36.7	41.1
90-day maximum	19.0	25.5	24.4	20.9	16.8	21.6	19.2	16.3	20.7	20.5	21.8
Group 3											
Date of minimum	238.2	228.1	248.7	226.8	198.2	189.0	217.6	223.0	224.3	236.1	269.0

Date of maximum	49.4	67.5	297.3	85.9	70.8	300.3	84.0	81.8	83.2	67.0	57.4
Group 4											
Rise rate	14.57	20.37	16.12	15.42	14.01	18.85	15.75	13.31	16.46	17.50	17.31
Fall rate	-5.82	-7.87	-6.33	-6.19	-5.54	-6.53	-6.38	-5.74	-6.53	-6.94	-6.86
Group 5											
January Low Flow	3.083	4.591	3.665	4.155	2.638	4.192	3.192	2.961	3.568	4.193	3.539
February Low Flow	2.897	4.292	3.265	3.440	2.024	3.771	3.001	2.536	2.770	3.507	3.646
March Low Flow	3.251	4.564	3.319	4.304	2.710	3.396	3.068	2.845	3.684	3.819	4.437
April Low Flow	3.236	4.050	2.586	3.171	2.317	2.143	2.226	2.121	2.816	2.849	3.374
May Low Flow	1.913	2.792	2.294	1.740	1.292	1.724	1.506	1.293	1.837	1.847	2.670
June Low Flow	1.430	2.131	1.356	1.460	1.118	1.745	1.065	0.875	1.208	1.489	1.716
July Low Flow	1.084	2.252	1.495	1.493	1.572	2.411	1.171	0.949	1.128	1.164	1.929
August Low Flow	1.587	2.392	1.684	2.062	1.799	2.539	1.277	0.980	1.643	1.378	2.381
September Low Flow	1.558	2.579	1.807	2.363	1.680	2.690	1.761	1.082	1.531	1.900	1.978
October Low Flow	1.497	2.348	1.814	1.789	1.576	2.633	1.381	1.392	1.723	1.553	1.985
November Low Flow	1.381	2.907	2.175	2.134	1.640	2.829	1.855	1.334	1.867	1.923	2.055
December Low Flow	2.665	3.911	3.052	2.687	1.971	2.873	2.124	2.143	2.196	2.523	2.846

Appendix C.2. Combined impacts under RCP 8.5.

*The climate models are listed in Table III-2.

	COMBINED IMPACTS (RCP 8.5)										
Simulations (Climate models)	1	2	3	4	5	6	7	8	9	10	11
Mean annual flow	9.75	9.13	8.55	9.86	9.62	8.24	8.46	8.8	8.54	9.24	9.78
Group 1											
January	17.06	13.25	16.19	18.92	16.58	10.29	14.92	11.87	11.56	15.84	15.73
February	15.49	14.49	11.14	15.77	17.39	11.15	11.28	16.00	15.67	16.73	14.13
March	20.09	15.79	11.07	19.11	15.47	8.92	14.45	20.28	18.80	17.02	19.00
April	7.74	10.40	7.91	7.85	4.96	5.70	7.41	8.88	6.69	6.35	8.36
May	3.79	3.76	7.34	3.32	3.12	3.10	2.87	5.56	4.64	5.02	6.07
June	1.32	4.52	2.03	3.33	3.16	3.54	7.28	1.98	1.26	2.00	4.21
July	3.28	4.02	2.43	6.74	5.02	5.93	4.23	3.88	3.52	2.84	4.18
August	4.62	4.02	4.07	5.91	5.35	4.92	4.53	4.25	3.58	3.81	5.78
September	6.33	6.58	8.59	4.46	5.61	10.93	4.92	5.80	8.01	9.63	7.13
October	8.39	7.39	8.40	8.48	14.21	15.35	10.75	6.48	6.43	7.90	8.81
November	14.49	10.01	8.62	7.16	10.17	9.04	7.19	7.05	10.04	12.59	8.81
December	12.25	13.27	13.49	10.92	10.50	5.65	8.70	11.27	11.32	10.31	11.14
Group 2											
1-day minimum	0.041	0.059	0.046	0.097	0.088	0.038	0.021	0.045	0.032	0.049	0.071
3-day minimum	0.050	0.069	0.052	0.109	0.100	0.043	0.027	0.056	0.037	0.061	0.083
7-day minimum	0.058	0.089	0.062	0.124	0.115	0.052	0.038	0.067	0.045	0.074	0.098
30-day minimum	0.158	0.330	0.215	0.320	0.342	0.172	0.203	0.253	0.132	0.217	0.384
90-day minimum	1.302	1.969	1.520	1.656	1.672	1.596	2.133	1.551	1.351	1.762	2.346
1-day maximum	400.7	334.0	338.5	338.7	341.0	295.8	339.0	311.0	433.6	372.2	268.0
3-day maximum	199.3	161.7	160.7	172.8	177.7	154.3	166.1	145.1	185.3	166.8	135.6
7-day maximum	104.6	87.0	82.8	93.7	95.6	89.4	84.4	81.1	95.5	86.6	78.6
30-day maximum	39.5	35.5	31.1	36.4	37.8	33.5	31.0	31.7	34.0	32.6	34.1
90-day maximum	22.1	18.9	17.7	20.6	19.7	17.9	17.4	17.9	18.2	18.5	20.1
Group 3											
Date of minimum	255.9	220.7	233.2	266.0	240.6	179.2	223.5	222.8	232.2	259.9	275.4

Date of maximum	346.2	43.2	320.2	103.1	94.5	181.4	95.0	62.2	55.4	28.3	67.9
Group 4											
Rise rate	17.44	16.70	16.92	17.81	16.79	16.38	17.39	17.30	18.04	18.09	17.17
Fall rate	-6.76	-5.95	-6.02	-6.52	-6.11	-5.52	-6.17	-6.37	-6.48	-6.67	-6.22
Group 5											
January Low Flow	2.964	2.642	2.199	3.140	2.683	1.521	2.441	2.748	2.344	3.460	3.022
February Low Flow	2.460	2.341	2.363	3.076	2.460	1.414	2.350	2.124	1.967	2.977	2.694
March Low Flow	3.200	2.732	2.479	3.453	2.988	1.614	2.325	3.158	2.692	3.315	3.276
April Low Flow	2.287	2.154	1.677	2.464	1.881	1.210	1.637	2.119	1.716	2.026	2.314
May Low Flow	1.159	1.199	1.481	1.304	0.970	0.747	0.813	1.311	1.022	1.370	1.713
June Low Flow	0.664	0.993	0.768	0.799	0.788	0.567	0.711	0.794	0.593	0.875	1.153
July Low Flow	1.178	1.049	0.682	1.360	1.426	0.596	1.107	1.089	0.888	0.972	1.210
August Low Flow	1.223	1.113	0.929	1.508	1.423	0.752	1.025	1.166	0.799	1.155	1.546
September Low Flow	1.397	1.322	1.055	1.656	1.538	1.338	1.367	1.052	1.103	1.410	1.584
October Low Flow	1.282	1.262	1.082	1.144	1.355	1.187	1.045	1.137	1.008	1.366	1.333
November Low Flow	1.390	1.501	1.443	1.428	1.575	1.317	1.295	1.339	1.165	1.772	1.645
December Low Flow	1.798	2.150	2.182	2.205	1.676	1.282	1.521	1.797	1.508	2.171	2.211